The use of multi-zone modelling for tunnel fire risk analysis

Johansson, Nils; Ronchi, Enrico; Scozzari, Rugiada; Fronterrè, Michele

2021

Document Version:
Publisher's PDF, also known as Version of record

The use of multi-zone modelling for tunnel fire risk analysis

Nils Johansson
Enrico Ronchi
Rugiada Scozzari
Michele Fronterrè

Department of Fire Safety Engineering
Lund University, Sweden
Lund 2021

Report 3242

The use of multi-zone modelling for tunnel fire risk analysis

Nils Johansson
Enrico Ronchi
Rugiada Scozzari
Michele Fronterrè

Lund 2021

The use of multi-zone modelling for tunnel fire risk analysis

Nils Johansson, Enrico Ronchi, Rugiada Scozzari, Michele Fronterrè

Report 3242
ISRN: LUTVDG/TVBB-3242-SE

Number of pages: 67

Keywords: tunnel fire, risk analysis, multi-zone model, fire safety

Abstract. Tunnel fire risk analysis are a useful tool to ensure adequate safety levels in tunnels. This report presents the work conducted to integrate a multi-zone modelling approach into a fire risk assessment tool, called ARTU. This work was performed to improve its fire modelling predictive capabilities compared to the currently adopted 1D fire modelling representation. This is deemed to allow for the use of multi-scale modelling, i.e., to select among different modelling approaches in relation to the scenarios under consideration. The multi-zone model integrated within ARTU is based on an existing tool, i.e., the MZ Fire model developed for large spaces which has been updated and adapted for tunnel environments. The integration of MZ Fire model into ARTU involved a set of developments needed specifically for tunnel fire scenarios (e.g. considering tunnel gradient, tunnel section representations, customization of outputs for use in a tunnel fire risk assessment tool, etc.). Those new features are here presented along with a sensitivity analysis looking at zone size. Benchmarking of the results produced is performed through comparison with data from the 2006 BeNeLux tunnel experiments and the 2015 Runehamar experiments. The multi-zone model results were also compared against results from the Fire Dynamics Simulator (FDS) for a set of tunnel configurations.

Avdelningen för brandteknik
Lunds universitet
P.O. Box 118
221 00 Lund

brand@brand.lth.se
http://www.brand.lth.se

Telefon: 046 - 222 73 60
Telefax: 046 - 222 46 12

Department of Fire Safety Engineering
Lund University
P.O. Box 118
SE-221 00 Lund, Sweden

brand@brand.lth.se
http://www.brand.lth.se/english

Telephone: +46 46 222 73 60
Fax: +46 46 222 46 12

Acknowledgements

The authors wish to acknowledge Cantene srl for sponsoring the project on which this report is based on.

Table of Contents

1. Introduction

Tunnels are important infrastructures as they facilitate the development of links in transportation networks, i.e. they often represent a viable solution to overcome road layout issues and shorten travel times (Ronchi, 2012). Tunnels often represent crucial nodes of a road network, as they may represent points of connection between two otherwise disconnected areas or even allow for transnational connection between countries. For this reason, tunnel fires can have catastrophic consequences in terms of traffic disruption, property damage, and, more importantly loss of lives (Carvel and Beard, 2005). While tunnel fires are far less frequent than fires in buildings (Carvel and Marlair, 2005; Rattei et al., 2014), they present unique characteristics which may contribute to make more difficult to extinguish them, too often leading to deadly consequences. In addition, several factors can increase the hazards of tunnels such as traffic densities, increased lengths, and higher fire loads due to transportation of dangerous goods (Bergmeister et al., 2004).

In this context, an appropriate risk assessment of existing and new facilities can be a useful tool to assess tunnel safety levels and inform decision makers and designers upon solutions to be adopted (Beard, 2010). This is an alternative tool to traditional prescriptive-based approaches, which instead have shown several shortcomings in relation to fire safety (Meacham and Custer, 1995). The introduction of the European Directive 2004/54/EC made tunnel risk assessment an integral part of tunnel design (European Commission, 2004). This could be performed adopting a variety of approaches. Probabilistic risk assessment approaches have shown great potential to consider uncertainties linked to both the selection of the scenarios themselves, the inputs of the analysis and tools used for the analysis (Nỳvlt et al., 2011).

Based on these premises, the Italian fire engineering and thermal science company Cantene srl developed a tunnel risk analysis tool called ARTU® (acronym in Italian for Risk Analysis in Tunnels). This tool adopts a probabilistic approach to estimate the expected number of fatalities per year in existing and new tunnels. ARTU uses an approach based on pseudo-random sampling from distributions to define hundreds of different fire and egress scenarios. In each scenario, values coming from statistical distributions are adopted for a set of random variables including pre-movement time and egress velocity, fire position, and the type of vehicle on fire. A deterministic approach is used to describe the interaction between fire products and people involved in each scenario. For the fluid dynamics representation, ARTU uses a third party software based on 1D fluid-dynamics which includes geometrical data and characteristics of the ventilation system. The software returns time-varying air temperature, air velocity, and volume airflow along the tunnel which is used as an input for the ARTU tool. Since it is a 1D tool it returns only one value for each variable at a set distance from the fire. One-dimensional (1D) modelling has been chosen for its low computational cost that make it possible to simulate a large number of different scenarios. A queue-formation model is used to determine the initial position of agents along the tunnel, taking into account data about traffic condition and volume. The path of each agent inside the tunnel through the exit is calculated assuming that the people in a straight or curved tunnel can only move in one direction (along the tunnel), which can be approximated with a 1D modelling approach. ARTU takes into account the presence of other agents in the surroundings and the reduction of visibility due to smoke. The estimation of damage is based on the effects of smoke on escaping agents, estimated by means of the FED (Fractional Effective Dose). For the majority of toxic products in a fire atmosphere, a given toxic endpoint such as incapacitation or death occurs when the victim has inhaled a particular product dose of toxicant (Purser and McAllister, 2016). As with toxic gases, an exposed occupant can be considered to accumulate a dose of convected heat over a period of time (NFPA, 2017). ARTU calculates the FED for each agent in the domain, based on oxygen, carbon monoxide, carbon dioxide concentration and gas temperature, obtained from the results of the 1D fluid-dynamics routine (Sandin et al., 2019). ARTU finally produces FN-curves. The latter represent cumulative frequency divided by the

number of fatalities for a given tunnel under consideration, thus being an indicator of the societal risk associated with the tunnel facility. Those curves can then be compared with the so-called ALARP diagram (as low as reasonably practicable) in relation to the regulatory framework to which the tunnel is subjected to.

Previous work (Sandin et al., 2019) has been conducted to perform a set of verification tests to ensure that the calculation methods implemented in ARTU work as intended from the perspective of the tunnel application domain and a set of validation tests against experiments performed in the Second Benelux tunnel (Lemaire and Kenyon, 2006) and the Runehamar tests (Ingason et al., 2015a).

At the time this report was written, Cantene srl was in the process of developing a new version of ARTU, to increase the accuracy of the fire representation. To improve the resolution of the fire modelling representation available in ARTU, Cantene initiated a research project together with the Division of Fire Safety Engineering at Lund University. Due to the fact ARTU estimation of risk is based on the analysis of a large number of different scenarios, actual fluid dynamics representation is based on 1D model. Despite its low computational requirement, this modelling approach prevents the representation of phenomena like smoke stratification and back-layering that can occur in presence of low longitudinal velocity. These phenomena are common in naturally ventilated tunnels with low slope when the fire is growing and not fully developed. Furthermore in mechanical ventilated tunnel, smoke stratification can be a desired effect during the egress of occupants, in order to assure a layer free of smoke in the lower part of tunnel section that is used as a mean of egress. ARTU's aim is to evaluate societal risk, namely expected number of fatalities per year, so its focus in on the first phase of fire, during egress procedures. A more detailed description of smoke stratification in the vicinity of fire and during the first phase of fire, when egress takes place, has the potential to better represent the interaction between occupants and fire, leading to a more accurate evaluation of societal risk.

In order to keep the computational time under a reasonable limit, field models have been excluded. Zone models have the potential to represent the stratification of smoke, but their use requires carefully consideration of: (i) the ratio between length and height of the simulated domain (Jones et al., 2009); (ii) the representation of ventilation devices used in tunnels, such as jet-fans, that may require dedicated model input calibration efforts (Sandin et al., 2019). The multi-zone model has been chosen in order to address these requirements and an analysis has been done to determine its limit of applicability. Once applicability limits are defined, the multi-zone model has been included in ARTU routine in a coupled hybrid modelling approach.

1.1 Aim and objectives

The aim of this work is to expand the fire modelling capabilities of ARTU by integrating a multi-zone modelling approach. This is deemed to enhance its fire modelling predictive capabilities and allow for the specific use of multi-scale modelling and in general to choose among different modelling approaches in relation to the scenarios under consideration. The multi-zone model integrated within ARTU is based on an existing tool, i.e., the MZ Fire model developed for large spaces (Johansson, 2021) which has been updated and adapted for tunnel environments. The integration of MZ Fire model into ARTU involved a set of specific developments needed specifically for tunnel fire scenarios (e.g. considering tunnel gradient, tunnel section representations, customization of outputs for use in ARTU, etc.). Benchmarking of the results produced by ARTU is performed through analysing the sensitivity of results to the zone size, and comparison with experimental data (validation) and results from Computational Fluid Dynamics (CFD) models such as the Fire Dynamics Simulator (FDS) (McGrattan et al., 2021).

The version of the MZ Fire model that has been applied in this project is labelled: MZ_Tunnel_01.

1.2 Report overview

The first chapter of this report introduces the project and the overall aim and objectives. Chapter 2 presented the method employed for the development and implementation of the MZ Fire model within ARTU. Chapter 3 presents a brief overview of existing approaches adopted for fire modelling in tunnels, particularly focusing on the main limitations of 1D models, existing multi-scale modelling approaches and why a multi-zone modelling approach was selected for implementation within ARTU. Chapter 4 introduces MZ along with its developments and adaptation to be used for tunnel fire risk assessment. Chapter 5 presents a set of tests performed for benchmarking the updated MZ Fire model against experimental data (validation) and results from the Fire Dynamics Simulator. Chapter 6 demonstrate the new features implemented in MZ during the project. Chapter 7 presents a sensitivity analysis conducted for a set of simple cases, aimed at investigating the impact of zone sizes on the updated MZ Fire model results. Chapter 8 discusses the domain of applications of MZ considering pros and cons of multi-zone modelling against other modelling approaches for different tunnel fire scenarios. Chapter 9 presents a general discussion on the new version of ARTU implementing multi-zone modelling. Finally, chapter 10 presents a set of conclusive remarks about the work conducted.

2. Method

The set of features to be developed was discussed and identified in dialog between the project partners. An interpretation of the features and how they could be integrated in the existing MZ Fire model was investigated by Lund University. A control and demonstration of each one of the implemented features in the model was performed.

A review of full-scale experimental tests was performed to identify suitable tests to be used in testing of the model and the new features for the tunnel environment. It is in general difficult to control and measure all variables in full-scale fire tests that are needed for simulating the test. This means that a difference between simulated and test results can be due to inaccurate inputs rather than inabilities of the model to describe the physical phenomena studied. To identify such issues a benchmark was also performed with an established fire model, FDS. Based on the results from the testing and benchmarking of the MZ Fire model recommendations for when to apply the model for tunnel situations was developed.

Finally, the MZ Fire model as implemented in the existing risk analysis tool, ARTU. This work was performed by Cantene.

3. Fire modelling in tunnels

This section provides an overview of the key concepts related to the modelling of fires in tunnels. This includes the characteristics of tunnel fires and existing modelling techniques, including coupled hybrid modelling approaches.

3.1. Characteristics of tunnel fires

Tunnel fires differ in many aspects from open fires (a fire without any interaction with its surrounding geometry or enclosure) and building fires (Ingason et al., 2015b). There are at least two important ways in which tunnel fires differ from the open fires: (i) the heat feedback from the surrounding environment; (ii) the effect of natural ventilation on the fire (Ingason et al., 2015b). The heat feedback to the fuel surface in open fires is governed by the flame volume. Tunnel lining, cross-sectional area and ventilation also play an important role in tunnels. A fire that develops in a tunnel interacts with the ventilation airflow and generates complex air flow patterns and turbulence in the vicinity of the fire. In the case of a slope inside the tunnel, buoyancy forces are created along the tunnel which could govern the movement of the air flow inside the tunnel. If the resulting longitudinal flow velocity is not high enough (about 3–3.5 m/s for most tunnels), a reverse flow of hot gases in the ceiling will be created, so-called backlayering. In addition, winds and atmospheric conditions outside the portals may have a strong influence on the ventilation system. Sudden changes in the air flow could easily occur due to pressure changes inside and outside the tunnel portals (Ingason et al., 2015b).

Tunnel fires differ from building compartment fires in at least three important ways: (i) the effects of the ventilation factor; (ii) the flashover conditions; (iii) the stratification development. The maximum HRR in compartment fires is usually dictated by the ventilation factor (opening areas and their height). In tunnels the situation is entirely different. The size of the fire and its position within the tunnel, the slope of the tunnel in the vicinity of the fire, the cross-sectional area where the fire takes place, the total length of tunnel, the type of the tunnel lining material (concrete, blasted rock) and the meteorological conditions at the entrance and exit are the factors that govern the natural ventilation within the tunnel system. The result of this is that the excess air available for combustion is an order of magnitude higher than in compartment fires which are governed by the ventilation factor. Tunnels are also often equipped with mechanical ventilation which consists of supply/exhaust fans and/or jet fans in the ceiling. These ventilation conditions differ significantly from compartment fires which are usually naturally ventilated through windows or other openings. There are many buildings equipped with mechanical ventilation, but the flow rate is relatively small as compared to the fire size, and usually when a fire becomes fully developed the windows break and the fire becomes dominated by the ventilation. Flashover is defined as the rapid transition to a state such that all the surfaces of the combustible materials within a compartment are involved in the combustion. Fires in compartments can easily grow to 'flashover' within a few minutes. Tunnel fires are not likely to grow to a conventional flashover, due to large heat losses from the fire to the surrounding walls, lack of fuel in relation to the volume size and containment of hot fire gases. Experiments and theoretical considerations show that flashover can easily occur in a train compartment or a truck cabin located inside a tunnel. Although flashover appears to be impossible in a tunnel fire, an under-ventilated fire in a tunnel is possible. This should be given special attention. In an under ventilated fire, the consequences of the activation of a powerful ventilation system may be significant. The flame volume may suddenly increase in size and length. The stratification formation of the smoke layer differs from compartment fires. In the early stages of compartment fires, an upper quiescent buoyant smoke layer is formed with a cold smoke free layer below. At a short distance from the point where the fire plume impinges on the tunnel ceiling, the smoke flow transits to a longitudinal flow on both sides in a tunnel with essentially no longitudinal ventilation and nearly no slope. Eventually such a layer will be become

thicker and descend towards the tunnel floor. If a longitudinal ventilation system is activated, this stratified layer will gradually disperse (Ingason et al., 2015b).

3.2. Tunnel fire modelling approaches

The main modelling methods for the study of fire and smoke in tunnels are here presented considering increasing complexity and computational cost.

One-dimensional (1D) network models represent a system as a one-dimensional network of nodes, containing a single set of variables such as temperature, density, mass and treated as homogeneous, and node connections that represent 1D transfer conduits between nodes (Ralph and Carvel, 2018). The 1D model returns time-varying air temperature, air velocity, and volume airflow along the tunnel. The benefit of using 1D representation of fluid-dynamics are: (i) 1D models have low computational requirements; (ii) 1D models give advantages for the analysis of a complex network system, constituted by a tunnel and its ventilation system, allowing a complete and compact description of the system. The intrinsic limitations of 1D models are because the flow quantities are assumed to be homogeneous in each cross-section. This assumption makes 1D models unsuitable for simulating the fluid behaviour in regions characterised by high temperature or velocity gradients, typically encountered close to the flames or in the regions where well-defined smoke stratification is found (Beard and Carvel, 2012).

Zone models represent a compartment as multiple uniform zones (typically two zones: a hot upper layer and a cooler lower layer). Zone models solve conservation equations between the uniform zones and typically include empirical relationships for phenomena such as fires and plume flow. Zone models are limited by the geometry they can represent (simple, cuboidal compartments) but are solved relatively quickly (Ralph and Carvel, 2018). Control volume modelling has the capacity to predict various aspects of fires in tunnels; however, any radical departure by the fire system from the conceptual basis of the control volume model can seriously affect the accuracy and validity of the approach. As any other model, zone models adopts certain assumptions, both conceptual and numerical, and it is essential for results to be interpreted in the light of them (Beard and Carvel, 2012). As an example, a typical assumption is that mass transport times within a control volume are instant. When applying control volume equations to tunnel fires, consideration should be given to the unique nature of some fire phenomena in tunnels. For example (i) an assumption that hot-layer properties are homogeneous along the length of the tunnel will only be tenable for very short tunnels; (ii) ambient and forced ventilation flows in tunnels may affect air entrainment in plumes; (iii) the relative velocities of hot and cold layers may mean that shear mixing effects at the interface may not be negligible (Beard and Carvel, 2012).

Field models, also called computational fluid dynamics (CFD) models, divide a domain into finite elements or volumes for which conservation equations are solved. Each finite element holds a set of conserved variables. Field models can be used to examine complex geometry but require large storage space, high computation requirements and have a high computational cost (Ralph and Carvel, 2018). CFD provides a powerful tool for the analysis of complex fire situations in tunnels. The details of tunnel geometry and ventilation systems can be represented, taking advantage of the three-dimensional prediction capability of modern CFD codes. The physical behaviour of the fluid is represented by means of mathematical models, and it is possible to extend the description of the fluid to include effects such as turbulence, buoyancy, combustion and heat transfer by radiation and convection, all in a single simultaneous calculation. When solutions are obtained, they should be reviewed taking into account the influence of grid size and time step, what influence do boundary conditions have on the solution, adequate convergence of solution (Beard and Carvel, 2012).

As systems in the built environment are getting bigger and more complex (Ralph and Carvel, 2018), hybrid approaches exploiting the advantages of different methods started arising. Computational limitations mean that the calculation domain must be curtailed, ignoring the two-way coupling between the total system and a fire. Coupled hybrid modelling (coupling of fire dynamics sub-models with a range of computational costs) expands the domain and analyses this two-way coupling within a reasonable timeframe (Ralph and Carvel, 2018). Coupled hybrid modelling is also called multiscale approach. In fire safety engineering, coupled hybrid modelling can be broken into three categories based on the selection of sub-models: (i) coupled field-zone; (ii) field-network; (iii) zone-network (see Ralph & Carvel, 2018 for a literature review for each category).

Different coupled hybrid model types are possible based upon the constituent sub-models adopted. The choice for which sub-model type to adopt is based upon what element of the built environment is being examined and the type and extent of output required to perform the desired analysis. Where tunnels are the subject of analysis, the majority of authors have adopted a field-network modelling methodology (Ralph and Carvel, 2018). The lack of adoption of a zone sub-model is because this model type, at least in its typical state, is not useful for a tunnel. A zone model does not typically account for lateral variation in parameters or lateral movement of mass; therefore, information related to smoke spread, back-layering and critical velocity in a longitudinally ventilated tunnel is not resolved. Some authors have attempted to use zone models in a "multicell" arrangement for tunnels (Ralph and Carvel, 2018).

4. Multi-zone modelling: the MZ Fire model for tunnel safety

The Multi-Zone (MZ) Fire model is a fire model that can be used to calculate the effects of a fire in an enclosure. The model consists of a single executable file that is runs from a terminal window. The user is required to write a simple text input file since there is no graphical user interface

The overall concept of a multi-zone model is presented in Figure , this general description has been presented in pervious publications (Suzuki et al., 2004). The enclosure is divided into several regions (horizontal) and layers (vertical) this means that the entire enclosure is made up of several smaller computational volumes or zones. The conservation mass and energy are applied for each zone.

The fire is specified as a heat release rate and the heat and hot gases rises upwards from the fire in a plume that enters the highest located layer in the fire region, *i*. The fire plume flow rises until it hits the ceiling. Air and hot gases are entrained in the plume from the layers that it passes through. Mass is transported horizontally to layers in adjacent regions due to hydrostatic pressure differences. The vertical flow of mass between layers is calculated based on the conservation of mass. The calculated properties (like temperature) are uniform in each zone (see Figure 1). The model extends into a three-dimensional volume with regions not only in the x- and z-direction, as illustrated in (Figures 1 and 2), but also in the y-direction.

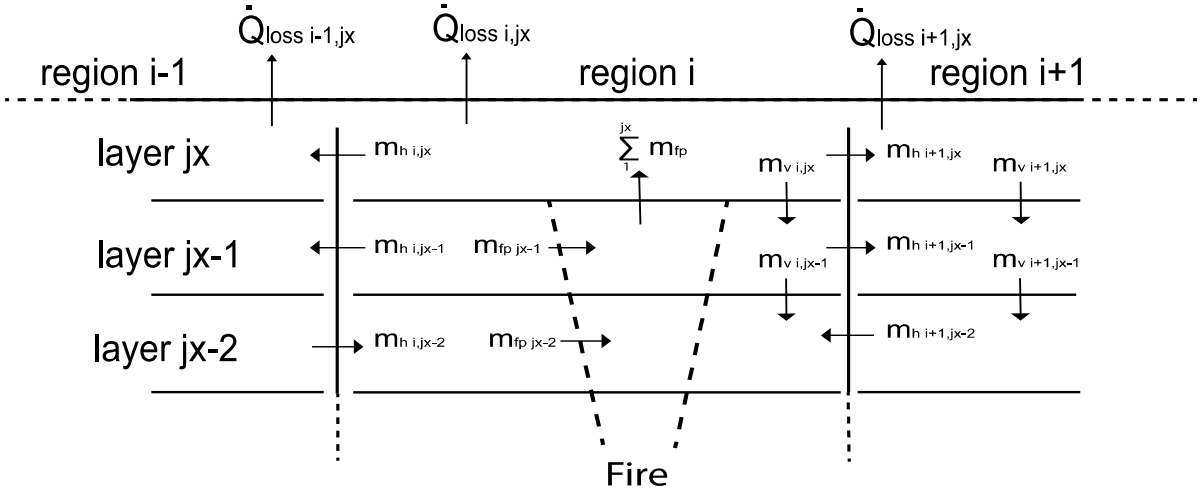

Figure 1. Principles of the multi-zone concept, re-drawn from Suzuki et al (Suzuki et al., 2004).

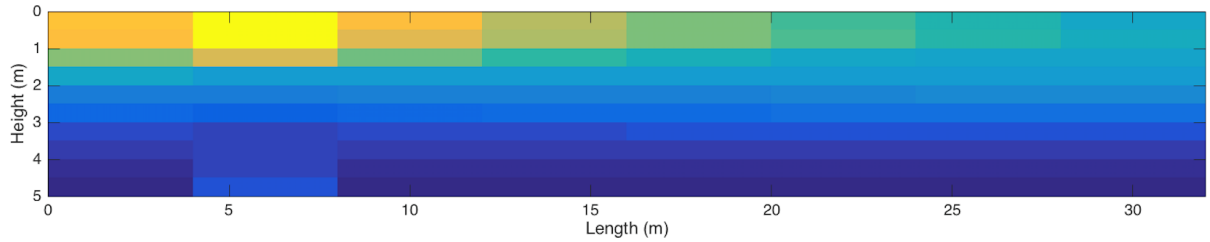

Figure 2. Illustration of results from an example calculation with the Multi-Zone Fire model in a room that is 32x20x5 m. The figure is rendered with MATLAB.

An overview of the most fundamental calculations performed in the MZ Fire model is presented in Section 4.1-4.8.

4.1. Conservation of mass

The conservation equation for mass is as follows:

$$\frac{d}{dt}(\rho_{i,j,k}V_{i,j,k}) = -\dot{m}_{fp,i,j,k} + \dot{m}_{x,i-1,j,k} - \dot{m}_{x,i,j,k} + \dot{m}_{y,i,j-1,k} - \dot{m}_{y,i,j,k} + \dot{m}_{z,i,j,k+1} - \dot{m}_{z,i,j,k} \quad [1]$$

where $\rho_{i,j,k}$, [kg/m^3] and $V_{i,j,k}$, [m^3] are the density and the volume of the *k*-th layer in the region with x-coordinate *i* and y-coordinate *j*, and $\dot{m}_{fp,i,j,k}$ [kg/s] is the mass flow rate entrained into the fire plume in that zone. The horizontal mass flow rate from the (i-1)-th and (j-1)-th region to the i-th and j-th region is represented by $\dot{m}_{x,i-1,j,k}$ and $\dot{m}_{y,i,j-1,k}$ respectively. The horizontal mass flow rate from the k-th down to the (k-1)-th is $\dot{m}_{z,i,j,k}$. The plume mass flow enters the top layer in each fire region; furthermore, there is no layer above the top layer, this means that the conservation of mass for the top layer becomes as follows:

$$\frac{d}{dt}(\rho_{i,j,k\_max}V_{i,j,k\_max}) = \sum_{n=1}^{k\_max-1} \dot{m}_{fp,i,j,n} - \dot{m}_{z,i,j,k\_max} + \dot{m}_{x,i-1,j,k\_max} - \dot{m}_{x,i,j,k\_max} + \dot{m}_{y,i,j-1,k\_max} - \dot{m}_{y,i,j,k\_max} \quad [2]$$

If there is no fire in the region the fire plume entrainment, $\dot{m}_{fp,i,j,k}$, will be zero.

4.2. Conservation of energy

The conservation equation for energy is as follows:

$$\frac{d}{dt}(c_p T_{i,j,k}\rho_{i,j,k}V_{i,j,k}) = -C_p\dot{m}_{fp,i,j,k}T_{i,j,k} + h_{x,i-1,j,k} - h_{x,i,j,k} + h_{y,i,j-1,k} - h_{y,i,j,k} + h_{z,i,j,k+1} - h_{z,i,j,k} - \dot{Q}_{w,i,j,k} + \dot{Q}_{r,i,j,k} \quad [3]$$

where c_p [J/kgK] and $T_{i,j,k}$, [K] is the specific heat and temperature of *k*-th layer in the region with x-coordinate *i* and y-coordinate *j*. The specific heat is calculated for each zone with the following expression, based on normal air properties.

$$c_p = 3\cdot10^{-4}\cdot T_{i,j,k}^2 - 0.1216\cdot T_{i,j,k} + 1014.4 \quad [4]$$

$\dot{Q}_{w,i,j,k}$ [W] in Eq. 3 is the convection heat loss to wall boundaries in contact with the zone and $\dot{Q}_{r,i,j,k}$ [W] is the net radiation heat to the zone. The energy flow, *h*, [W] depends on the direction of the mass flow over the zone boundaries. The vertical energy flow, $h_{z,i,j,k}$, is calculated as:

$$h_{z,i,j,k} = c_p\dot{m}_{z,i,j,k}T_{i,j,k} \quad (\dot{m}_{z,i,j,k} > 0) \quad [5a]$$
$$h_{z,i,j,k} = c_p\dot{m}_{z,i,j,k}T_{i,j,k-1} \quad (\dot{m}_{z,i,j,k} \leq 0) \quad [5b]$$

The horizontal energy flow rate, in the x-direction, $h_{x,i,j,k}$, is calculated as:

$$h_{x,i,j,k} = c_p\dot{m}_{x,i,j,k}T_{i,j,k} \quad (\dot{m}_{x,i,j,k} > 0) \quad [5c]$$
$$h_{x,i,j,k} = c_p\dot{m}_{x,i,j,k}T_{i+1,j,k} \quad (\dot{m}_{x,i,j,k} \leq 0) \quad [5d]$$

The horizontal energy flow rate, in the y-direction, $h_{y,i,j,k}$, is calculated similar as in the x-direction.

The conservation of energy for the top layer is calculated as:

$$\frac{d}{dt}\left(c_p T_{i,j,k\_max}\rho_{i,j,k\_max}V_{i,j,k\_max}\right)=$$

$$=\sum_{k=1}^{k\_max-1} C_p\dot{m}_{fp,i,j,k}T_{i,j,k}+\dot{Q}_{c,i,j}+h_{x,i-1,j,k\_max}-h_{x,i,j,k\_max}+h_{y,i,j-1,k\_max}-h_{y,i,j,k\_max}-h_{z,i,j,k\_max}-\dot{Q}_{w,i,j,k\_max}+\dot{Q}_{r,i,j,k\_max} \quad [6]$$

where, $\dot{Q}_{c,i,j}$ [W] is the convective heat released by the combustion transported to the top layer through the fire plume in the fire region. $\dot{Q}_{c,i,j}$ is zero in non-fire regions.

4.3. Mass flows

Horizontal mass flow in the x-direction, $m_{x,i,j,k}$, [kg/s] is calculated as below.

$$m_{x,i,j,k}=C_d A_x\sqrt{2\rho_{i,j,k}\left(\Delta P_{i,j,k}-\Delta P_{i+1,j,k}\right)} \qquad (\Delta P_{i,j,k}-\Delta P_{i+1,j,k}\geq 0) \quad [7a]$$

$$m_{x,i,j,k}=C_d A_x\sqrt{2\rho_{i,j,k}\left(\Delta P_{i+1,j,k}-\Delta P_{i,j,k}\right)} \qquad (\Delta P_{i,j,k}-\Delta P_{i+1,j,k}<0) \quad [7b]$$

The horizontal mass flow in the y-direction, $m_{y,i,j,k}$, [kg/s] is calculate similar as in the x-direction. The vertical mass flow, $m_{z,i,j,k}$, is solved from the conservation of mass equation (Eq. 1 and 2). $\Delta P_{i,j,k}$ is the pressure difference between the zone and ambient conditions.

4.4. Temperature

Equation 3 can be rewritten as:

$$\frac{d}{dt}\left(c_p T_{i,j,k}\rho_{i,j,k}V_{i,j,k}\right)=C_p\rho_{i,j,k}V_{i,j,k}\frac{dT_{i,j,k}}{dt}+C_p T_{i,j,k}\frac{d}{dt}\left(\rho_{i,j,k}V_{i,j,k}\right) \quad [8]$$

The governing equation for temperature of each zone is derived by substituting Eq. 1 and 3 into Eq. 8 and rearranging, see Eq. 9.

$$\frac{dT_{i,j,k}}{dt}=\frac{1}{c_p\rho_{i,j,k}V_{i,j,k}}\left[h_{x,i-1,j,k}-h_{x,i,j,k}+h_{y,i,j-1,k}-h_{y,i,j,k}+h_{z,i,j,k+1}-h_{z,i,j,k}-\dot{Q}_{w,i,j,k}+\dot{Q}_{r,i,j,k}-C_p T_{i,j,k}\left(\dot{m}_{x,i-1,j,k}-\dot{m}_{x,i,j,k}+\dot{m}_{y,i,j-1,k}-\dot{m}_{y,i,j,k}+\dot{m}_{z,i,j,k+1}-\dot{m}_{z,i,j,k}\right)\right] \quad [9]$$

Substituting Eq. 2 and 6 into Eq. 8 results in the following equation for the top layer.

$$\frac{dT_{i,j,k\_max}}{dt}=\frac{1}{c_p\rho_{i,j,k}V_{i,j,k\_max}}\left[\sum_{k=1}^{k\_max-1} C_p\dot{m}_{fp,i,j,k}T_{i,j,k}-C_p T_{i,j,k\_max}\sum_{k=1}^{k\_max-1}\dot{m}_{fp,i,j,k}+\dot{Q}_{c,i,j}+h_{x,i-1,j,k\_max}-h_{x,i,j,k\_max}+h_{y,i,j-1,k\_max}-h_{y,i,j,k\_max}-h_{z,i,j,kk\_max}-\dot{Q}_{w,i,j,k\_max}+\dot{Q}_{r,i,j,k\_max}-C_p T_{i,j,k\_max}\left(\dot{m}_{x,i-1,j,k\_max}-\dot{m}_{x,i,j,k\_max}+\dot{m}_{y,i,j-1,k\_max}-\dot{m}_{y,i,j,k\_max}-\dot{m}_{z,i,j,k\_max}\right)\right] \quad [11]$$

4.5. Plume entrainment

Plume mass flow is calculated with Heskestad's plume model (Heskestad, 1983).

$$\dot{m}_{fp}=0.071\dot{Q}_c^{1/3}(z-z_0)^{5/3}+1.92\cdot 10^{-3}\dot{Q}_c \quad [12a]$$

$$\dot{m}_{fp}=0.0058\dot{Q}_c\frac{z}{L} \quad [12b]$$

Where $\dot{Q}_c$ is the convective part of the heat release rate, and z_0 is the virtual origin which is calculated with:

$$z_0 = 0.083\dot{Q}^{2/3} - 1.02D \quad [13]$$

The mean flame height, *L*, is calculated with:

$$L = 0.235\dot{Q}^{2/3} - 1.02D \quad [14]$$

The mass flow entrained into the plume in a certain zone, $\dot{m}_{fp,i,j,k}$, is calculated as:

$$\dot{m}_{fp,i,j,k} = \dot{m}_{fp}(z) - \dot{m}_{fp}(z-1) \quad [15]$$

By using the Heskestad equation it is possible to calculate the plume mass flow below the flame height (see Equation 12b). The MZ Fire model will automatically select plume model (12a or 12b) when calculating the mass flow at a certain height depending on the calculated flame height (Equation 14). However, it should be kept in mind that the plume equation is developed from data of pool fires up to a diameter of 2.5 m (Kung and Stavrianidis, 1982) that is assumed to be axisymmetric and not influenced by wind.

4.6. Heat release rate

The user specifies the heat release rate in the input file. The heat release rate can be specified as a growth rate (alfa-t^2) followed by a steady phase, or with a ramp (time and heat release values). The heat release rate is not affected by the surrounding conditions (e.g., radiant heat feedback or oxygen concentration) the user needs to account for that when specifying the heat release rate.

4.7. Heat transfer

Heat is transferred to solid obstructions through convection and radiation, and through 1-D conduction in obstructions. Heat is transferred between zones through the flow of hot gases and radiation.

4.8. Momentum

The driving mechanism behind the transport of smoke in the MZ Fire model is temperature differences between the different zones (Section 4.3). This makes the implementation difficult when momentum forces become important. To account for momentum resulting from when a fire plume hits the ceiling and a horizontal flow created, an empirical ceiling jet model is used (see Equation 16). The ceiling jet velocity is introduced as a hydrodynamic pressure in the model.

$$u = 0.96\left(\frac{\dot{Q}}{H}\right)^{1/3} \quad [16]$$

4.9. New features in the MZ Fire model for tunnel fire risk analysis

The original MZ Fire model (Johansson, 2021) is developed for smoke filling and temperature calculations of large volumes. Several tunnel specific features, which are not included in the original model, have been identified and implemented in this project.

4.9.1. Longitudinal ventilation

Longitudinal ventilation exists in tunnel to limit traffic emission during normal operation and to control movement of smoke in case of fire. Consequently, the possibility to account for the longitudinal gas velocity is important when analysing fire safety in tunnels. Therefore, a feature to include longitudinal ventilation is included in the MZ Fire model.

The feature is applied on the boundary of the simulated domain (e.g., tunnel openings, see Figure 3) as a gas velocity entering or leaving a vent. The gas velocity can be set as transient (i.e., time-dependent) with the help of a ramp-function.

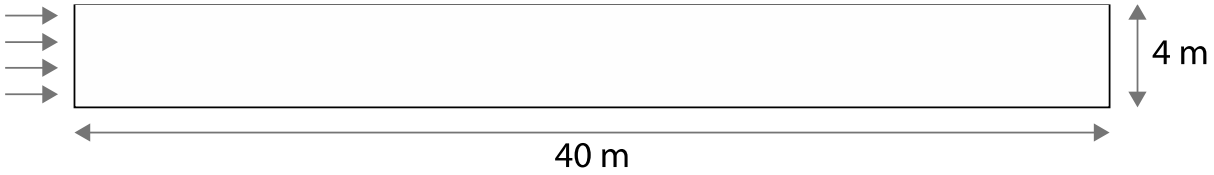

Figure 3. Visualisation of how longitudinal ventilation is applied from the left side of this 40 m long and 4 m hight tunnel.

A demonstration of the use of longitudinal ventilation is presented in Chapter **Error! Reference source not found.**.

4.9.2. Tunnel gradient

The hydrostatic pressure difference between two tunnel openings located at different elevations will cause a so-called chimney effect and affect the flow of smoke in case of fire. The gradient and the length of the tunnel both have a large effect on the pressure difference. So, a tunnel gradient feature is included in the MZ Fire model. This is done by modifying the height of each region (see Figure 4). The feature allows the possibility to set a uniform tunnel gradient in one-direction in the tunnel.

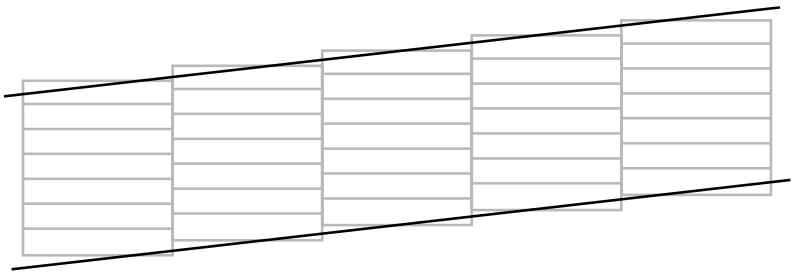

Figure 4. Visualisation of how each region is displaced in order to account for the tunnel gradient.

A demonstration of the use of using the gradient function is presented in Chapter 6.1.

4.9.3. Vertical cross-section

Obstructions in the original MZ Fire model are modelled as 2-D planes that are placed on zone boundaries. This means that the vertical cross-section needs to be rectangular. The cross-section in tunnels will seldom be rectangular, instead the ceiling is often curved. The shape of the cross-section can have great influence the movement of smoke in tunnels and a feature to account for non-rectangular cross-sections is therefore included in the MZ Fire model. The main principle of the feature is that 3-D obstructions, which fill up only a part of the zones, can be included (see Figure 5). When applying the feature, it is important not to overlap the 3-D obstructions.

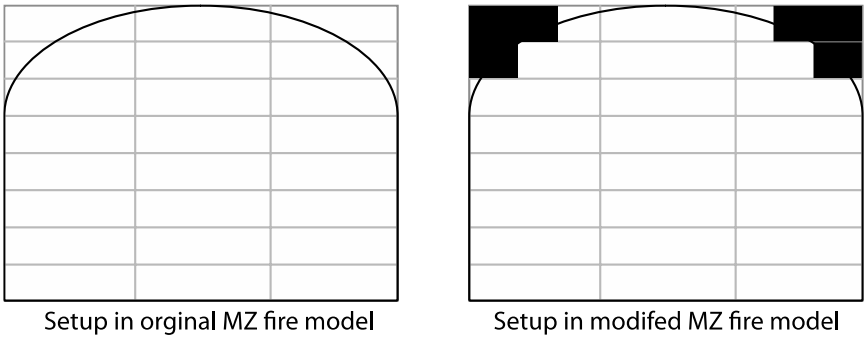

Figure 5. Visualisation of the original model (left) and how obstructions can be taken to a non-uniform cross-section (right).

A demonstration of the use of non-uniform cross-sections is presented in Chapter 6.3.

4.9.4. Smoke density

The original MZ Fire model does not allow for smoke density as an output. This is now included in the modified version of the model.

5. Benchmark testing

As any other model or simulation tool, the reliability of the data produced must be evaluated with a dedicated set of tests. In this context, verification is often intended as the process of making sure that the conceptual or mathematical implementation of a given model is correctly performed for the given type of application of the tool (International Standards Organization, 2014). Validation is performed to evaluate that the results produced by the model match with the expected phenomenon in the real world (International Standards Organization, 2014). Once different versions of a tool are released, it is therefore necessary to make sure that the tool perform as expected. This practically means that verification and validation tasks should not be considered as a one-time effort for tools involving simulations, but rather an ongoing process which should be performed along with software development.

Given the implementation of the updated MZ model within ARTU, it was therefore deemed necessary to perform a set of benchmark testing to evaluate the predictive capabilities of MZ in comparison to both experimental data as well as other modelling tools. It was decided to compare the MZ results against a more refined CFD tool, the Fire Dynamics Simulator (FDS), version 6.7.4 (McGrattan et al., 2021).

5.1. Testing with the BeNeLux tunnel fire tests

The BeNeLux tunnel consists of six bores, is 840 m long and runs under the New Meuse River outside Rotterdam. The slope gradient is 4.4 %, with the lowest point located in the middle of the tunnel. In 2000 and 2001, fourteen full-scale fire tests were performed in the tunnel. The fire tests were performed in a bore for road traffic with a width of 9.85 m, and the test site was located 265 m from the northern portal. The ventilation system was in the south part, and the measurements were performed from 50 m upstream to 200 m downstream of the fire. In this study five of the full-scale tests as used for benchmarking, these were selected since they have been used since they recently were used for another benchmark study at Lund University (Sandin et al., 2019). A summary of the ventilation and fire conditions in the five tests are presented in Table 1, and the HRR curves from the five tests are presented in Figure 6.

Table 1. Type of ventilation and fire in the five BeNeLux tests used in the report.

Test	Ventilation	Type of fire	Max HRR (MW)
6	Natural ventilation	Car	5
7	Longitudinal ventilation max 6 m/s	Car	5
8	Natural ventilation	Canvas covered wooden pallets	20
9	Longitudinal ventilation max 6 m/s	Canvas covered wooden pallets	20
14	Longitudinal ventilation max 1 m/s	Wooden pallets	25

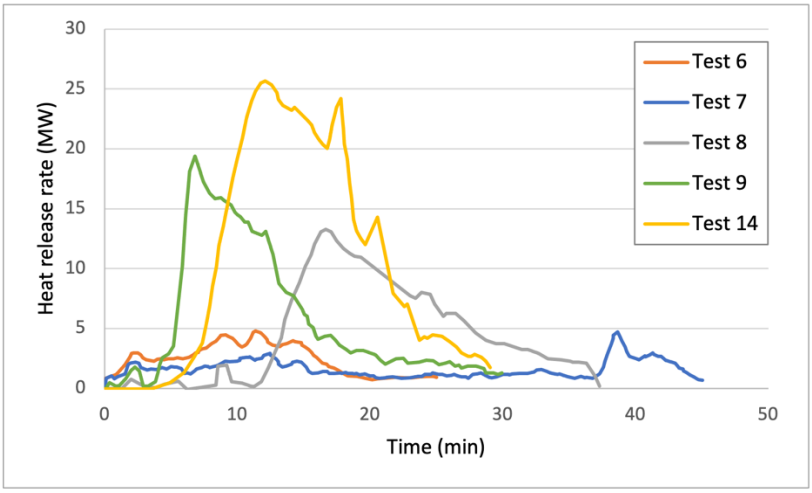

Figure 6. Measured HRR in the five BeNeLux tests used in the report.

Experimental data on temperatures at 1 and 2 m above the floor is available for test 6, 8 and 9. A comparison calculated of average gas temperatures with the MZ Fire model and FDS at increasing distanced from the fire sources is presented for test 6 (Figures 7 and 8) and for test 9 (Figures 9 and 10) below. The full results for all five studied tests are available in Appendix A.

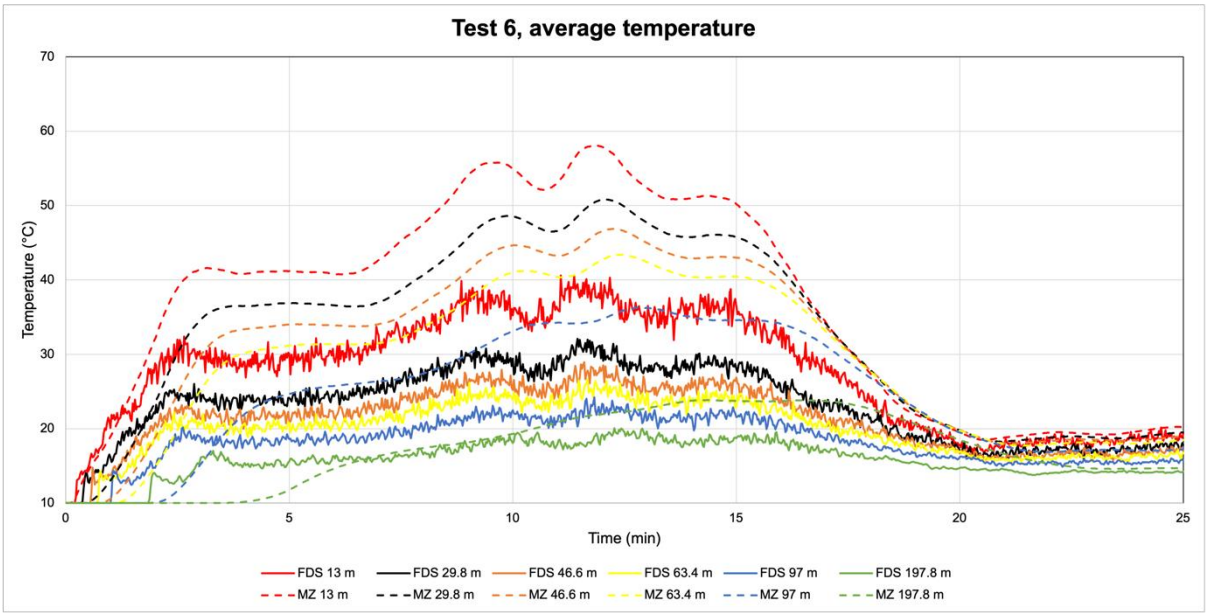

Figure 7. Average cross section temperature calculated with FDS and MZ at different positions from fire source test 6.

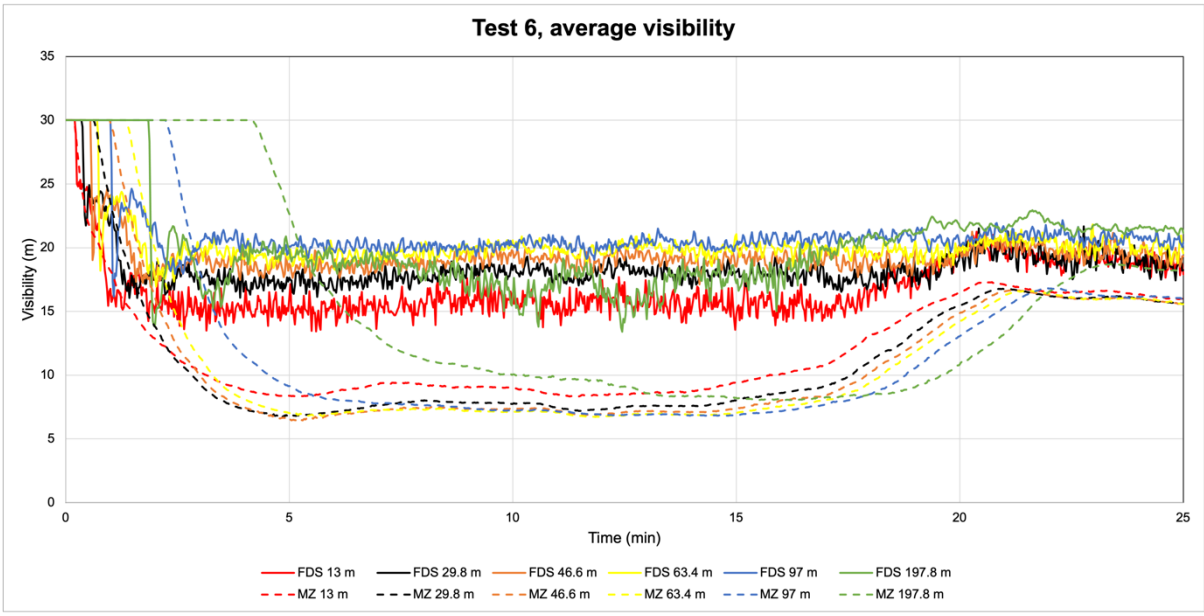

Figure 8. Average cross section visibility calculated with FDS and MZ at different positions from fire source test 6.

The overall correspondence between FDS and MZ is considered good for test 6. The average cross-section temperatures are higher in MZ (see Figure 7). However, at larger distance from the fire (> 100 m) the temperature increase is slower with the MZ Fire model. The average cross section visibility is in general worse in MZ than in FDS (see Figure 8), but as for the temperature the travel time for the gases is longer in MZ than FDS. The experimental gas temperature (average of 1 and 2 m height) is predicted rather well with MZ except at 200 m, where it is underpredicted (see Appendix A).

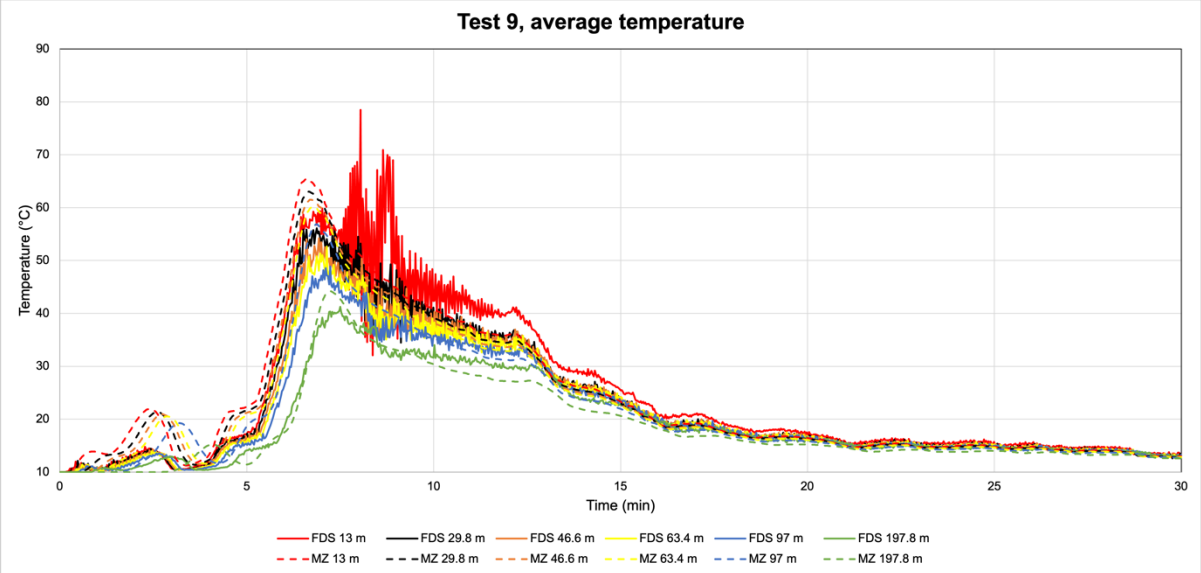

Figure 9. Average cross section temperature calculated with FDS and MZ at different positions from fire source test 9.

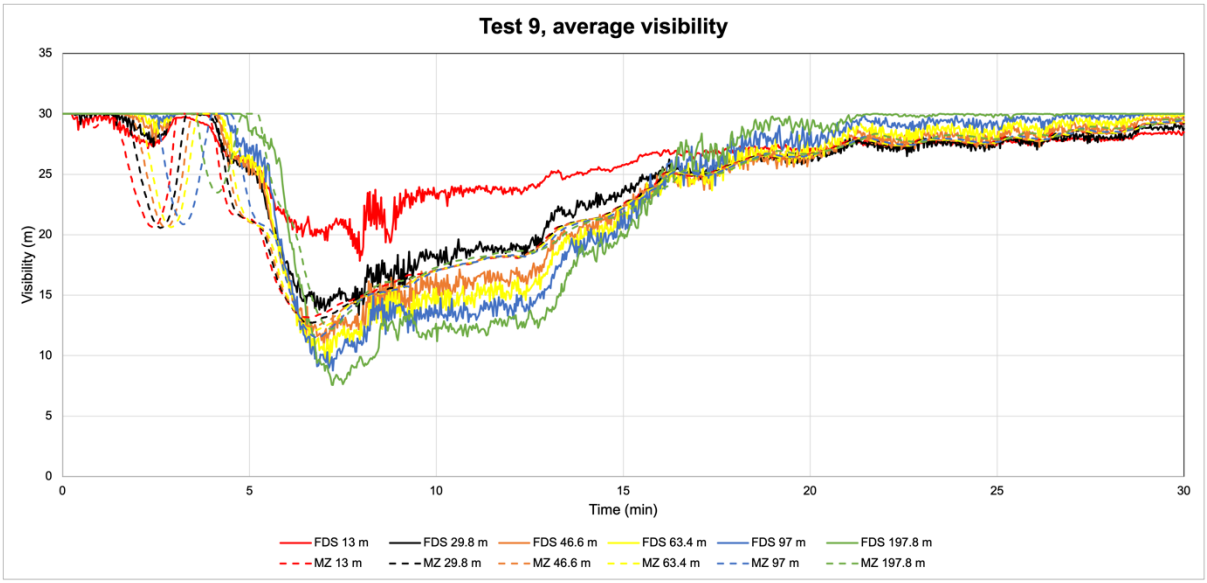

Figure 10 Average cross section visibility calculated with FDS and MZ at different positions from fire source test 9.

The overall correspondence between FDS and MZ is considered good for test 9 (see Figure 9 and Figure 10). The upper temperatures are in general overpredicted, while the lower temperatures are underpredicted compared to FDS (see Appendix A). Regarding visibility the MZ model gives conservative predictions compared to FDS. Compared to experimental results are the lower temperatures (at 1-2 m) underpredicted by MZ (see Appendix A).

5.2. Testing with the Runehamar tunnel fire tests

It has been shown that the HRR from tunnel fires can exceed those tested in the BeNeLux fire tests significantly (NFPA, 2017; PIARC, 1999) and design fires reported are in the order of 4-200 MW (CETU, 2010). Therefore, to complement the Benelux tunnel fire test, data from the Runehamar tunnel fires tests (Ingason et al., 2015a) were used in the benchmark exercise.

The Runehamar tunnel fire tests were conducted in Norway in 2003. The tunnel had a total length of around 1600 m and the fire was positioned in a downhill slope about 530 m from the west portal (see Figure 11). A total of five large-scale fire tests and benchmarking against one of these tests (Test T1) is performed in this report. Test T1 was selected since this test included the highest HRR and it has been well described in previous studies (Li et al., 2012).

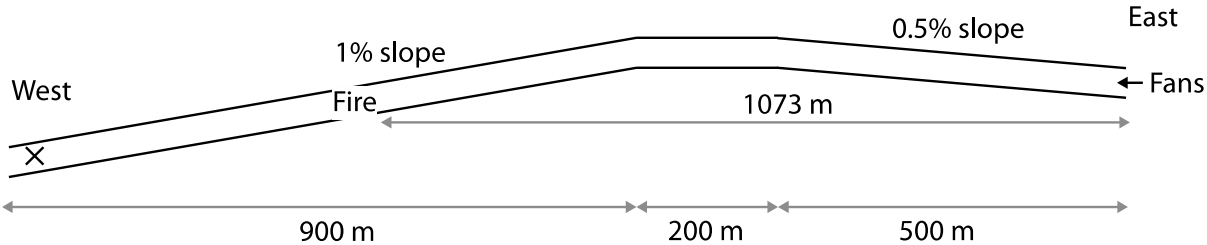

Figure 11. The Runehamar tunnel. Measurements were primarily made at the "x" located 458 m west of the fire.

The fire load in Test T1 consisted of wood and PE plastics that comprehended a total of around 11 tones. The HRR, which was estimated using the oxygen consumption method, reached a maximum of 205 MW (see Figure 12) after 18.3 minutes.

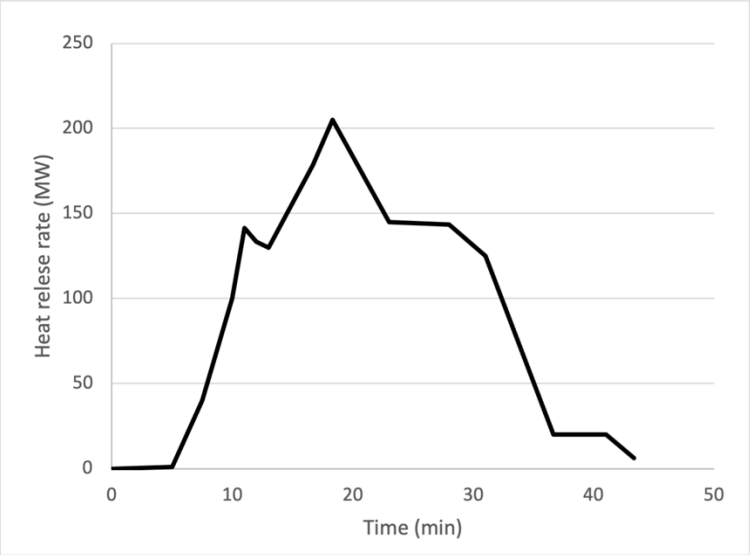

Figure 12. Heat release rate in the Runehamar test T1.

The result from the benchmarking is presented in Figure 13 to 15.

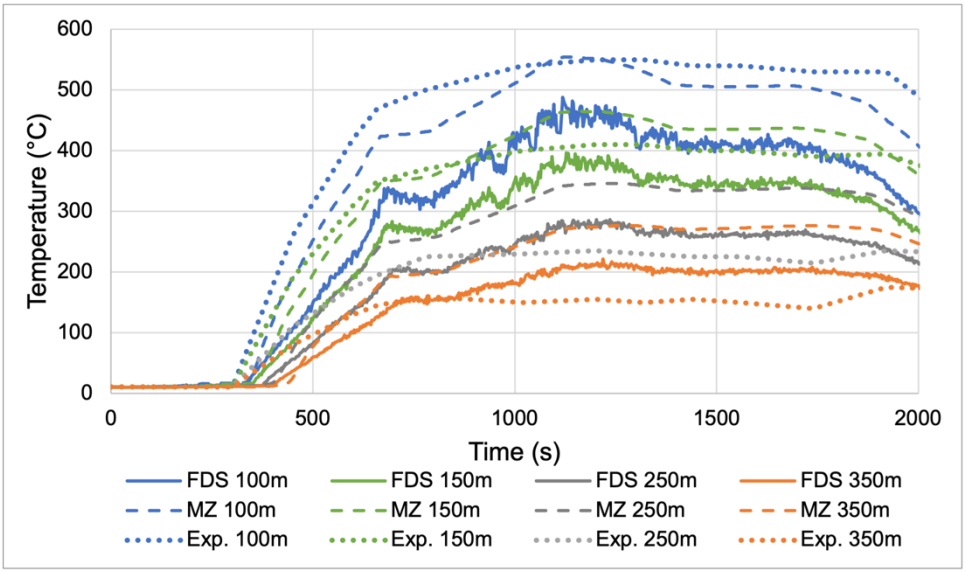

Figure 13. Gas temperatures 458 m west of the fire.

At 458 m west of the fire both the MZ Fire model and FDS overpredicts the temperatures in the simulations. One reason for this overestimation is most likely uncertainties in the inputs related to the heat transfer to the boundaries and the fact that no account was taken to the construction (fire protection boards) that was in place at the location of the fire to protect the tunnel in the experiment. Another possible reason is the very large HRR which is challenging to capture in the simulation models. However, in this case both simulation models produce conservative results.

When comparing results from the MZ Fire model and FDS, MZ predicts a higher temperature closer to the ceiling, while FDS predicts higher temperatures than MZ at lower levels. The average temperature over the height is however similar.

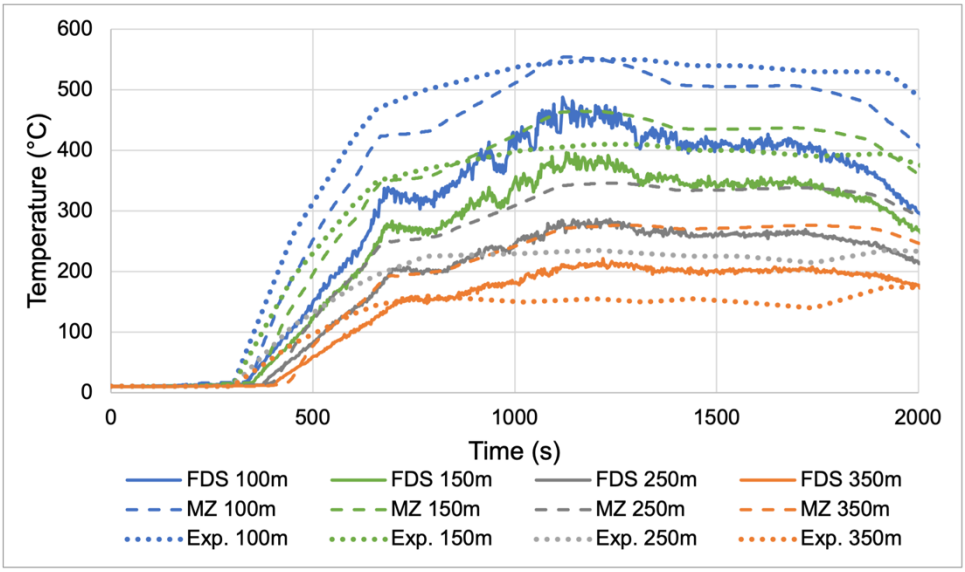

Figure 14. Ceiling gas temperatures at different distances from the fire.

The ceiling jet temperatures closer to the fire source (100-150 m) are predicted well by the MZ Fire model, while the temperatures further away (250+ m) are overpredicted, this is in line with the results in Figure 13.

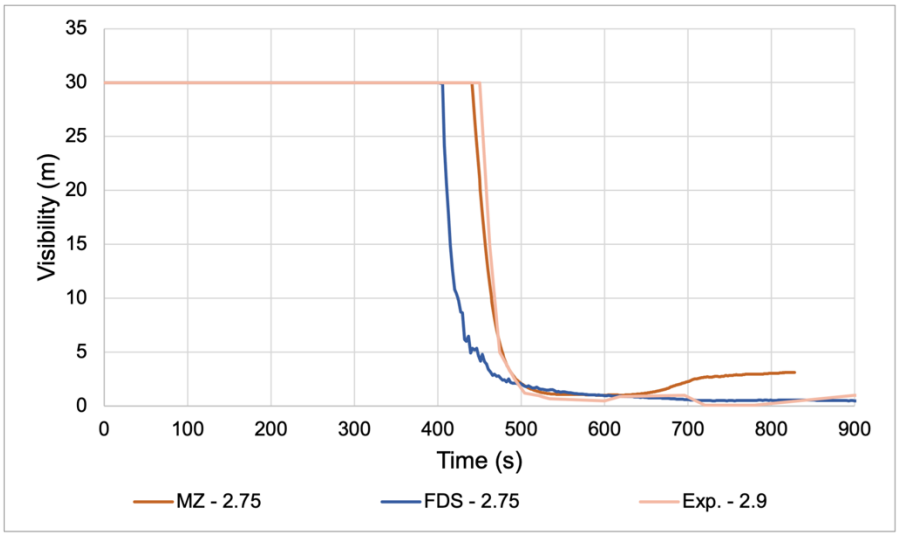

Figure 15. Visibility 458 m west of the fire.

The visibility in the MZ Fire model at 458 m from the fire and at an elevation of 2.75 m corresponds well to the experimental data in Figure XX. FDS results in slightly more conservative values as a visibility of 10 m is reached about 60 seconds prior to what was seen in the experiment.

6. Demonstration of the features

A 40 m long, 12 m wide and 4 m high tunnel (see Figure 16) is used to demonstrate the three features: longitudinal ventilation, tunnel gradient and vertical cross section. The fire source is located 18 m from the left portal and a total heat release rate of 4,000 kW. The left and right portals are modelled as opened vents (except when longitudinal ventilation is studied). In each one of the cases the vertical cross section temperature is presented after 600 seconds at three different positions (A, B and C).

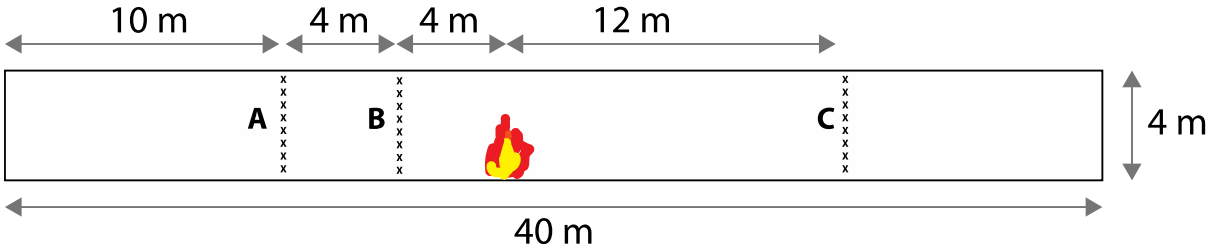

Figure 16. Scenario used in the demonstration of features.

6.1. Longitudinal ventilation

The tunnel presented in Figure 17 is used in a test of influence of longitudinal ventilation. Three different ventilation velocities (0 m/s, 2 m/s and 4 m/s) entering from the left portal (see Figure 17) are simulated and compared. The right portal is modelled as an open vent. The result from the study is presented as a vertical temperature and obscuration profiles at positions A, B and C after 600 seconds in Figures 18 to 20.

Figure 17. Scenario used in the demonstration of the longitudinal ventilation feature.

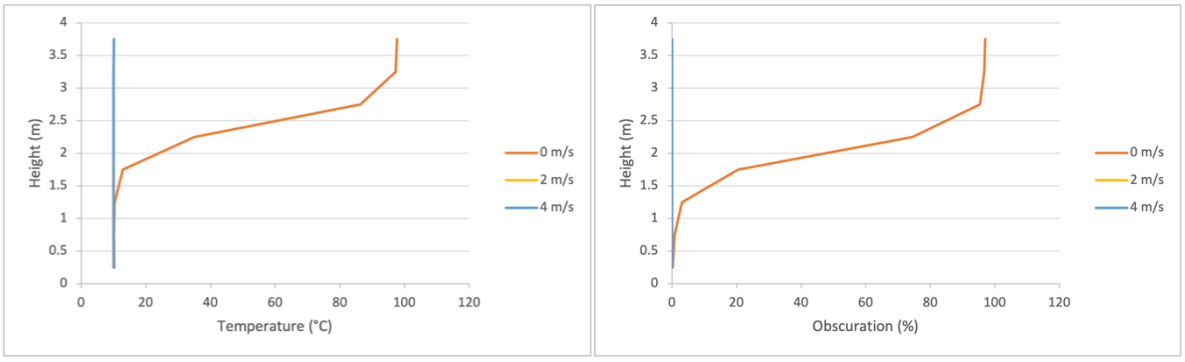

Figure 18. Temperature (left) and obscuration (right) at 10 m (A) in the analysis of longitudinal ventilation.

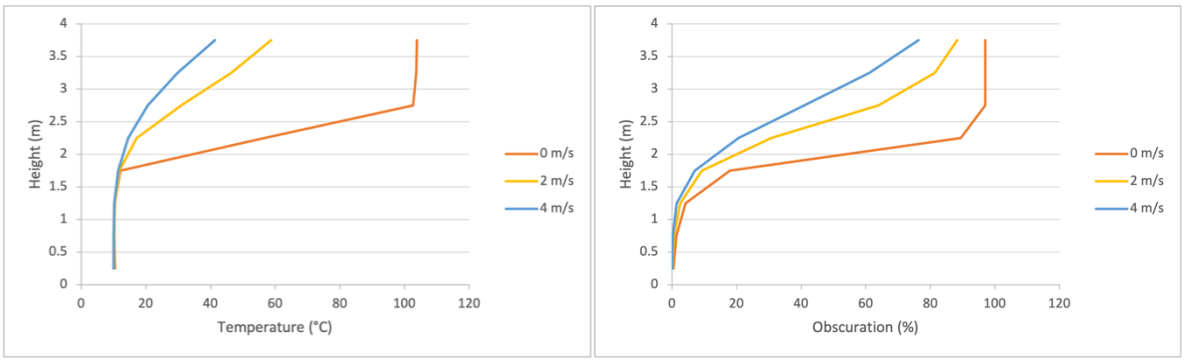

Figure 19. Temperature (left) and obscuration (right) at 14 m (B) in the analysis of longitudinal ventilation.

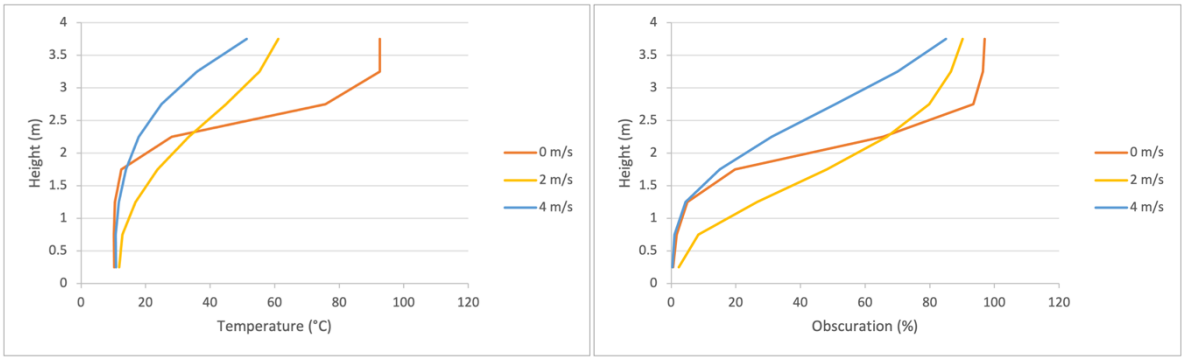

Figure 20. Temperature (left) and obscuration (right) 30 m (C) in the analysis of longitudinal ventilation.

The longitudinal ventilation velocities of 2 and 4 m/s will prevent backlayering to position A. This is anticipated and can be seen in Figure 17. Some backlayering will occur to position B but the gas temperature will be much less than when there is no longitudinal ventilation (see Figure 18). Upstream the fire (position C) temperatures will decrease with increasing velocities (see Figure 19) probably due to a higher airflow. The airflow will also affect the obscuration and thus also the visibility. The obscuration is affected on slightly lower levels compared to the temperature (e.g., in Figure 18 it can be seen that the temperature is not affected below 1.5 m, but there is a slight influence on the obscuration at this level).

6.2. Tunnel gradient

The tunnel presented in Figure 20 is used in a test of influence of a gradient in the tunnel. Three different uniform tunnel gradients are demonstrated (0°, 2.5° and 5°) as schematically presented in Figure 21. The result from the study is presented as a vertical temperature profile at positions A, B and C after 600 seconds in Figures 22 to 24.

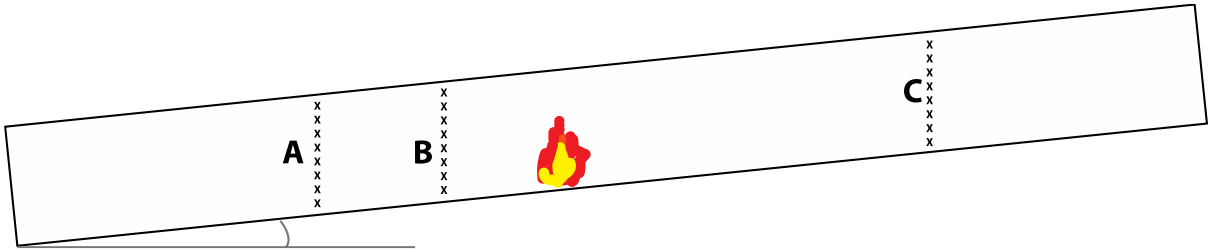

Figure 21. Scenario used in the demonstration of the tunnel gradient function.

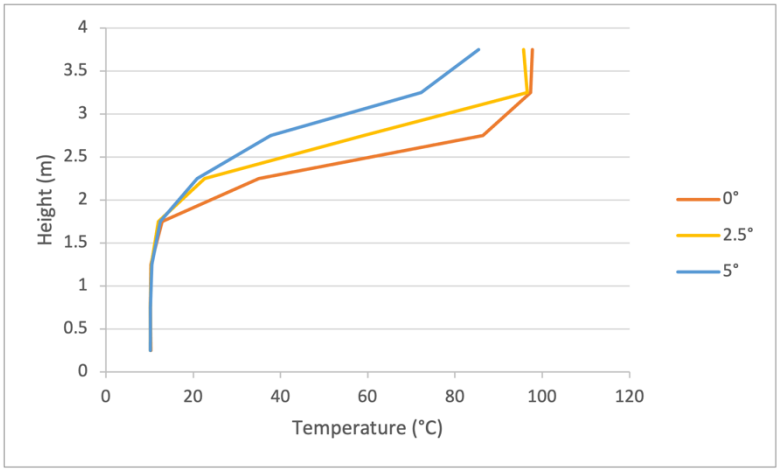

Figure 22. Temperature at 10 m (A) in the analysis of tunnel gradient.

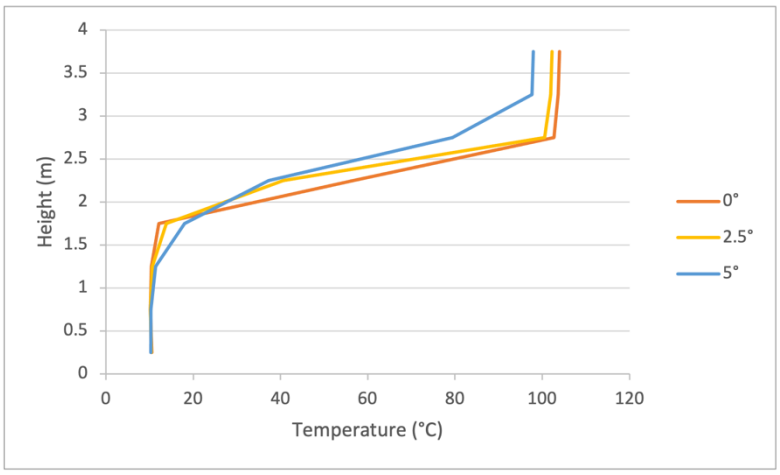

Figure 23. Temperature at 14 m (B) in the analysis of tunnel gradient.

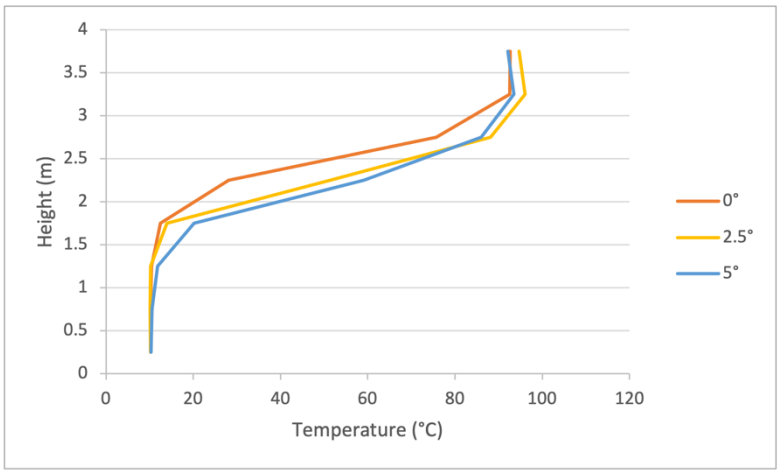

Figure 24. Temperature at 30 m (C) in the analysis o of tunnel gradient.

An increasing tunnel gradient will decrease the backlayering as can be seen at positions A and B (see Figure 22 and Figure 23). Upstream the fire (position C) an increasing gradient will cause a slightly higher temperature but also a lower height to the smoke layer (see Figure 24).

6.3. Vertical cross section

The tunnel presented in Figure 16 is used in a test of influence of reducing the vertical cross section. Three different vertical cross sections are demonstrated (see Figure 25). The cross sections in Scenario 1 and Scenario 2 are covered by obstructions to 15% and 8.33% respectively, compared to the base case. Scenario 1 is 3.6 m heigh, while Scenario 2 has the full height. The result from the study is presented as a vertical temperature profile at positions A, B and C after 600 seconds in Figures 26 to 28.

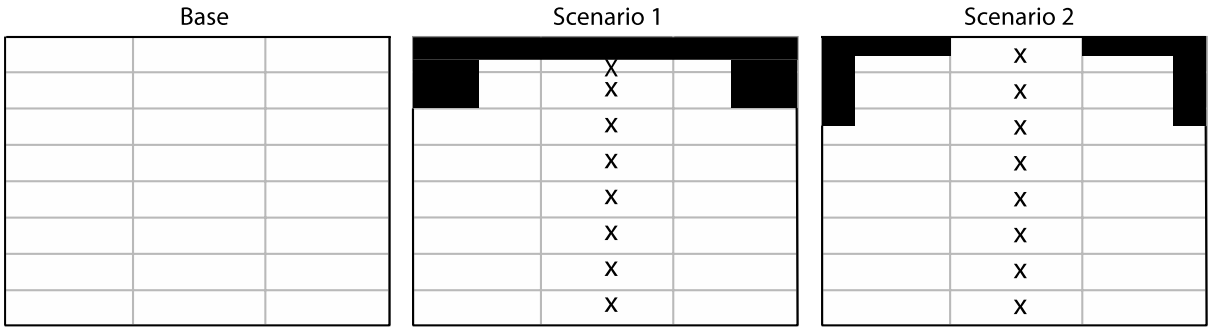

Figure 25. Three different vertical cross-sections tested (x – marks the position of temperature measurements. .

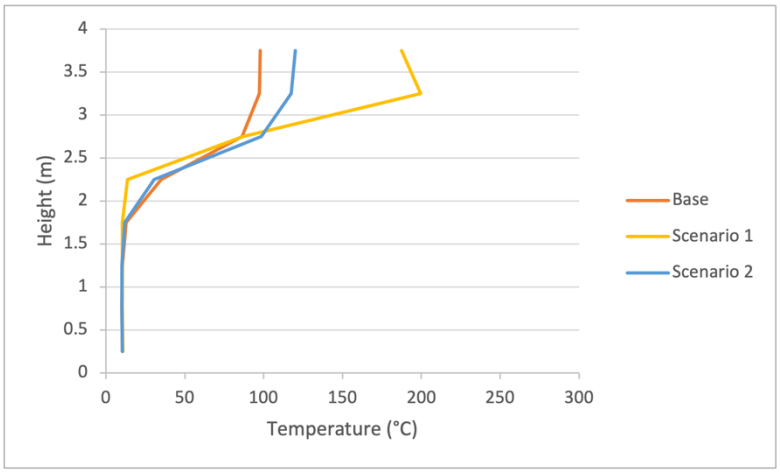

Figure 26. Temperature at 10 m (A) in the analysis of reduced vertical cross section.

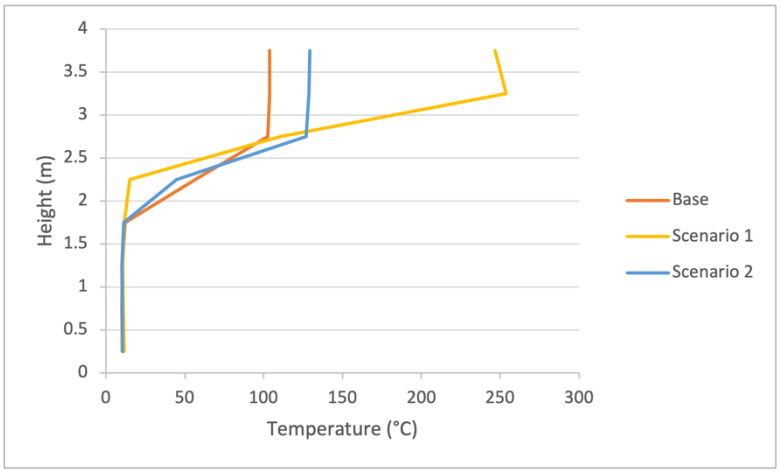

Figure 27. Temperature at 14 m (B) in the analysis of reduced vertical cross section.

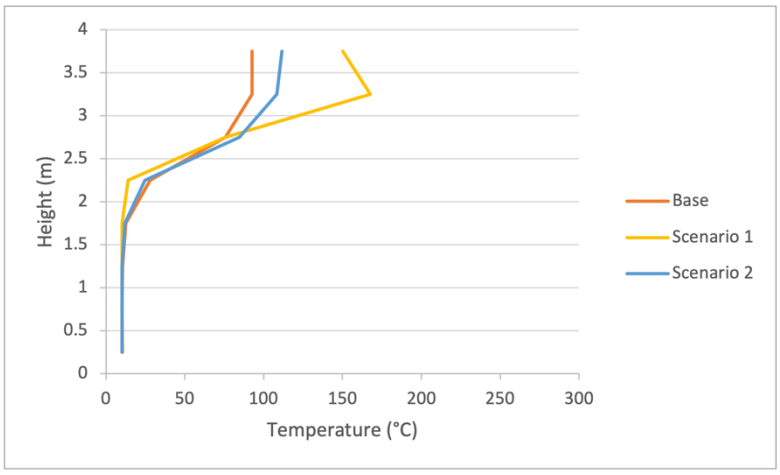

Figure 28. Temperature at 30 m (C) in the analysis of reduced vertical cross section.

A reduction of the cross section will increase the gas layer temperature under the ceiling as can be seen in Figures 26 to 28. The temperature in Scenario 1 will be higher than Scenario 2 because the volume is reduced more in Scenario 1. The higher temperature will cause the larger density differences compared to the ambient air and this will increase the gas velocity. This is probably the reason for that the hot gas layer is descending further down in Scenario 1 and 2.

7. Sensitivity analysis of zone size

A 120 m long, 12 m wide and 4 m high tunnel (see Figure 29) is used in a test of influence of zone size on gas temperature and visibility. The fire source is located 18 m from the left portal and a total heat release rate of 8,000 kW. The left and right portals are modelled as opened vents.

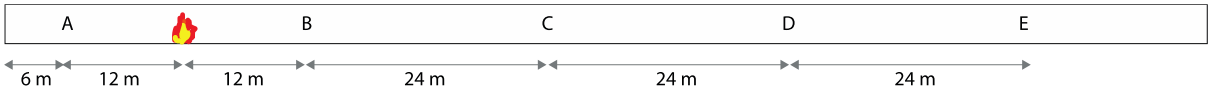

Figure 29. Scenario used in the zone size sensitivity analysis.

Three different zone lengths (in the direction of the tunnel length) are studied (4, 8 and 12 m). The zone width and height are kept constant. The division into zones in the x-direction is illustrated in Figure 30, black is the 4 m zone, red is the 8 m zone, and green is the 12 m zone.

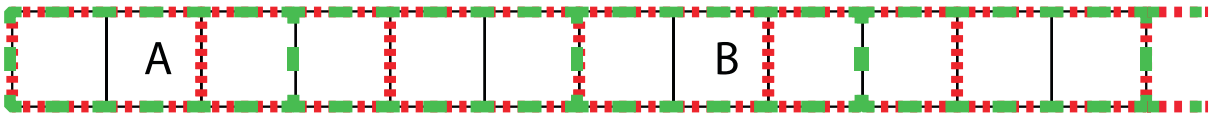

Figure 30. Scenario used in the zone size sensitivity analysis.

The vertical temperature and obscuration are presented after 600 seconds at five different positions (A, B, C, D and E) in Figures 31-35.

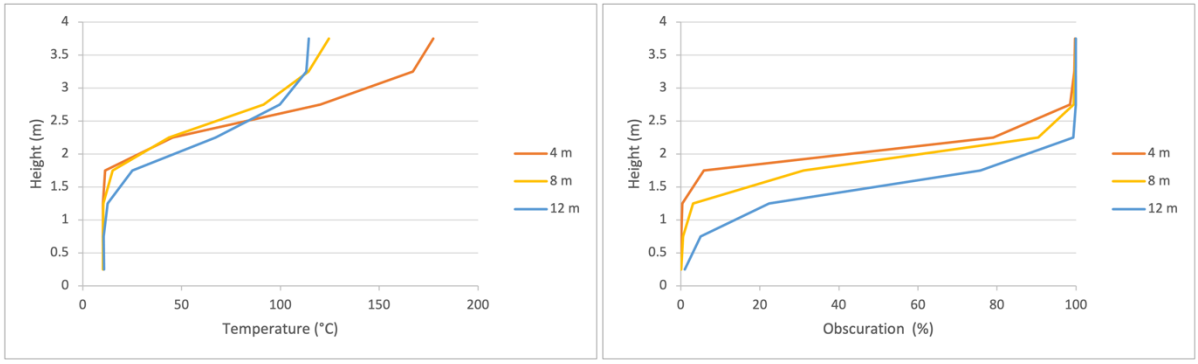

Figure 31. Temperature (left) and obscuration (right) at 6 m (A) in the zone size sensitivity analysis.

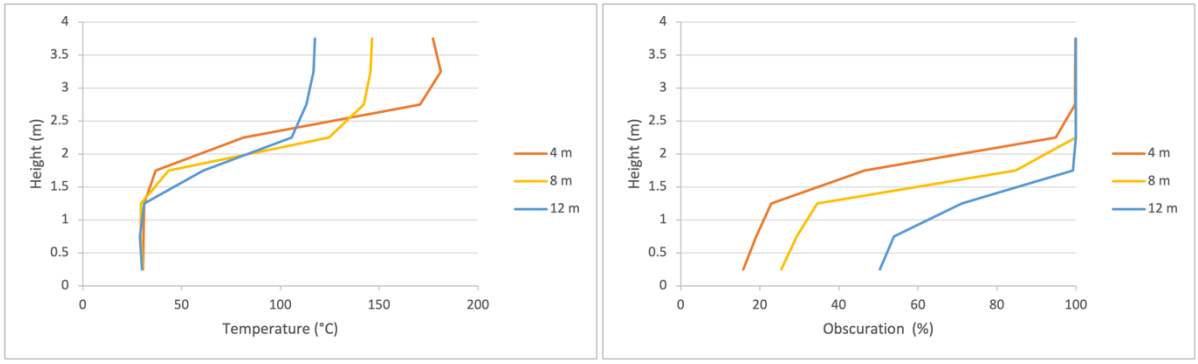

Figure 32. Temperature (left) and obscuration (right) at 30 m (B) in the zone size sensitivity analysis.

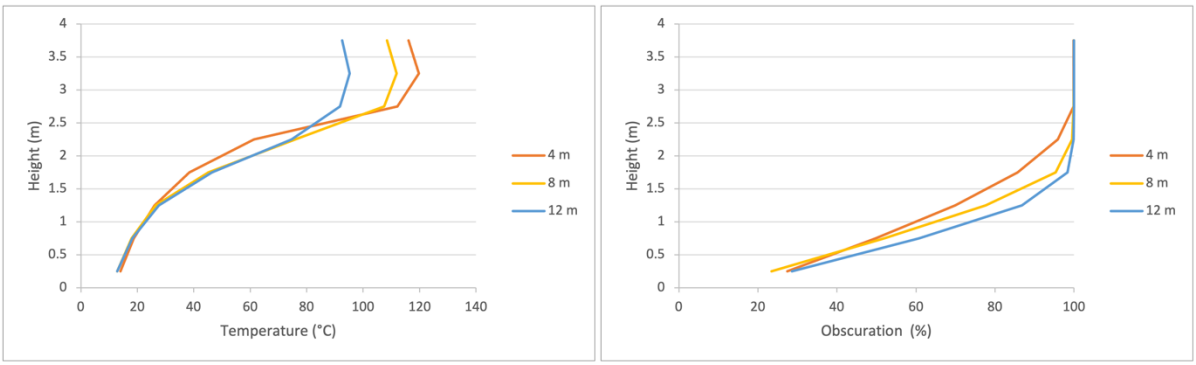

Figure 33. Temperature (left) and obscuration (right) at 54 m (C) in the zone size sensitivity analysis.

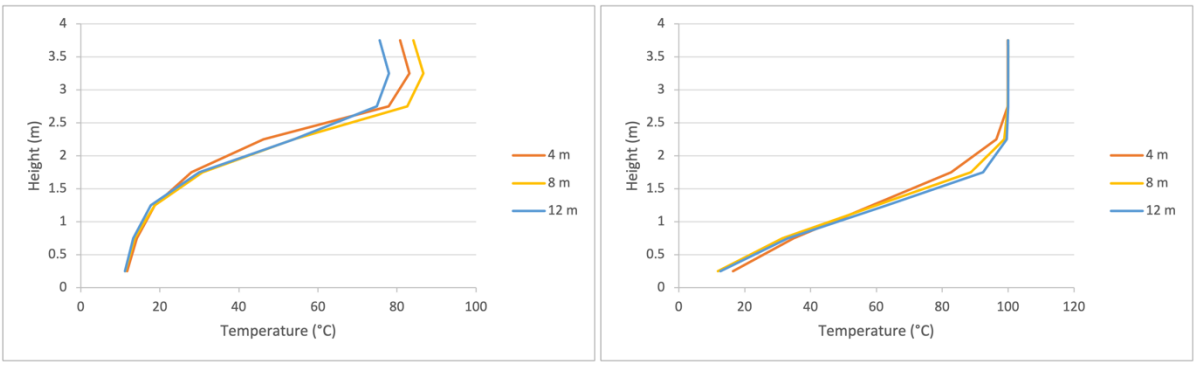

Figure 34. Temperature (left) and obscuration (right) at 78 m (D) in the zone size sensitivity analysis.

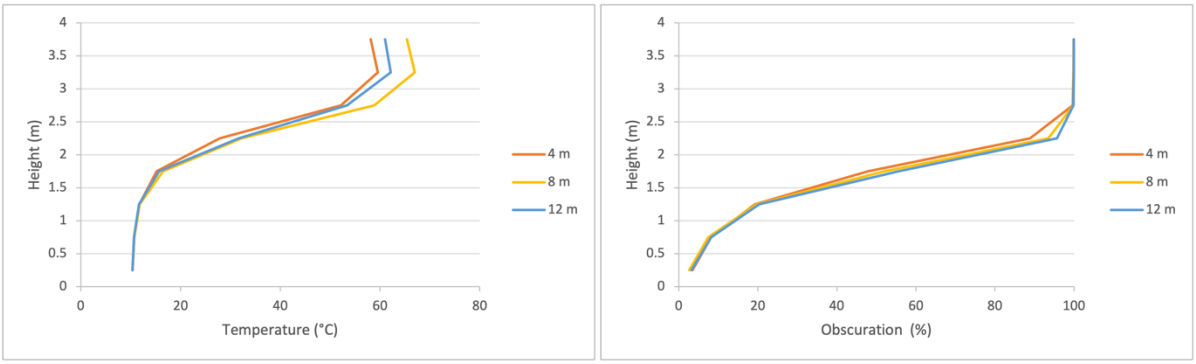

Figure 35. Temperature (left) and obscuration (right) at 102 m (E) in the zone size sensitivity analysis.

The difference in temperature is partly due to that the larger the zone, the more averaged will the temperature be. However, from Figure 31 to Figure 35 it can be seen that the zone size dependence is reduced further away from the fire and at a distance of 100+ m it is rather small. Closer to the fire source the zone size seems to be more important, however the differences that can be seen between the different zone sizes close to the fire (Figure 31 and Figure 32) are not propagated to the more distant zones.

The time dependent temperature and obscuration at 1.75 m above the floor are presented at three different positions (A, C and E) in Figures 36 to 38.

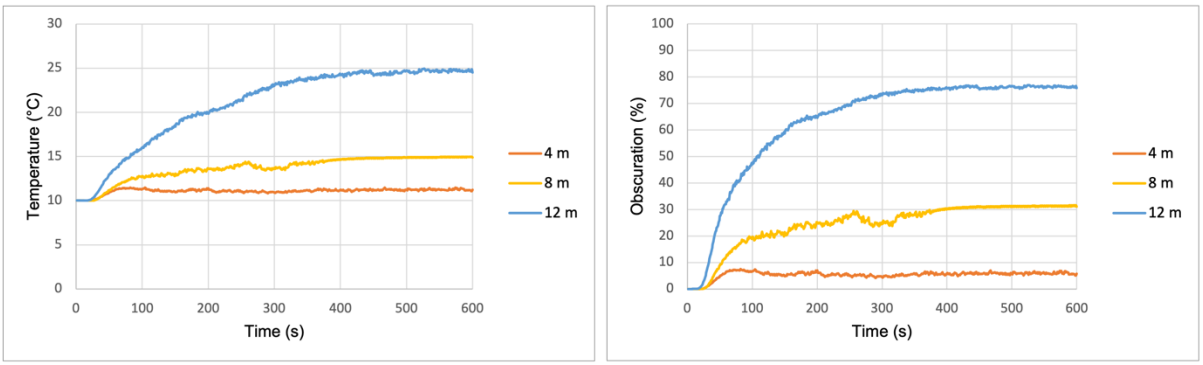

Figure 36. Time dependence of temperature (left) and obscuration (right) 1.75 m above the floor at 6 m (A) in the zone size sensitivity analysis.

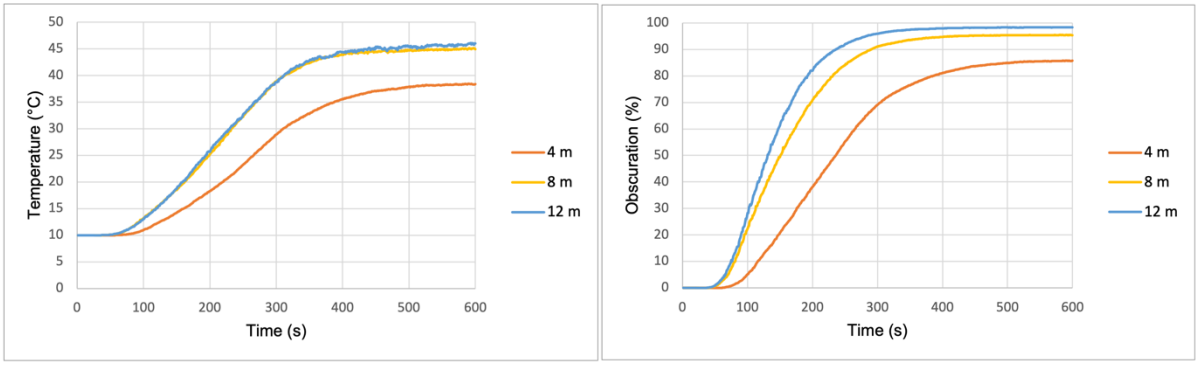

Figure 37. Time dependence of temperature (left) and obscuration (right) 1.75 m above the floor at 54 m (C) in the zone size sensitivity analysis.

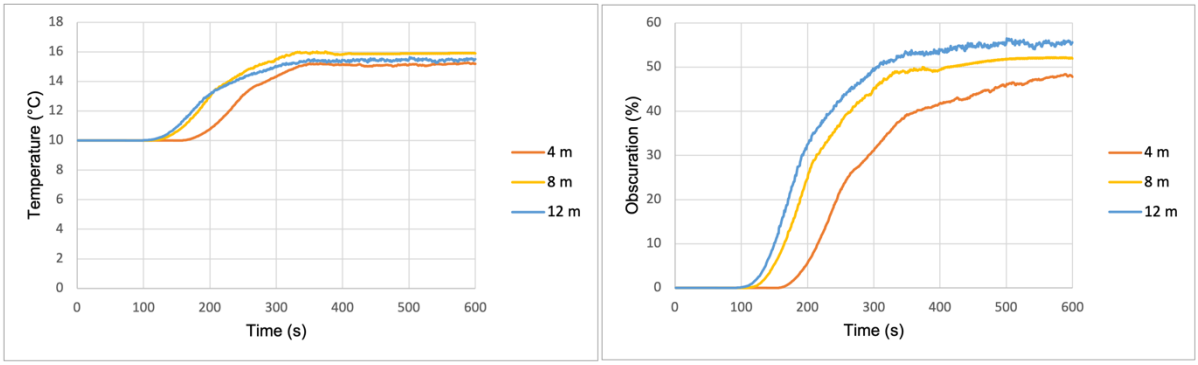

Figure 38. Time dependence of temperature (left) and obscuration (right) 1.75 m above the floor at 102 m (E) in the zone size sensitivity analysis.

From the time dependent results (Figures 36 to 38) the zone size will influence the transport time of the fire effluents. A larger zone will decrease the transport time, and thus create a more conservative results regarding calculating time to untenable conditions for people. However, there will possibly be a larger error within the zone if a comparison would be made to a more detailed model since the output is an average over the entire zone.

8. Domains of application of MZ for tunnel fire risk analysis

The MZ fire model is developed primary for smoke filling and gas temperature calculations in large volumes in buildings, and the model has proven to be able to predict the fire conditions in such environments well (Johansson, 2021).

Fire dynamics in tunnels are different than the case of buildings. The fire can be very large in size, and it will cause a large momentum in the flow. The driving mechanism behind the transport of smoke in the original MZ fire model is temperature differences between the different zones. This makes the implementation difficult when momentum forces become important. To overcome this problem the momentum right above the fire plume have been compensated for by introducing the hydrodynamic pressure caused by the ceiling jet (see Equation 16).

Other additional features have been added to adapt the MZ Fire model for use in tunnels in this work. One of these features is the possibility to take some account of the tunnel cross being non-uniform. The feature is based on a reduction of the zone volume in zones where 3D-obstructions are placed. This means that other effects that might be due to differences in heat transfer or plume entrainment due to reduced tunnel height is not accounted for.

Other issues relate to the modelling of the fire and the fire plume. The fire plume applied in the model (see Section 4.5) is based on empirical data for pool fires up to a diameter of 2.5 m. This is much smaller than many of the design fires used in tunnels. The plume is also assumed to be axisymmetric which means that no account is taken to the influence of the longitudinal ventilation flow on the shape or bending of the flame and plume. These issues will most likely add uncertainties to the MZ fire model results close to the fire (< 50 m).

The Benchmarking against the BeNeLux tunnel fire tests is satisfying on an overall level. Some reasons for concern should be raised when the longitudinal velocity is high (e.g. as in BeNeLux Test 9 where it was 6 m/s), in such cases it seems like the MZ fire model will underpredict the smoke decent and consequently the temperature and visibility at lower levels.

The MZ fire model generally performs well for heat release rates in the magnitude of 5-20 MW and in the range of 50-200 m from the fire. It is harder to evaluate the model for higher HRR:s due to the lack of data, but the results for the benchmarking against Runehamar tests indicate that the MZ model will result in higher temperatures closer to the ceiling and lower temperatures at lower levels, compared to FDS. However, in this case both FDS and the MZ fire model gave in general more conservative estimates comparted to the experiment, which indicates that simulate large heat release rates (100MW) in confined space is challenging regardless the modelling technique (zone or field model).

The zone size should vary with the size of the fire. In previous studies (Johansson, 2021) a zone of 4 m x4 m has been used and found reasonable for fire safety analysis in buildings when the fire is well within the 16 m^2 of the zone. A zone height of 0.5 m has also been seen to be reasonable. However, in the sensitivity analysis of the zone size it was seen that there were only small effects on temperature and visibility in the far field (> 100 m) when the zone length was increase by a factor of 2-3 for an 8 MW fire. Where the so-called far field is located depends on studied scenario, for example a large fire will probably extend the far field.

All in all, it can be stated that the MZ fire model (version MZ_tunnel_0) is considered to be applicable for tunnels to study conditions in the range of 100-200 m from tunnel fires sizes up to a size of 20 MW. This suggest that the use of MZ is particularly suitable in the first phase of fire, when the released power from the fire is in this order of magnitude. For larger fires there are indications that the model works well, especially for gas temperatures underneath the ceiling.

9. Discussion

The MZ Fire model provides an alternative modelling concept to simple one-dimensional models and the more advanced CFD models. The strength of the MZ Fire model compared to the simpler models is that it is possible to get the vertical and horizontal distribution of e.g., temperature and visibility in the simulated domain. Regarding more advanced models, the benefit of the MZ Fire model is that the simulation time is much smaller.

Regarding the general validity, the MZ Fire model has previously been evaluated for smoke filling and gas temperature calculations in large volumes in buildings. However, the fire dynamics in tunnels are different than for that in buildings (see Chapter 3). In this work the original MZ Fire model has been modified to be able account for some tunnel specific phenomena. These modifications included the possibility to:

- apply a longitudinal ventilation flow
- account for a slope in the tunnel
- account for a non-uniform vertical cross section in the tunnel

Example input-files that demonstrate how these features can be used are available in Appendix B.

A benchmarking exercise were conducted to study how well the MZ Fire model performs for tunnel fire scenarios. Data from experimental tests as well as results from FDS simulations were used in this exercise. The benchmarking was done on a limited number of tests, but these included a range of different heat release rates (5-200 MW) and two different tunnel configurations. Consequently, these tests are considered to give a good representation of possible tunnel fire scenarios. From the benchmarking it can be concluded that MZ Fire model generally performs well 50-200 m from the fire for heat release rates in the magnitude of 5-20 MW (BeNeLux fire tests) and moderate longitudinal ventilation flows. However, for the studied scenario with a very high heat release rate (Runehamar fire test) the MZ Fire model results in higher temperatures closer to the ceiling and lower temperatures at lower levels, compared to FDS. However, it was difficult to benchmark against the experimental data since some of the input data needed for accurately replicating experiment was not available. Even so, both FDS and the MZ Fire model in general gave more conservative estimates compared to the experiment.

Even if the results are promising caution should be taken when using the model, since it includes several simplifying assumptions. For example, the MZ Fire model uses an empirical plume model that does not account for the effect of forced ventilation on the air entrainment in in the plume. Another example is that mixing between zones due to the ventilation is not accounted for (this will probably be an issue if the longitudinal ventilation flow is high). The conducted benchmarking is limited and for conditions that are outside the scenarios studied in this report (e.g. very high gradient of high longitudinal ventilation) great care should be taken when using the MZ Fire model.

It should be kept in mind that the MZ Fire model is a complement to other models and tools. For some situations a simpler one-dimensional model might be adequate and for other situations more advanced models, like FDS, might be needed. The individual engineer needs to have a good knowledge of tunnel fire dynamics and the different models at hand to be able to make a correct judgment on the type of model to apply.

In addition to further evaluation and benchmarking of the MZ Fire model there are aspects of the MZ Fire model that could be developed further. The possibility to improve the feature of adapting the tunnel cross section for non-uniform cases is one such thing. The feature is currently based on a reduction of the zone volume in zones where 3D-obstructions are placed. The feature could possibly be improved by accounting for changes in heat transfer when a 3D obstruction is

introduced. Another aspect that can be looked at is the possibility to use other types of plume models and if mixing between layers can be accounted for.

The result dependence on zone size was investigated to a limited extent in this work. Further studies of this issue should be conducted. There is most likely a relationship between zone size, fire size and the longitudinal ventilation flow. This can for example result in that a large fire size will probably not require as small zones as applied in the benchmark testing (Chapter 5). The influence of zone size on the results is not an issue linked only to the MZ Fire model, as it is also necessary to analyse the impact of the cell size when conducting CFD calculations, with e.g. FDS.

10. Conclusion

This project successfully implemented a multi-zone model called the MZ Fire model (version MZ_tunnel_01) within a risk analysis tool called ARTU. MZ has been originally developed for large compartments, while it has been now updated and tested specifically for tunnel fires. This work leads to enhanced capabilities of ARTU, as it currently allows to switch from simpler and quicker 1D simulations of tunnel fire dynamics to a more refined representation. Multi-zone modelling represents a fair compromise between computational cost and result accuracy, thus still allowing the adoption of a probabilistic approach for the overall tunnel fire risk assessment. In fact, ARTU makes use of pseudo-random sampling from distributions and possibly thousands of simulations need to be run. Therefore, the possibility to switch between a more or less refined representations of tunnel fire dynamics (still having computational times that do not impede the use of this approach) offers more flexibility to the tunnel fire safety designer and expands the possible range of applicability of ARTU.

References

Beard, A., Carvel, R., 2012. Handbook of tunnel fire safety. ICE publishing.

Beard, A.N., 2010. Tunnel safety, risk assessment and decision-making. Tunn. Undergr. Space Technol. 25, 91–94.

Bergmeister, K., Francesconi, S., del Brennero SpA, A., 2004. Causes and Frequency of Incidents in Tunnels. UPTUN-Work Package 1–2.

Carvel, R., Beard, A., 2005. The handbook of tunnel fire safety. Thomas Telford, London.

Carvel, R., Marlair, G., 2005. A history of fire incidents in tunnels.

CETU, C. d'Études des T., 2010. Guide to road tunnel safety documentation.

European Commission, E., 2004. Directive 2004/54/CE on minimum safety requirements for tunnels in the Trans-European Road Network (29/04/2004).

Heskestad, G., 1983. Virtual origins of fire plumes. Fire Saf. J. 5, 109–114.

Ingason, H., Li, Y.Z., Lönnermark, A., 2015a. Runehamar tunnel fire tests. Fire Saf. J. 71, 134–149.

Ingason, H., Li, Y.Z., Lönnermark, A., 2015b. Tunnel Fire Dynamics. Springer New York, New York, NY. https://doi.org/10.1007/978-1-4939-2199-7

International Standards Organization, 2014. ISO 16730-1 Fire Safety Engineering – Procedures and requirements for verification and validation of calculation methods. International Standards Organization.

Johansson, N., 2021. Evaluation of a zone model for fire safety engineering in large spaces. Fire Saf. J. 120, 103122. https://doi.org/10.1016/j.firesaf.2020.103122

Jones, W.W., Peacock, R.D., Forney, G., Reneke, P.A., 2009. CFAST – Consolidated Model of Fire Growth and Smoke Transport (Version 6). Technical Reference Guide. NIST Special Publication 1026. National Institute of Standards and Technology.

Kung, H.-C., Stavrianidis, P., 1982. Buoyant plumes of large-scale pool fires. Symp. Int. Combust. 19, 905–912. https://doi.org/10.1016/S0082-0784(82)80266-X

Lemaire, T., Kenyon, Y., 2006. Large Scale Fire Tests in the Second Benelux Tunnel. Fire Technol. 42, 329–350. https://doi.org/10.1007/s10694-006-8434-4

Li, Y.Z., Ingason, H., Lönnermark, A., 2012. Numerical simulation of Runehamar tunnel fire tests. na.

McGrattan, K.B., Randall, M., Marcos, V., Simo, H., Jason, F., 2021. Fire dynamics simulator (version 6) :: user's guide (No. 1019). National Institute of Standards and Technology, Gaithersburg, MD. https://doi.org/10.6028/NIST.SP.1019

Meacham, B.J., Custer, R.L., 1995. Performance-based fire safety engineering: an introduction of basic concepts. Sage Publications Sage CA: Thousand Oaks, CA.

NFPA, N.F.P.A., 2017. Standard for road, tunnels, bridges, and other limited access highways (NFPA 502).

Nỳvlt, O., Prívara, S., Ferkl, L., 2011. Probabilistic risk assessment of highway tunnels. Tunn. Undergr. Space Technol. 26, 71–82.

PIARC, F., 1999. Fire and Smoke Control in Road Tunnels. PIARC Tech. Comm. C5 Road Tunn.

Purser, D.A., McAllister, J.L., 2016. Assessment of Hazards to Occupants from Smoke, Toxic Gases, and Heat, in: Hurley, M.J., Gottuk, D.T., Hall, J.R., Harada, K., Kuligowski, E.D., Puchovsky, M., Torero, J.L., Watts, J.M., Wieczorek, C.J. (Eds.), SFPE Handbook of Fire Protection Engineering. Springer New York, New York, NY, pp. 2308–2428. https://doi.org/10.1007/978-1-4939-2565-0_63

Ralph, B., Carvel, R., 2018. Coupled hybrid modelling in fire safety engineering; a literature review. Fire Saf. J. 100, 157–170. https://doi.org/10.1016/j.firesaf.2018.08.008

Rattei, G., Lentz, A., Kohl, B., 2014. How frequent are fire in tunnels-Analysis from Austrian tunnel incident statistics, in: Proceedings from the Seveth International Conference on Tunnel Safety and Ventilation, Graz, Austria. pp. 5–11.

Ronchi, E., 2012. Evacuation modelling in road tunnel fires (Doctoral Dissertation). Politecnico di Bari, Bari, Italy.

Sandin, K., Grenberg, K., Husted, B.P., Scozzari, R., Fronterrè, M., Ronchi, E., 2019. Verification and Validation of the ARTU (Tunnel Fire Risk analysis) tool.

Suzuki, K., Tanaka, T., Harada, K., Yoshida, H., 2004. An application of A Multi-layer Zone Model to A Tunnel fire. Fire Saf. Sci. 6, 7b–2.

Appendix A – Results from benchmarking, BeNeLux fire tests

The complete results from the benchmarking against the BeNeLux tests 6, 7, 8, 9 and 14 are presented in this appendix.

Test 6 (5MW, natural ventilation)

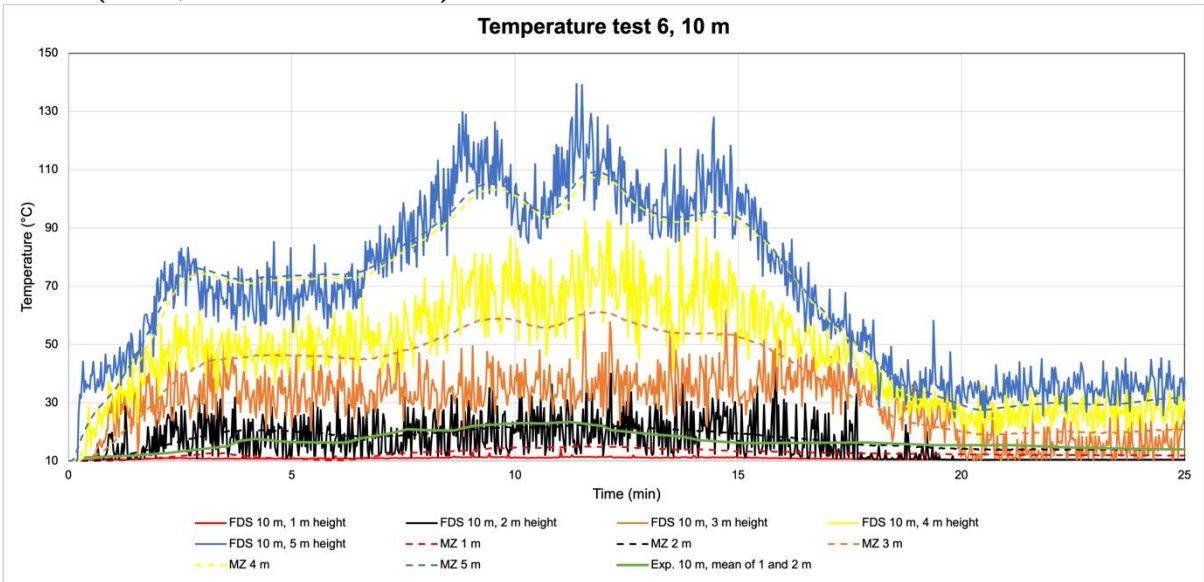

Figure A.1. Temperature calculated with FDS and MZ 10 m from fire source test 6.

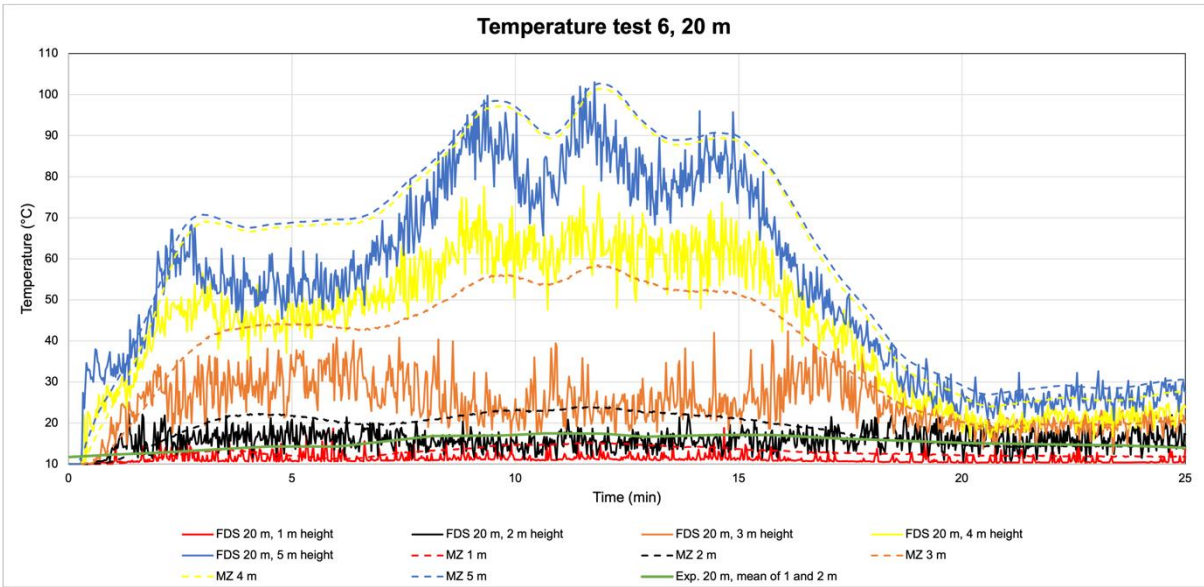

Figure A.2: Temperature calculated with FDS and MZ 20 m from fire source test 6.

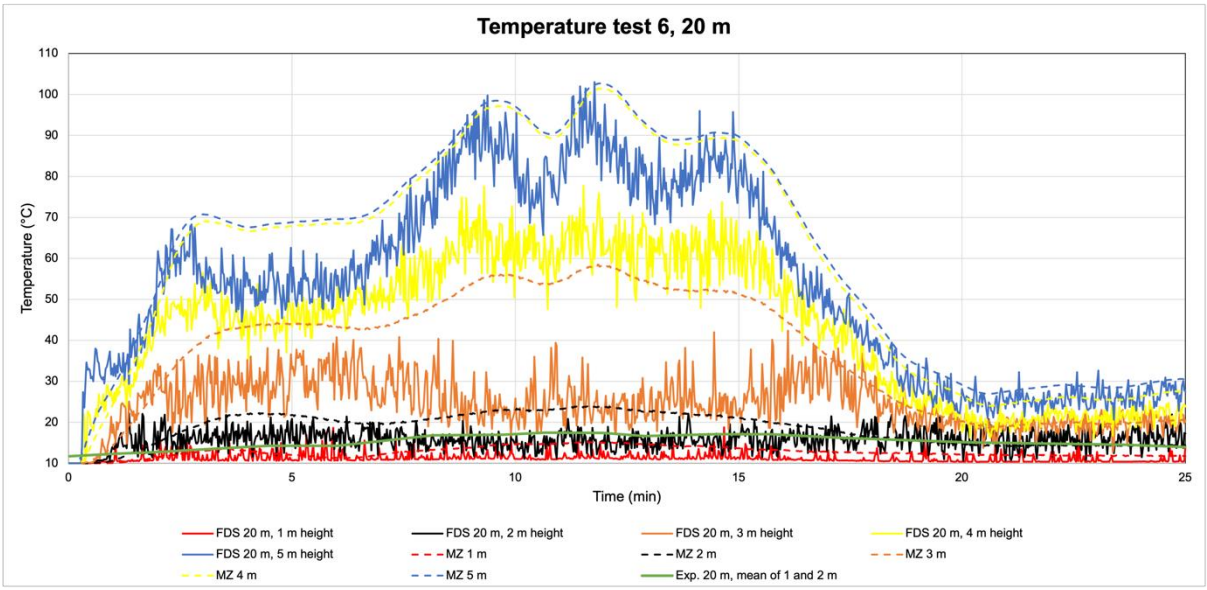

Figure A.3. Temperature calculated with FDS and MZ 50 m from fire source test 6.

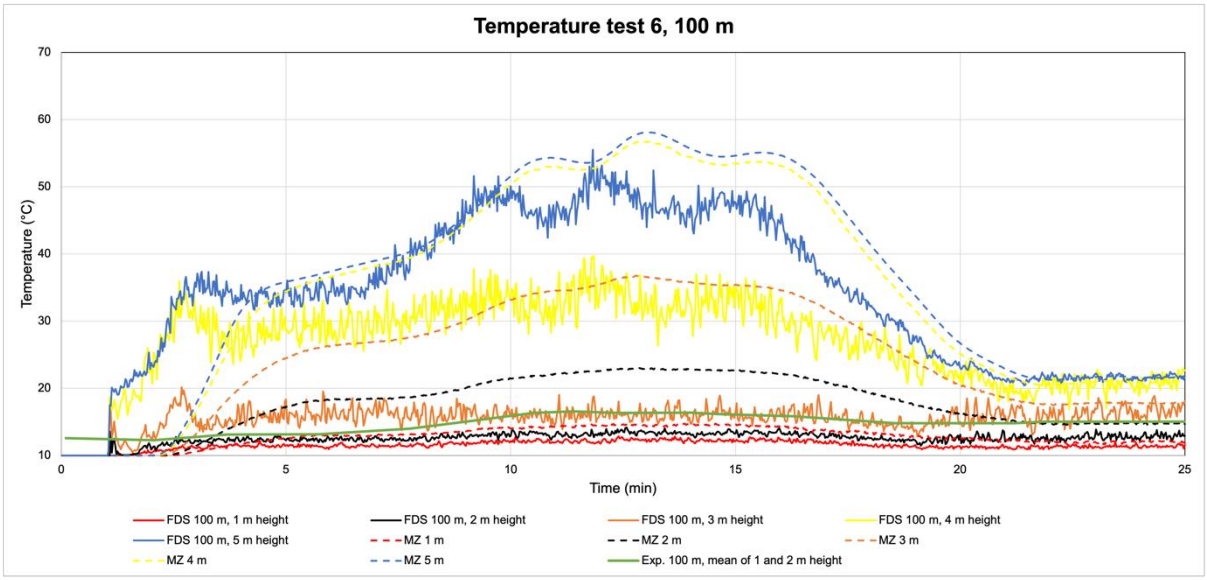

Figure A.4. Temperature calculated with FDS and MZ 100 m from fire source test 6.

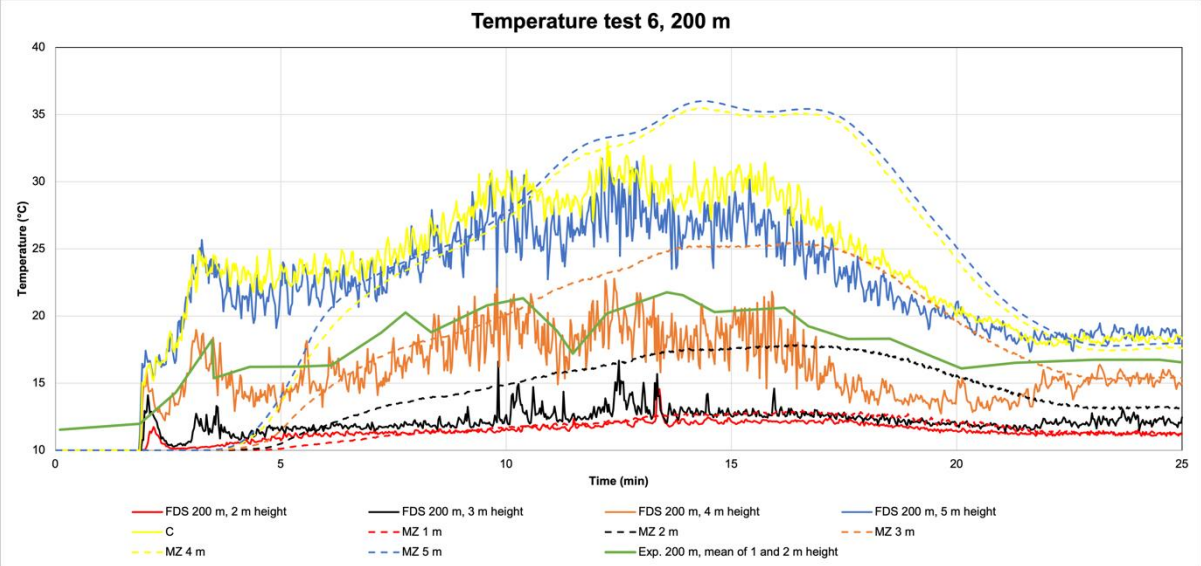

Figure A.5. Temperature calculated with FDS and MZ 200 m from fire source test 6.

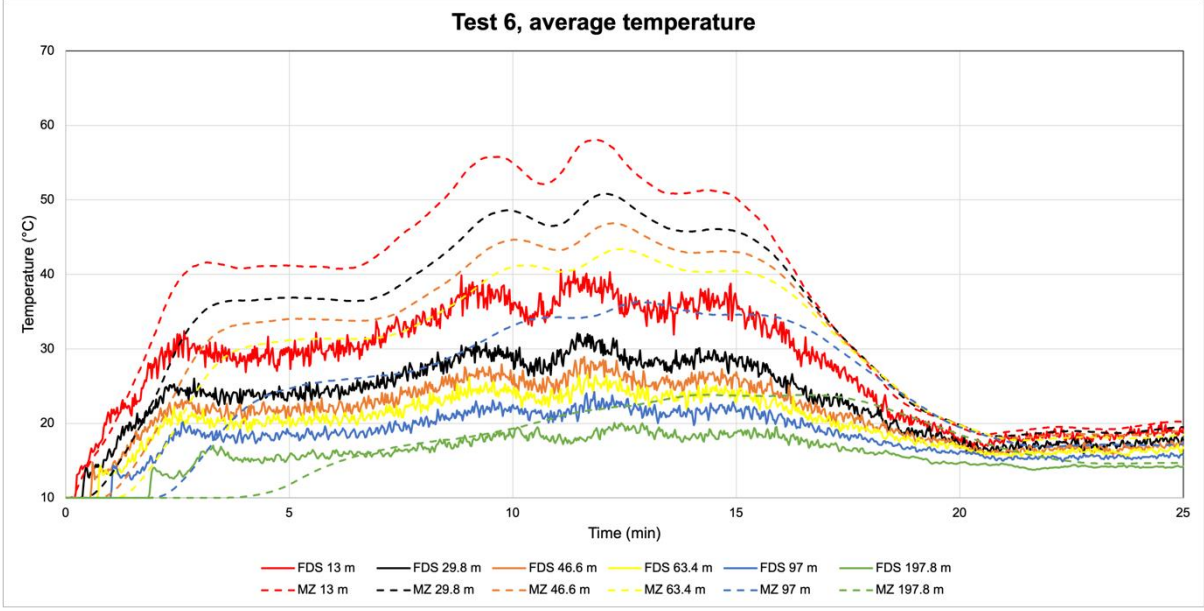

Figure A.6. Average cross section temperature calculated with FDS and MZ at different positions from fire source test 6.

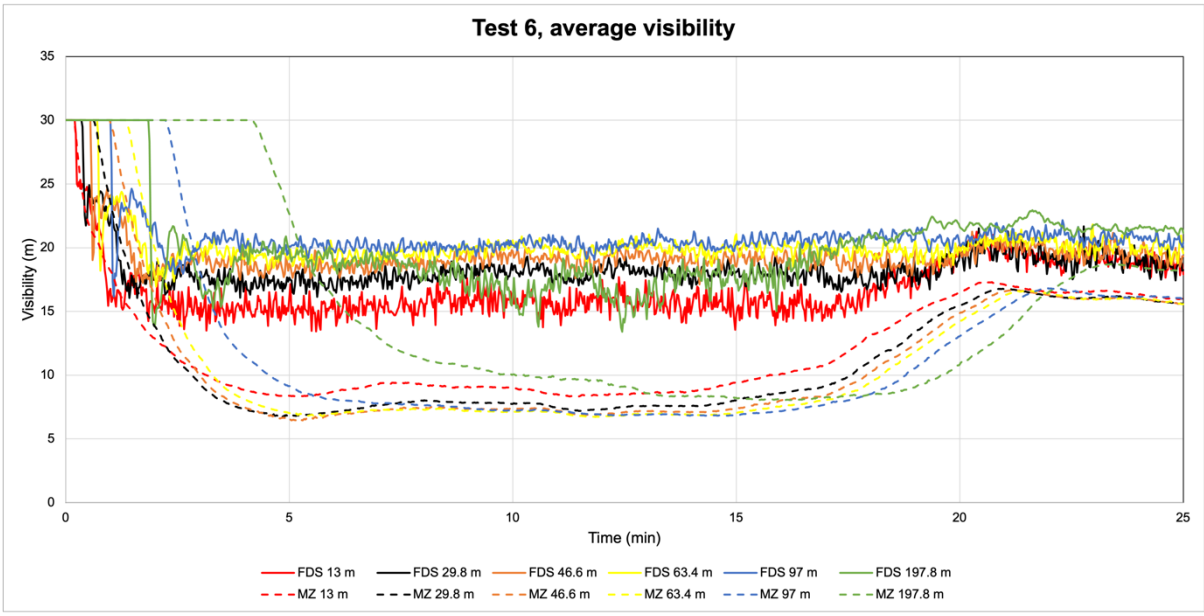

Figure A.7. Average cross section visibility calculated with FDS and MZ at different positions from fire source test 6.

Comment on the results test 6:

The overall correspondence between FDS and MZ is considered good for test 6. MZ results in slightly higher temperatures compared to FDS (see Figures B.1-B.5). The average cross-section temperatures are also higher in MZ (see Figure A.6). However, at larger distance from the fire (> 100 m) the temperature increase is slower with the MZ Fire model. The average cross section visibility is in general worse in MZ than in FDS (see Figure A.7), but as for the temperature the travel time for the gases is longer in MZ than FDS.

The experimental gas temperature (average of 1 and 2 m height) is in general predicted rather well MZ except at 200 m, where it is underpredicted (see Figure A.5).

Test 7 (5MW, Longitudinal ventilation max 6 m/s)

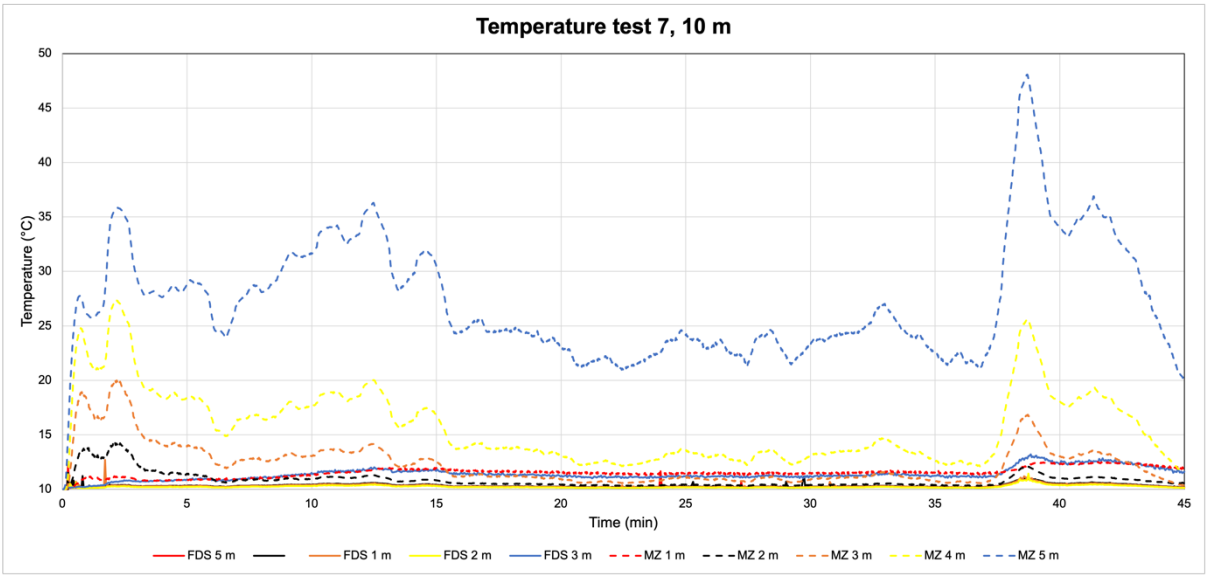

Figure A.8. Temperature calculated with FDS and MZ 10 m from fire source test 7.

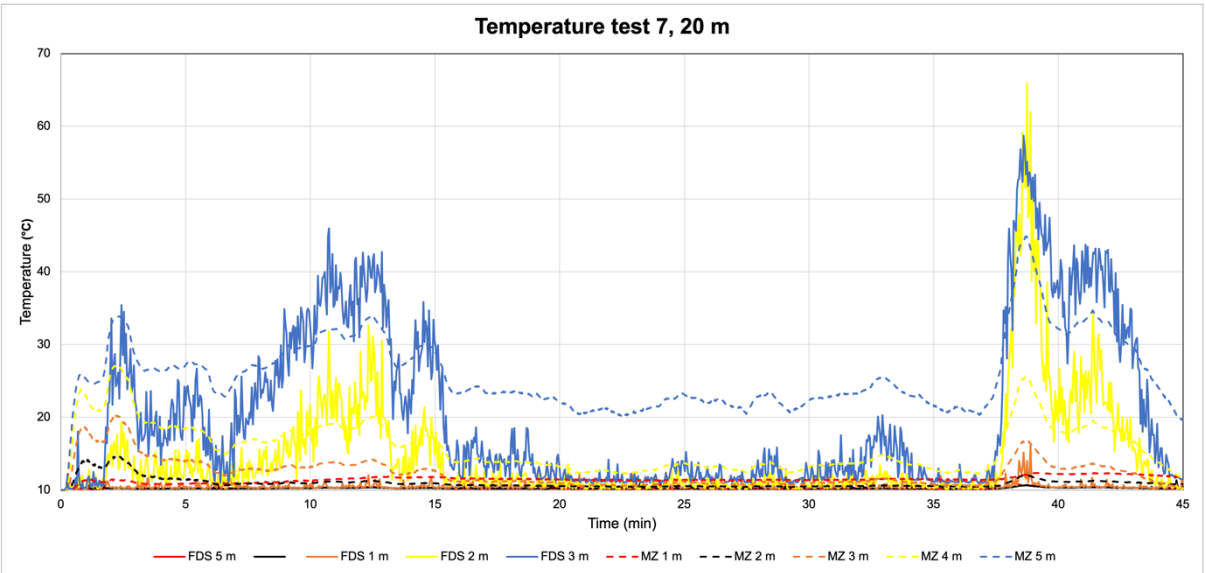

Figure A.9. Temperature calculated with FDS and MZ 20 m from fire source test 7.

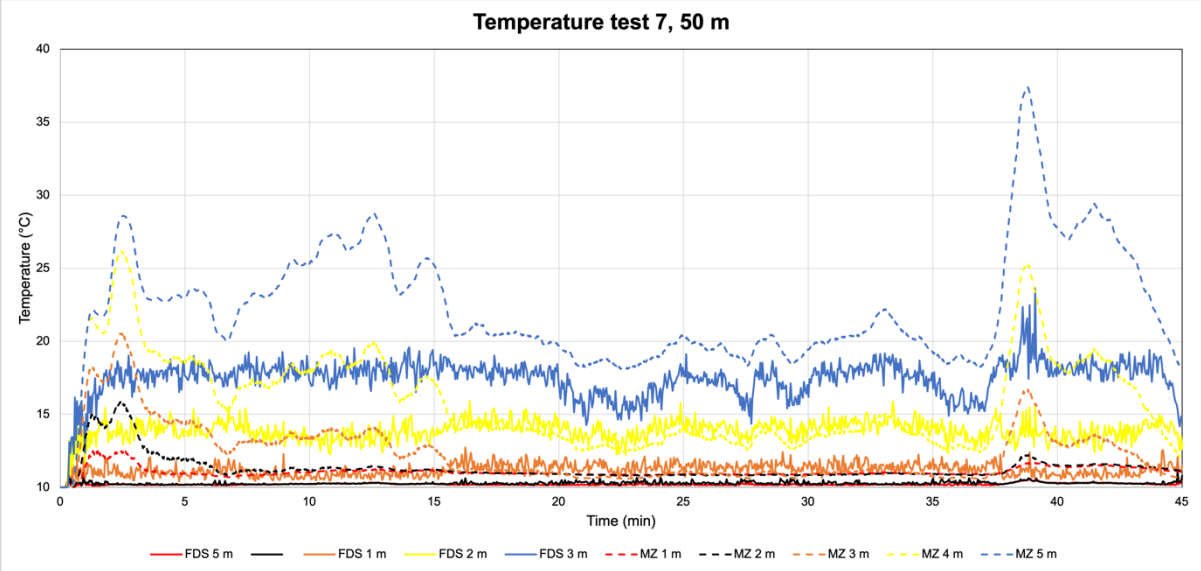

Figure A.10. Temperature calculated with FDS and MZ 50 m from fire source test 7.

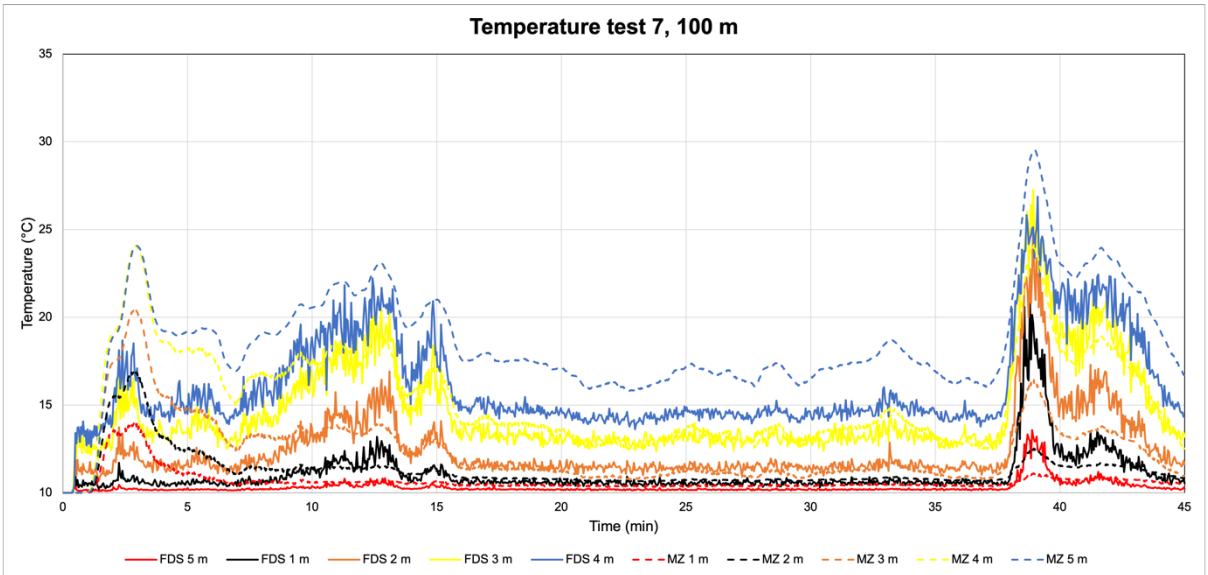

Figure A.11. Temperature calculated with FDS and MZ 100 m from fire source test 7.

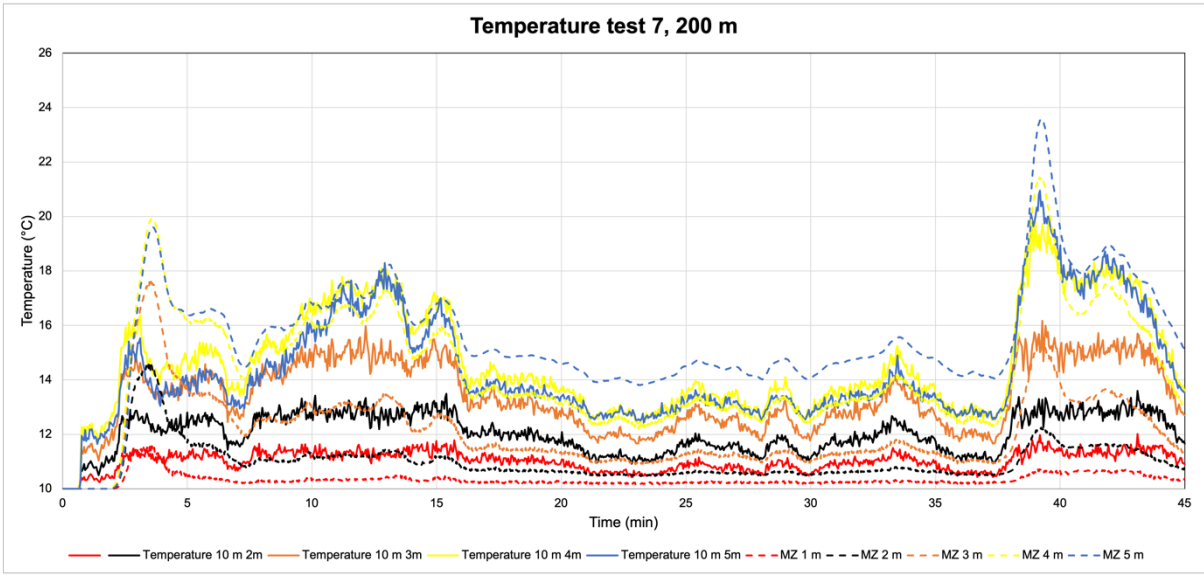

Figure A.12. Temperature calculated with FDS and MZ 200 m from fire source test 7.

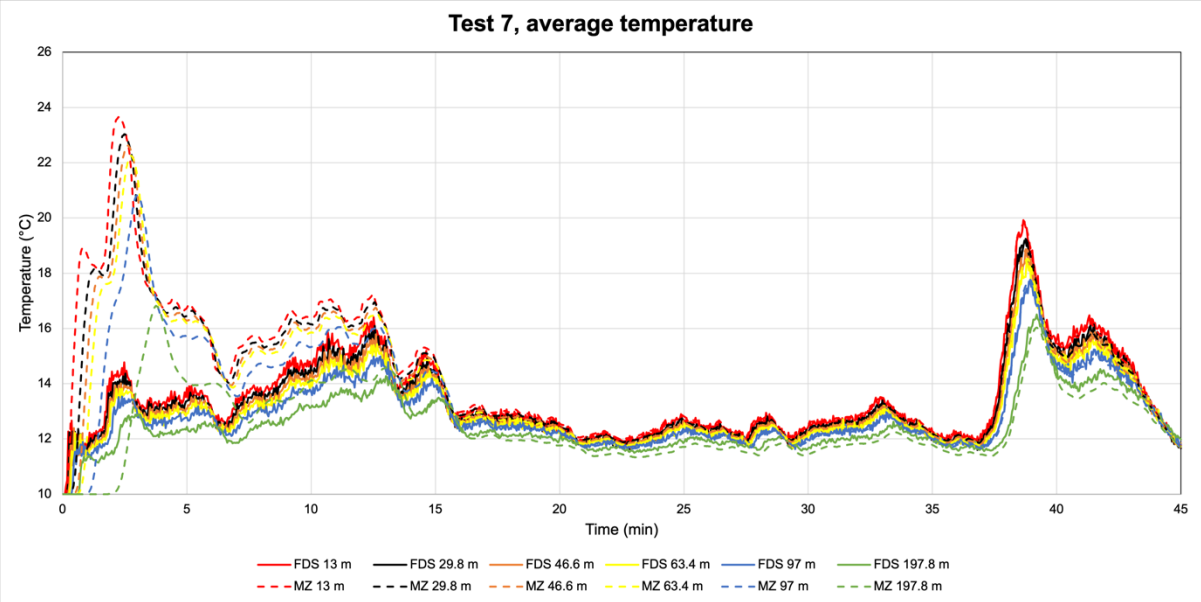

Figure A.13. Average cross section temperature calculated with FDS and MZ at different positions from fire source test 7.

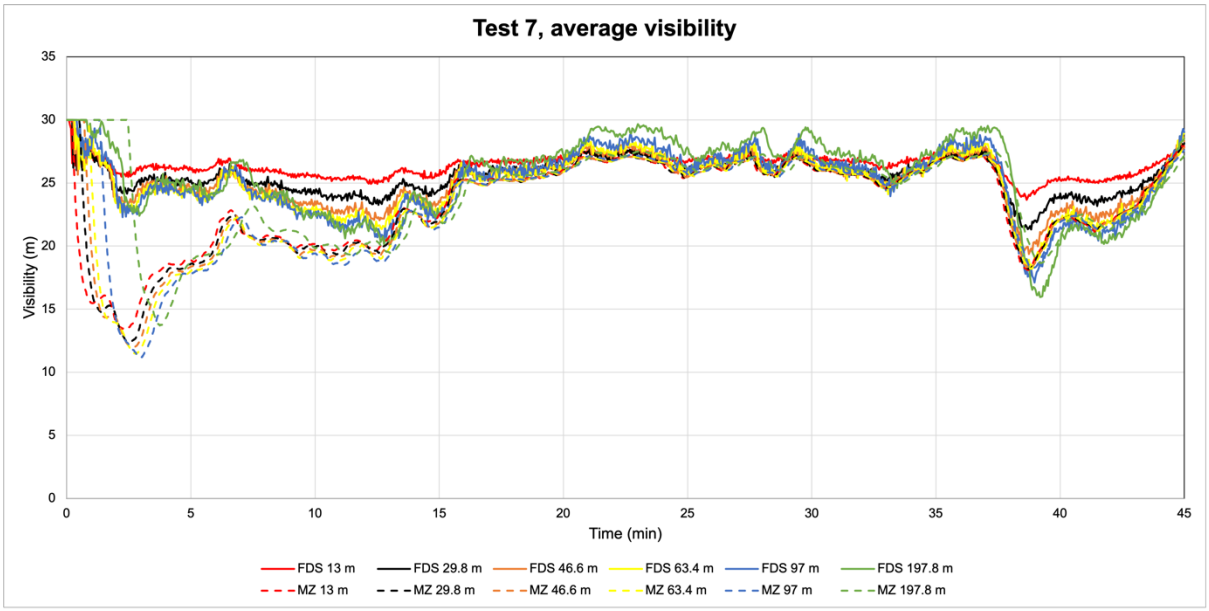

Figure A.14. Average cross section visibility calculated with FDS and MZ at different positions from fire source test 7.

Comment on the results test 7:

The overall correspondence between FDS and MZ is considered very good for test 7. MZ results in slightly higher temperatures than FDS (see Figures B.8-B.12) but the average cross-section temperatures are similar (see Figure A.13). The average cross section visibility is corresponding well (see Figure A.14).

No comparison to experimental test data was done for Test 7.

Test 8 (20MW, natural ventilation)

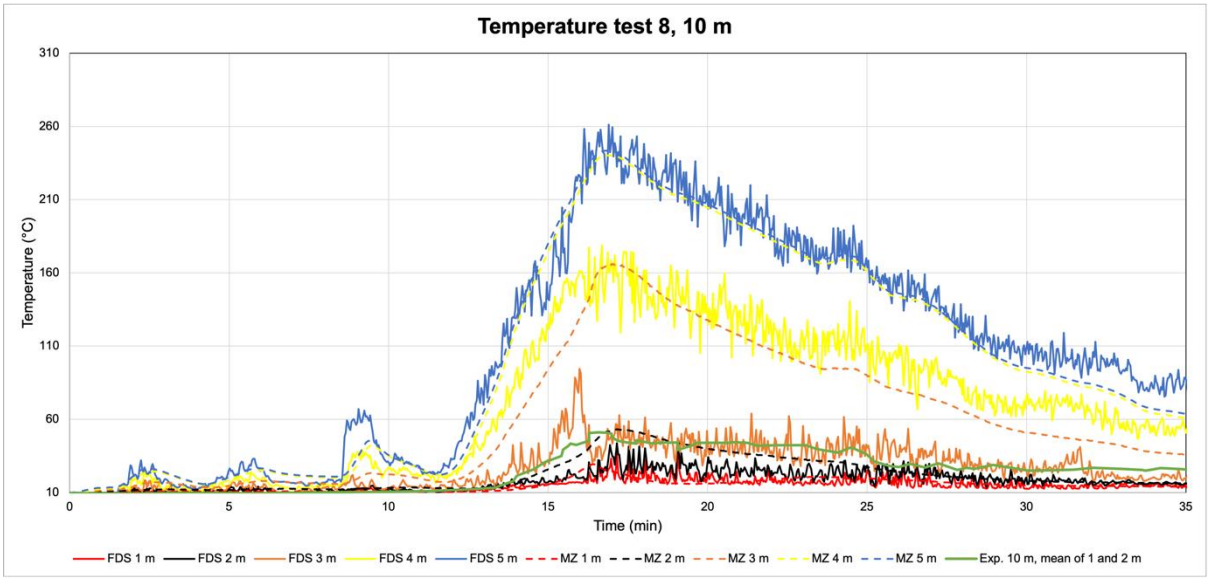

Figure A.15. Temperature calculated with FDS and MZ 10 m from fire source test 8.

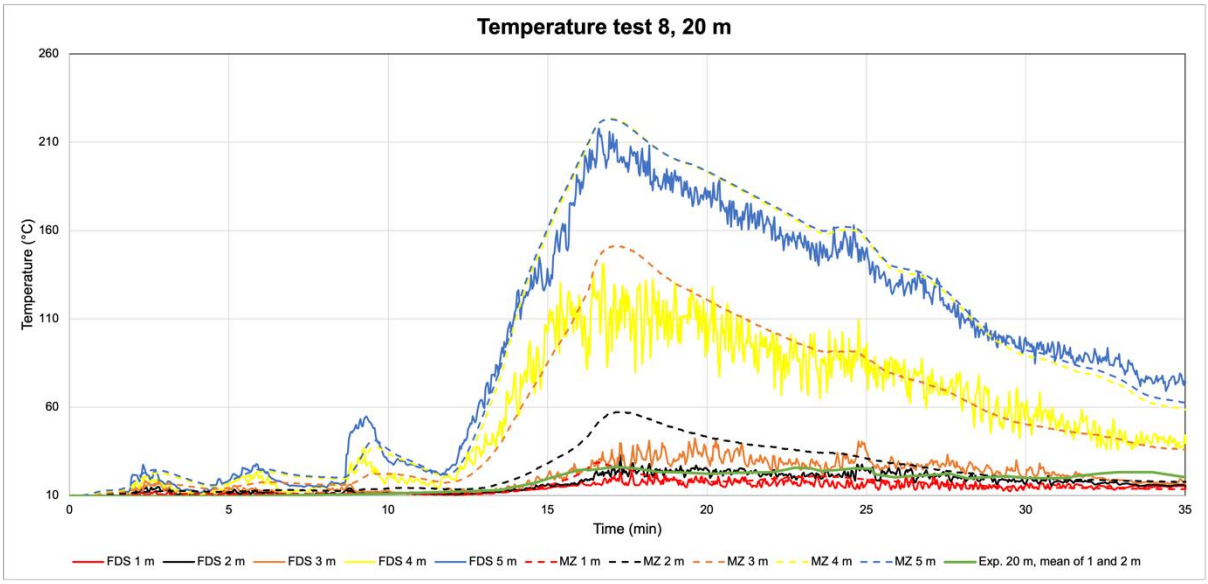

Figure A.16. Temperature calculated with FDS and MZ 20 m from fire source test 8.

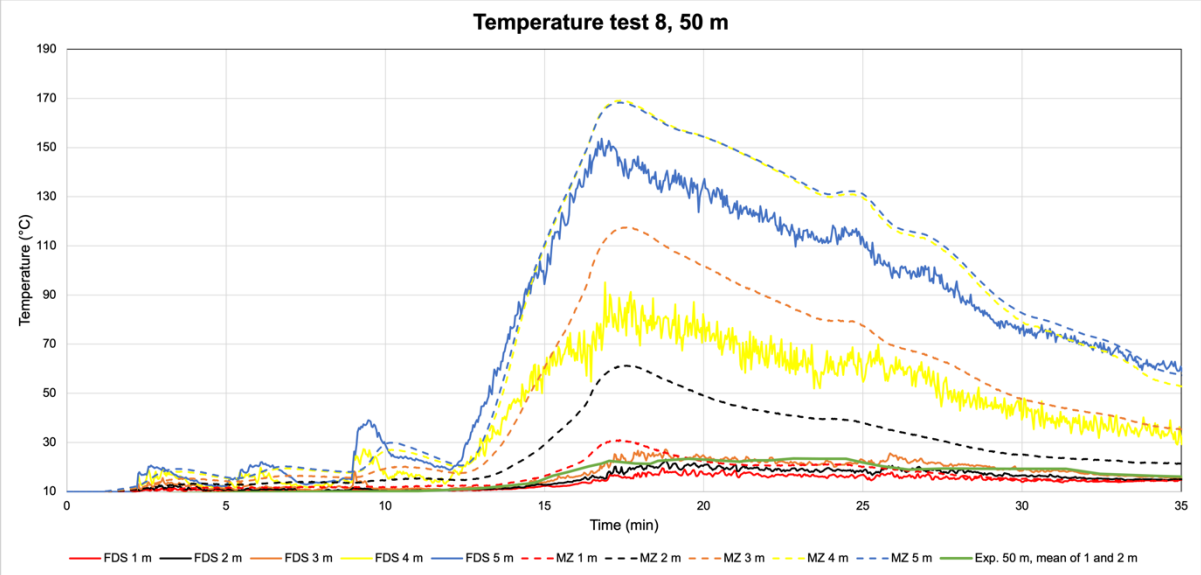

Figure A.17. Temperature calculated with FDS and MZ 50 m from fire source test 8.

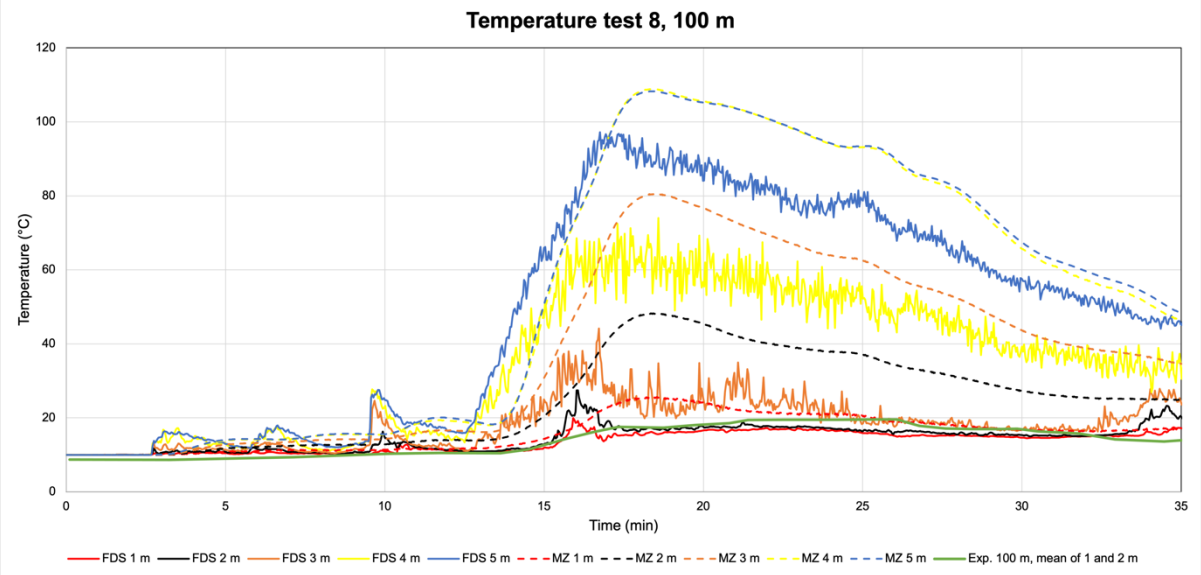

Figure A.18. Temperature calculated with FDS and MZ 100 m from fire source test 8.

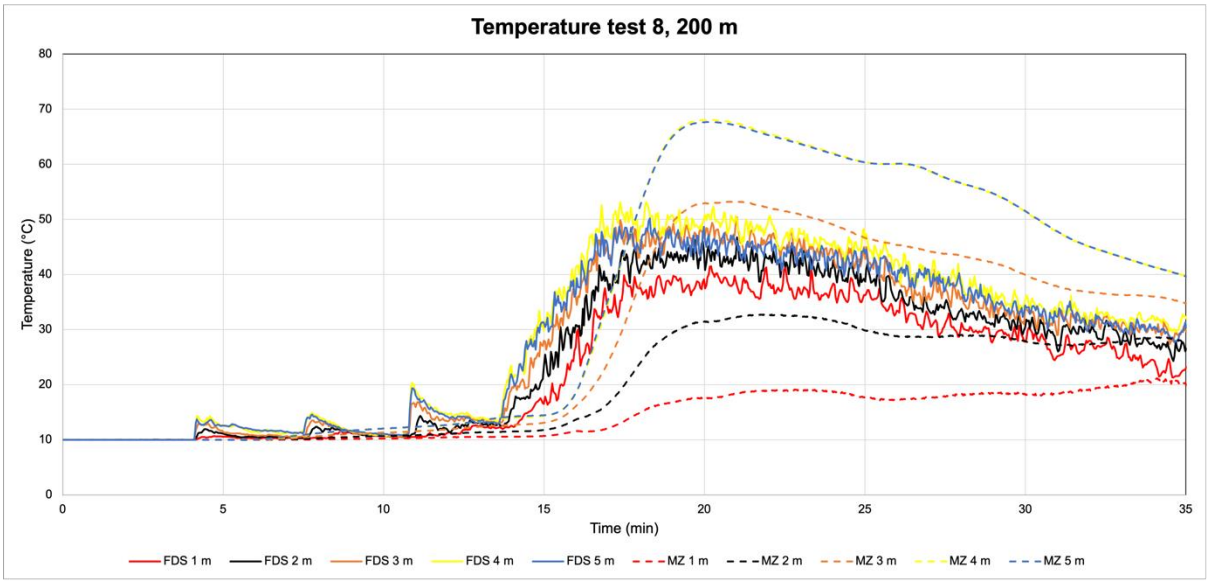

Figure A.19. Temperature calculated with FDS and MZ 200 m from fire source test 8.

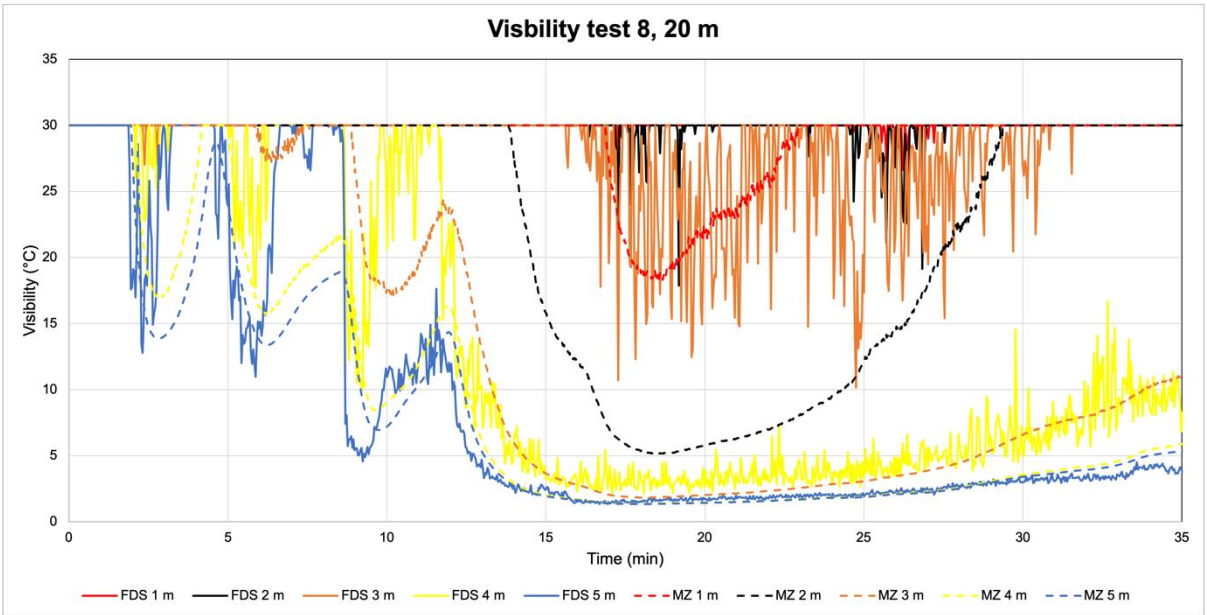

Figure A.20. Visibility calculated with FDS and MZ 20 m from fire source test 8.

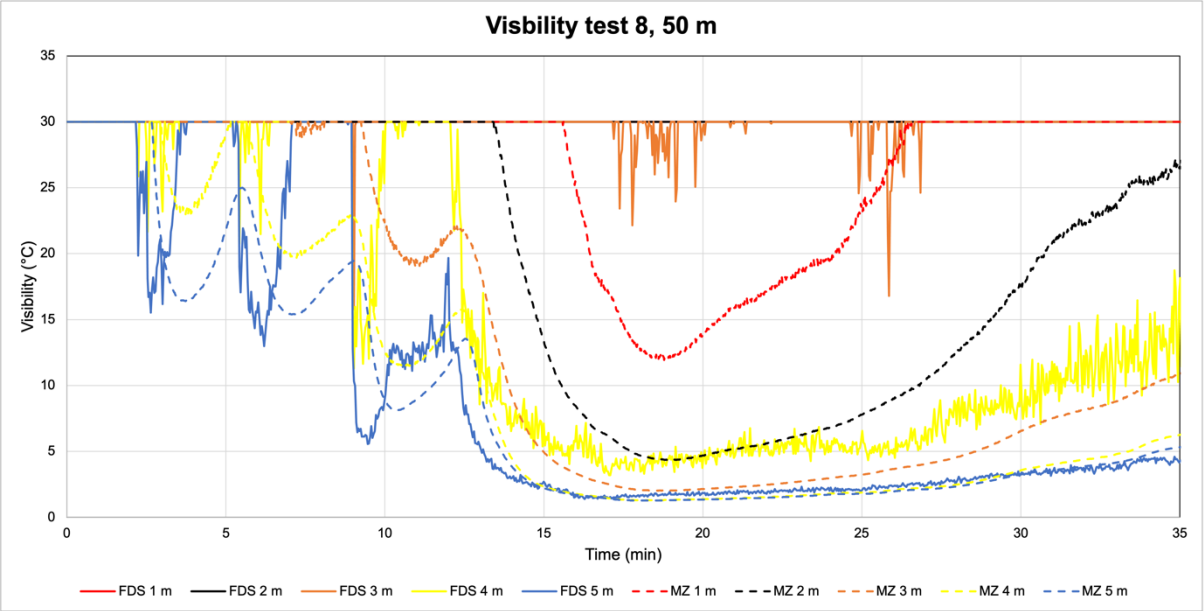

Figure A.21. Visibility calculated with FDS and MZ 50 m from fire source test 8.

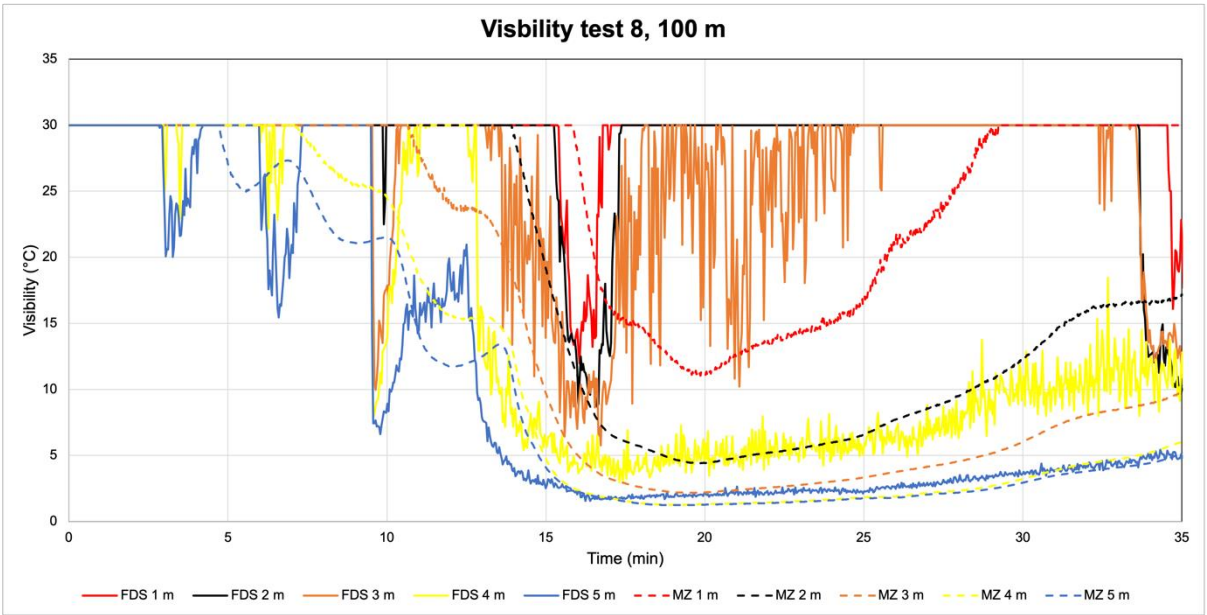

Figure A.22. Visibility calculated with FDS and MZ 100 m from fire source test 8.

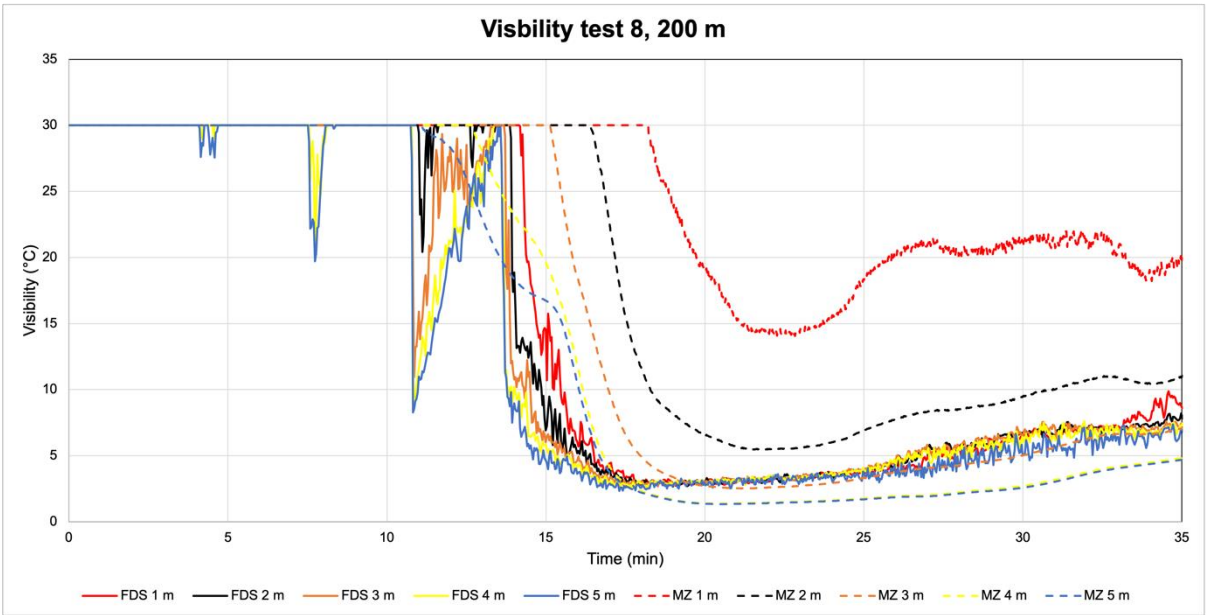

Figure A.23. Visibility calculated with FDS and MZ 200 m from fire source test 8.

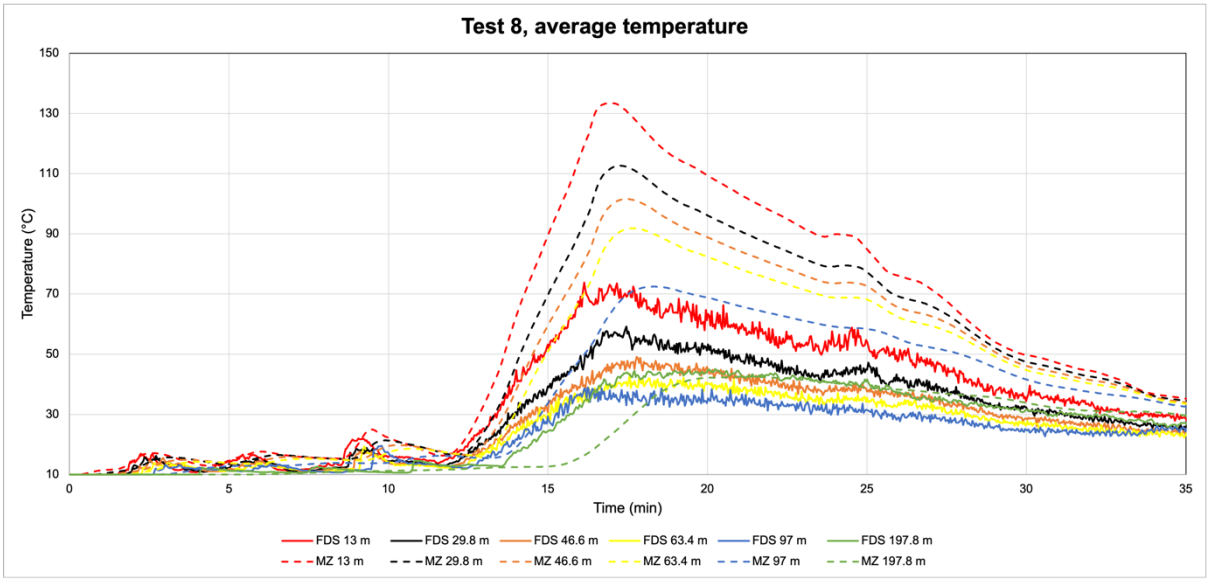

Figure A.24. Average cross section temperature calculated with FDS and MZ at different positions from fire source test 8.

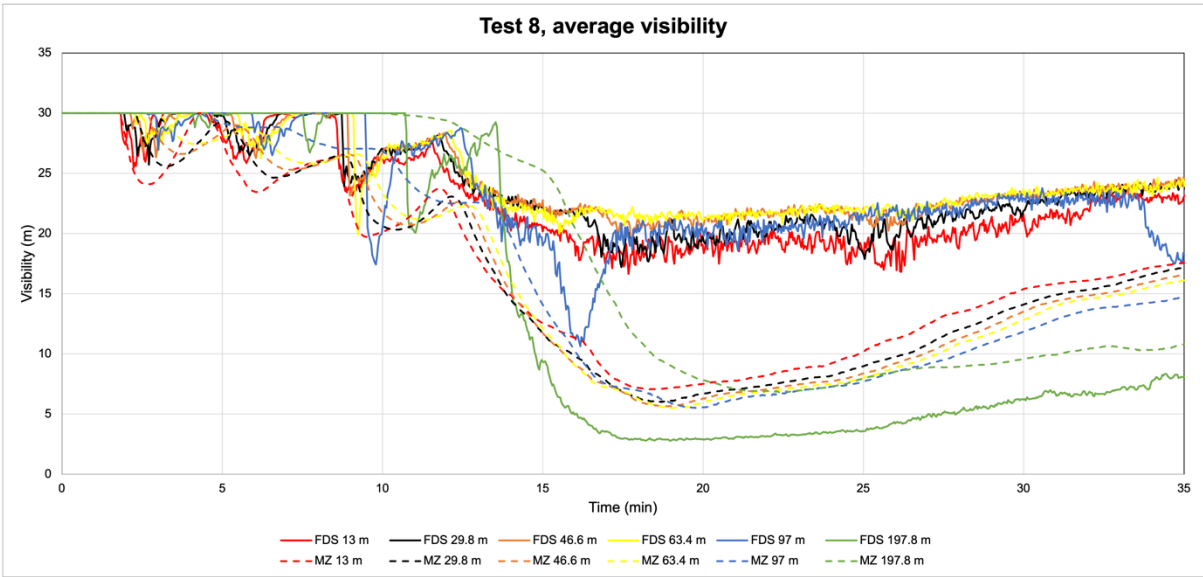

Figure A.25. Average cross section visibility calculated with FDS and MZ at different positions from fire source test 8.

Comment on the results test 8:

The overall correspondence between FDS and MZ is considered good for test 8, and the trends are similar as in test 6. Up to 100 m MZ performs conservative calculations but at larger distances the temperature increases, and visibility decreases slower than in FDS. Compared to the experimental data the predictions with MZ are good and on the conservative side up to 100 m.

Test 9 (20MW, Longitudinal ventilation max 6 m/s)

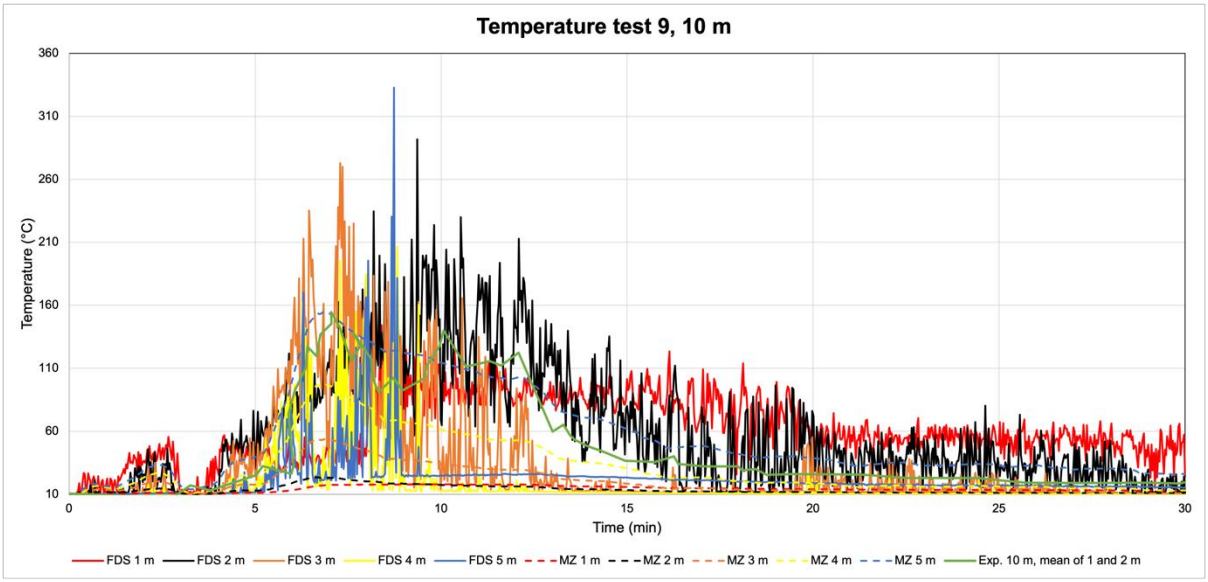

Figure A.26. Temperature calculated with FDS and MZ 10 m from fire source test 9.

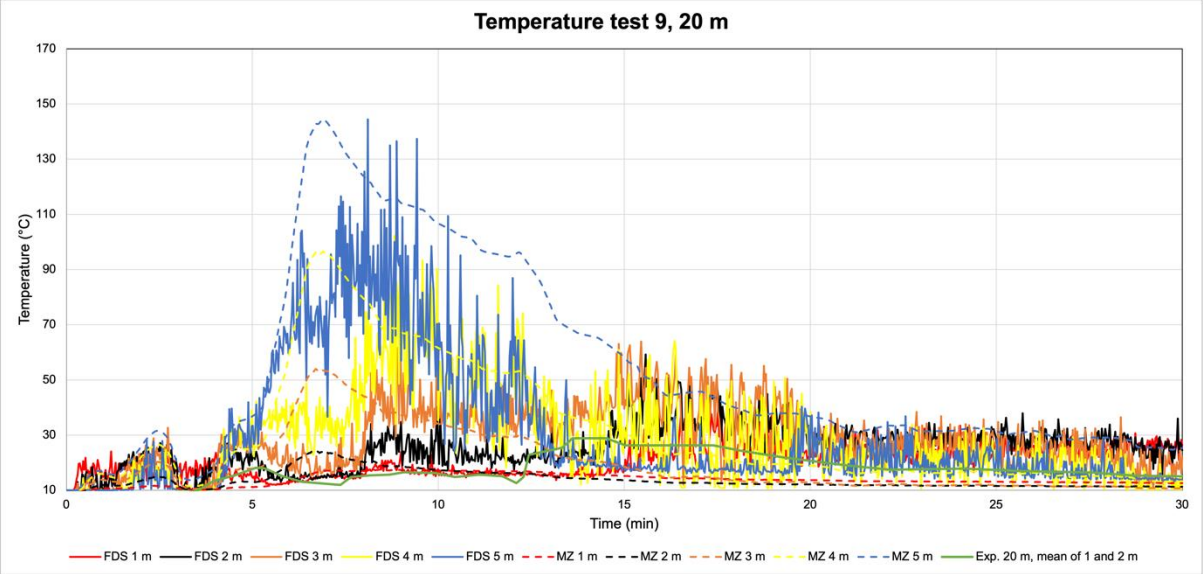

Figure A.27. Temperature calculated with FDS and MZ 20 m from fire source test 9.

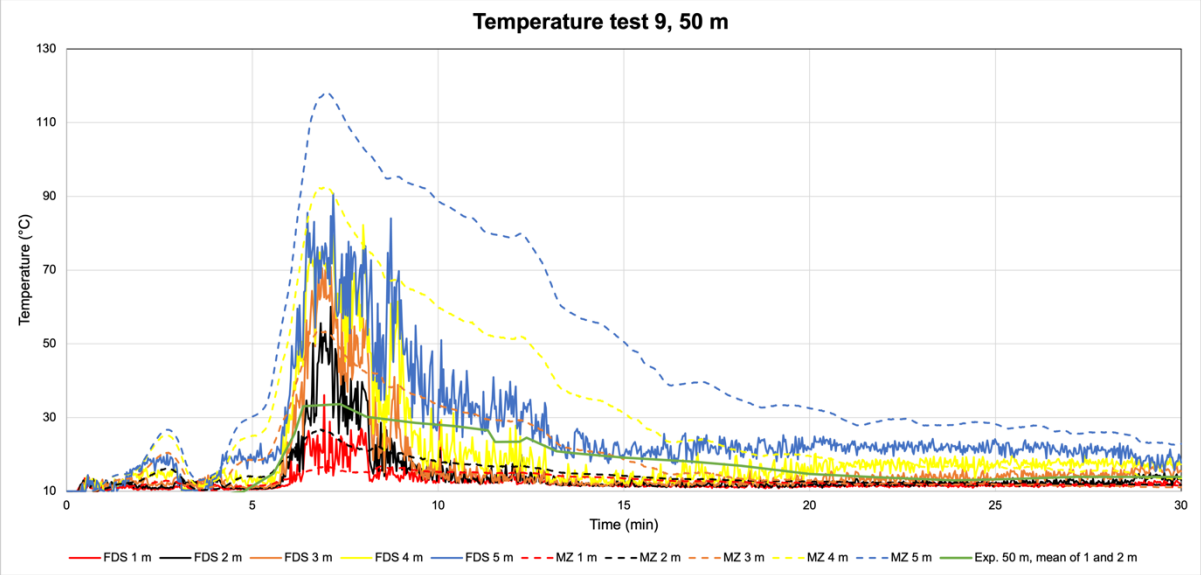

Figure A.28. Temperature calculated with FDS and MZ 50 m from fire source test 9.

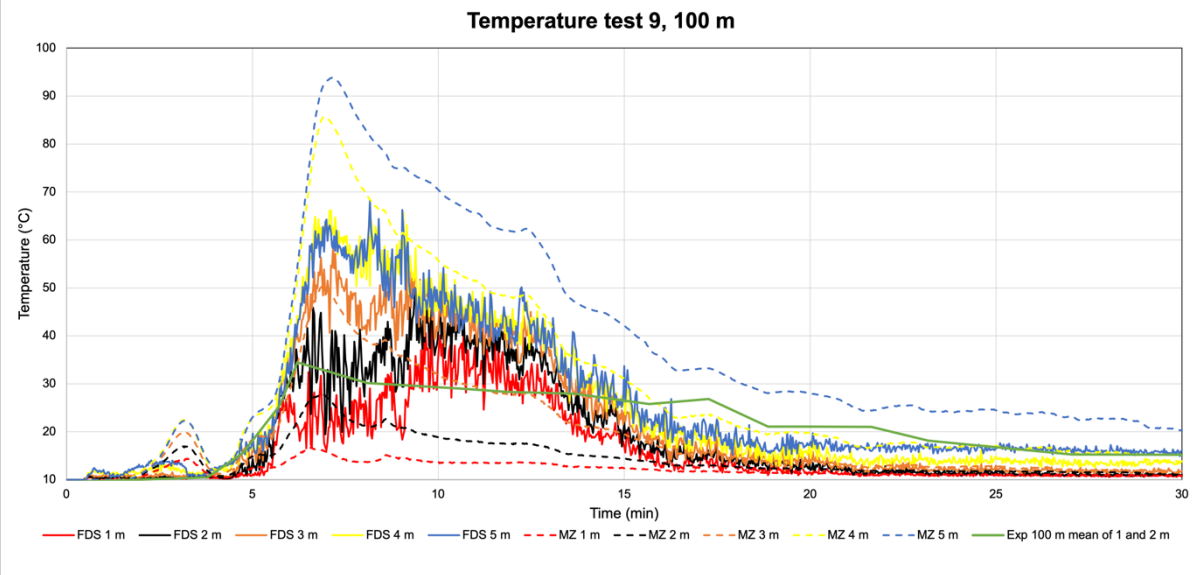

Figure A.29. Temperature calculated with FDS and MZ 100 m from fire source test 9.

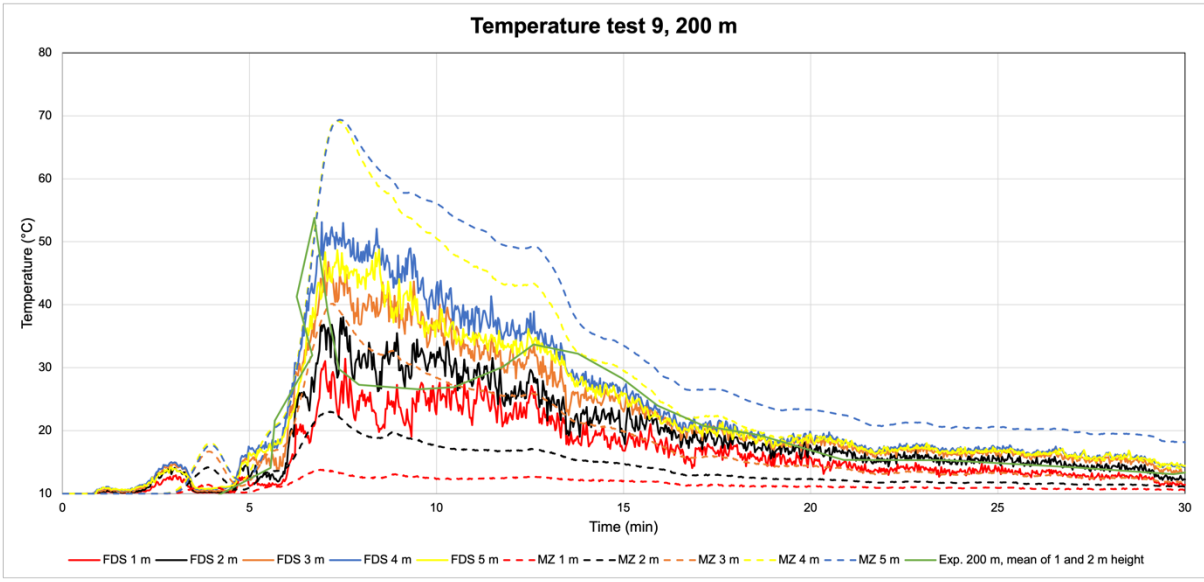

Figure A.30. Temperature calculated with FDS and MZ 200 m from fire source test 9.

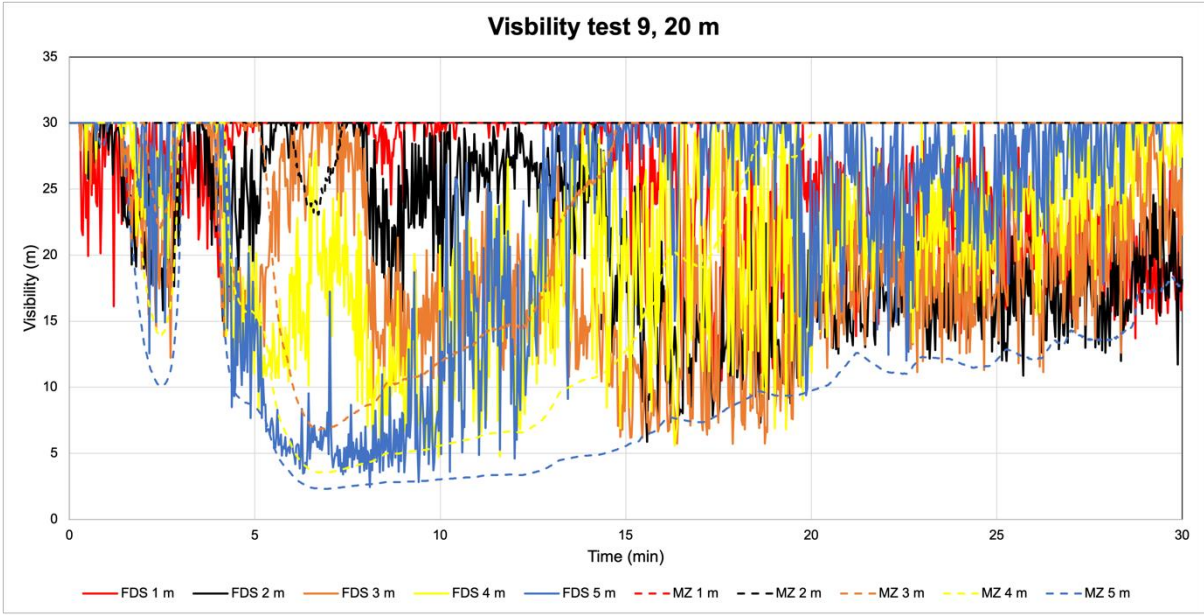

Figure A.31. Visibility calculated with FDS and MZ 20 m from fire source test 9.

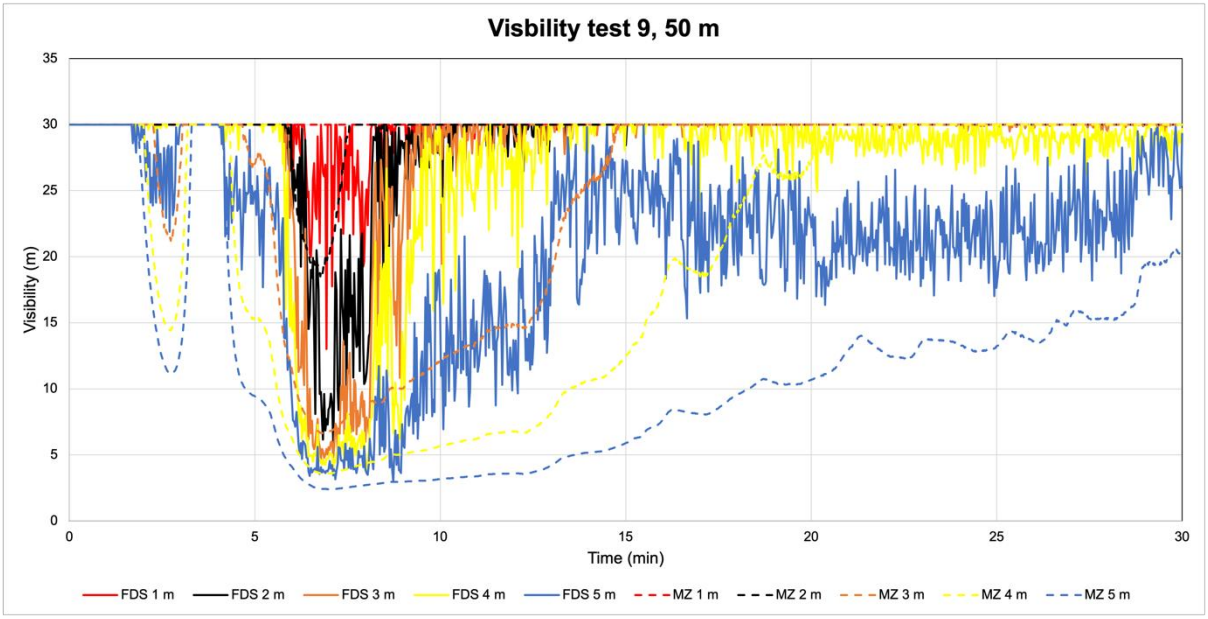

Figure A.32. Visibility calculated with FDS and MZ 50 m from fire source test 9.

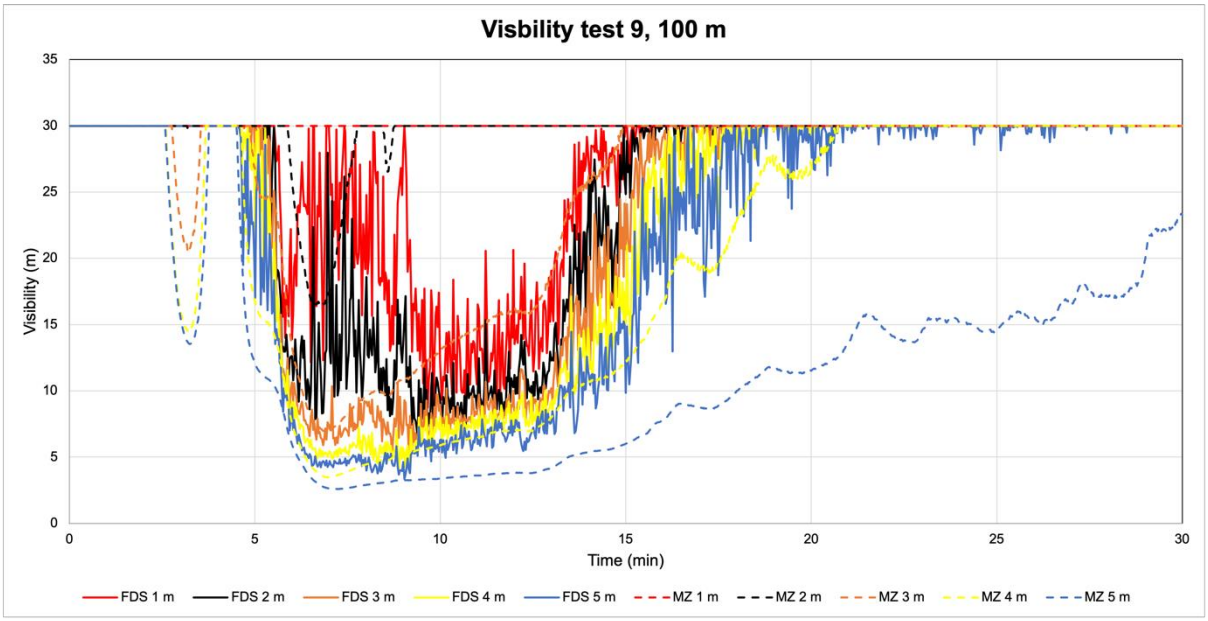

Figure A.33.Visibility calculated with FDS and MZ 100 m from fire source test 9.

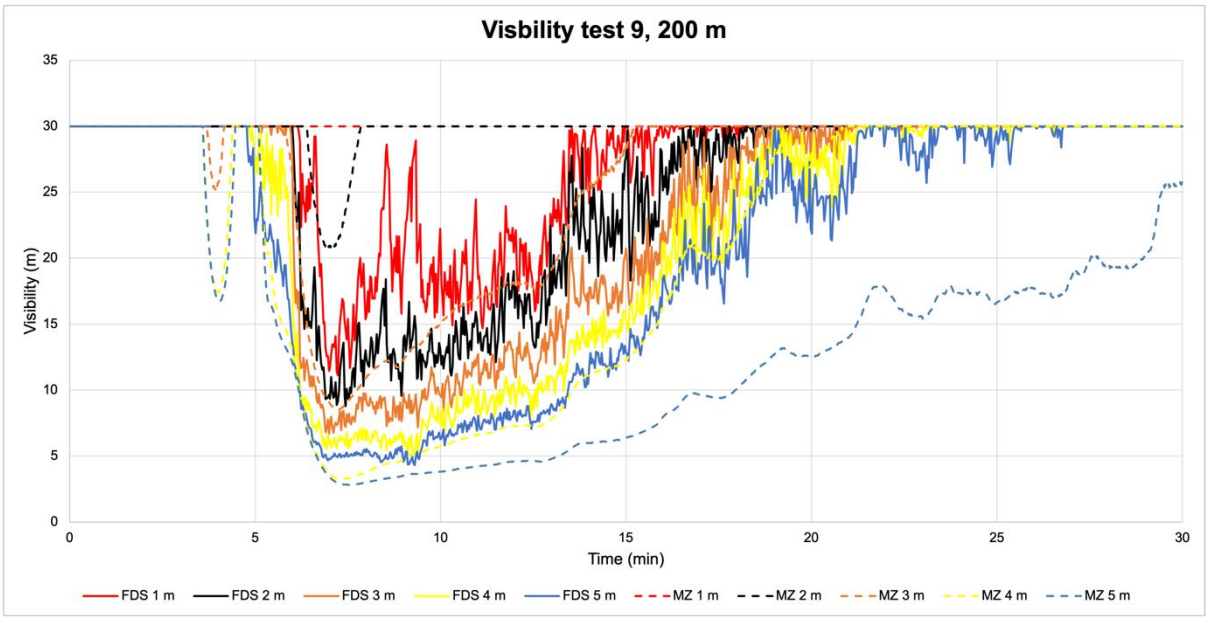

Figure A.34. Visibility calculated with FDS and MZ 200 m from fire source test 9.

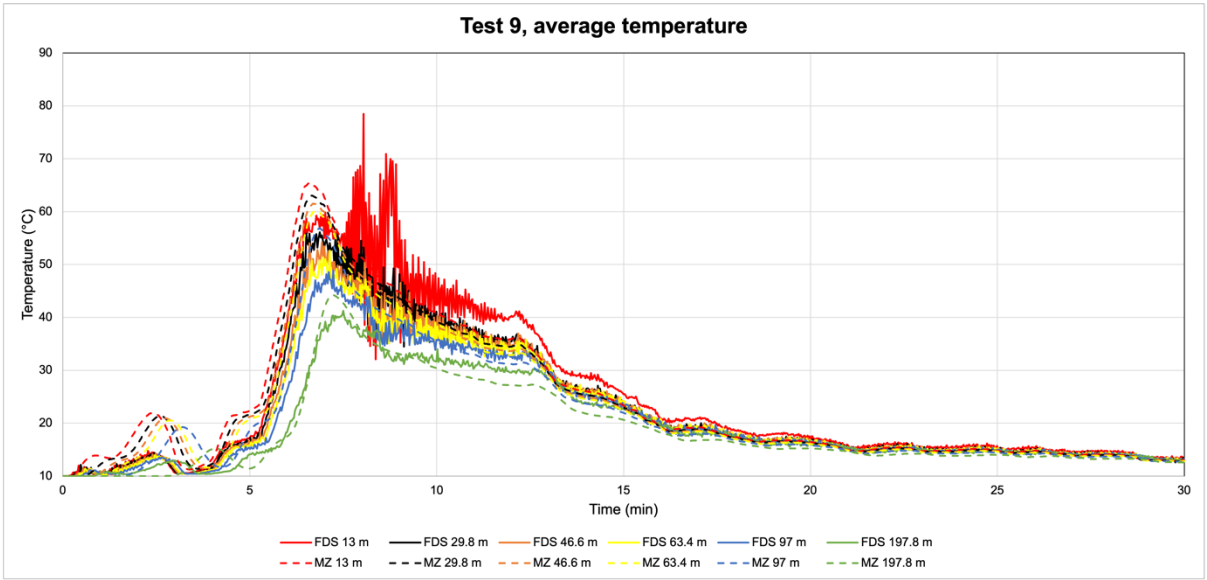

Figure A.35. Average cross section temperature calculated with FDS and MZ at different positions from fire source test 9.

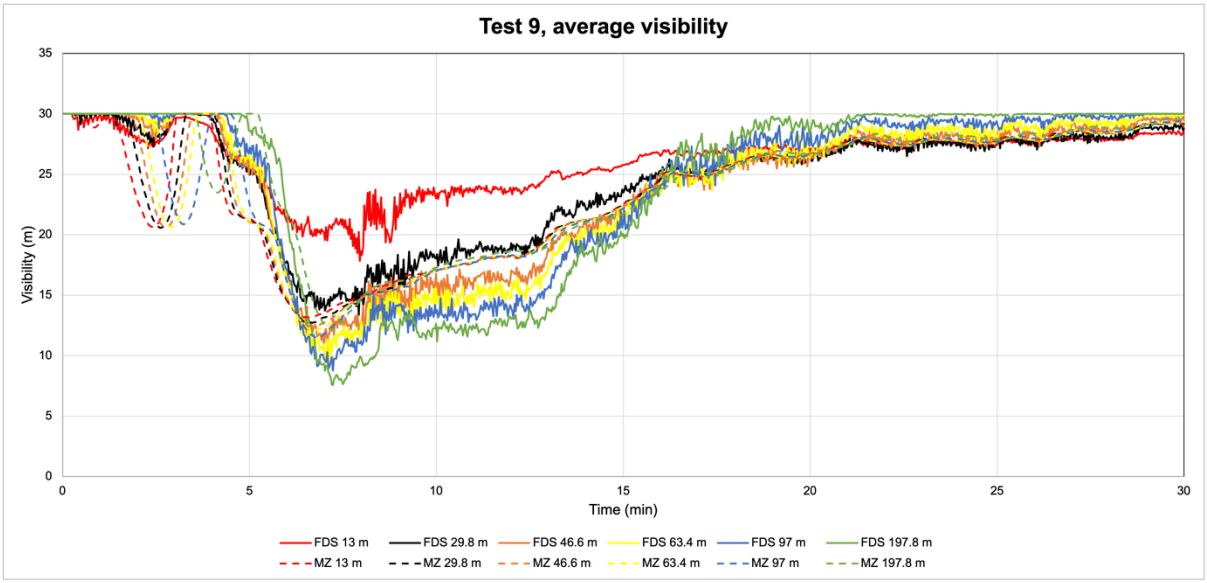

Figure A.36. Average cross section visibility calculated with FDS and MZ at different positions from fire source test 9.

Comment on the results test 9:

The overall correspondence between FDS and MZ is considered good for test 9. The upper temperatures are in general overpredicted, while the lower temperatures are underpredicted compared to FDS. The lower temperatures (at 1-2 m) are also underpredicted by MZ compared to the experimental results.

Regarding visibility the MZ model gives conservative predictions compared to FDS.

Test 14 (25MW, Longitudinal ventilation max 1 m/s)

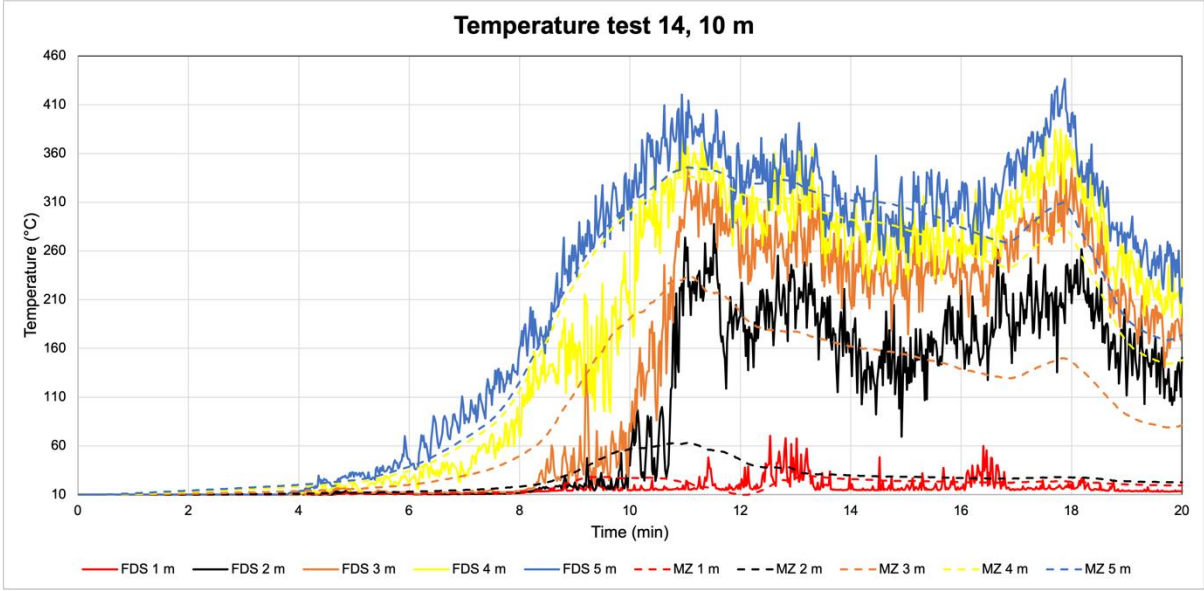

Figure A.37. Temperature calculated with FDS and MZ 10 m from fire source test 14.

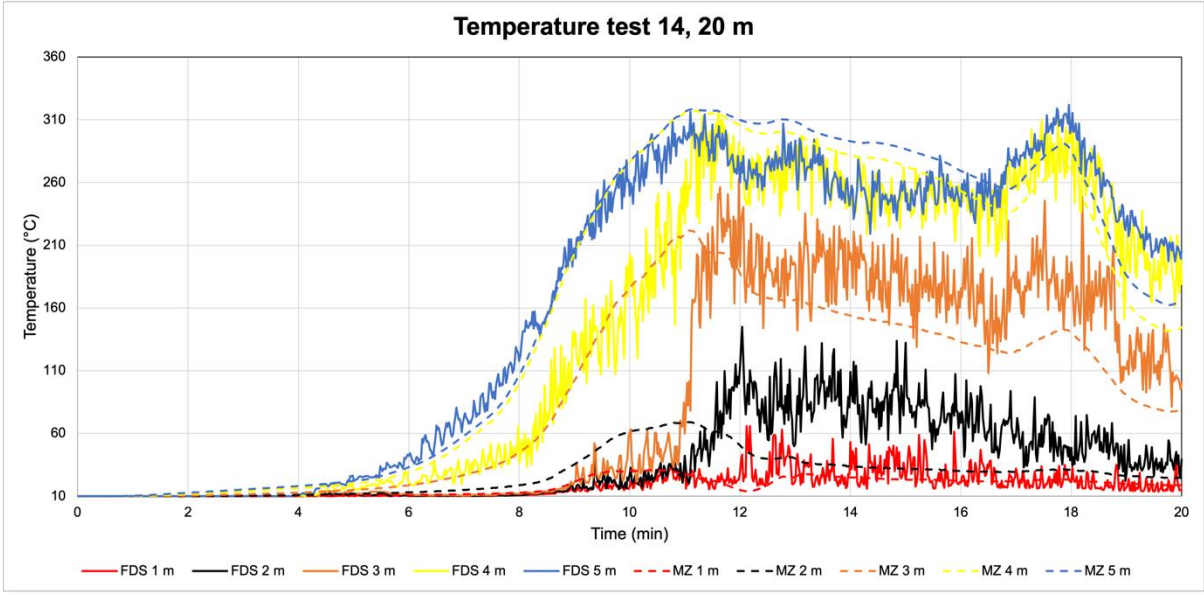

Figure A.38. Temperature calculated with FDS and MZ 20 m from fire source test 14.

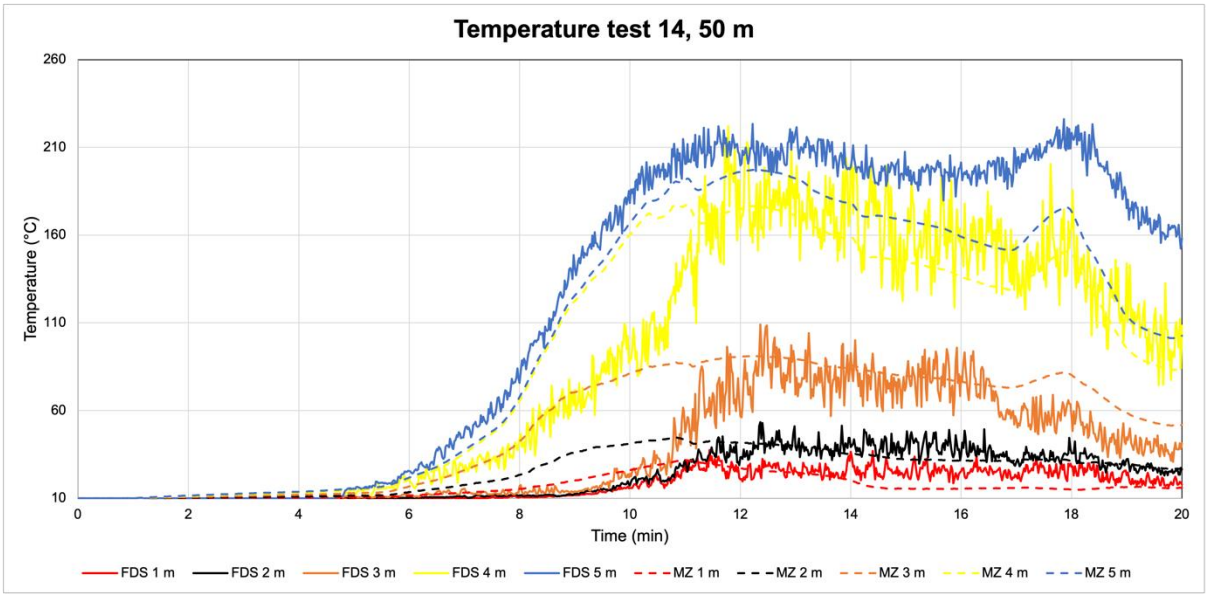

Figure A.39. Temperature calculated with FDS and MZ 50 m from fire source test 14.

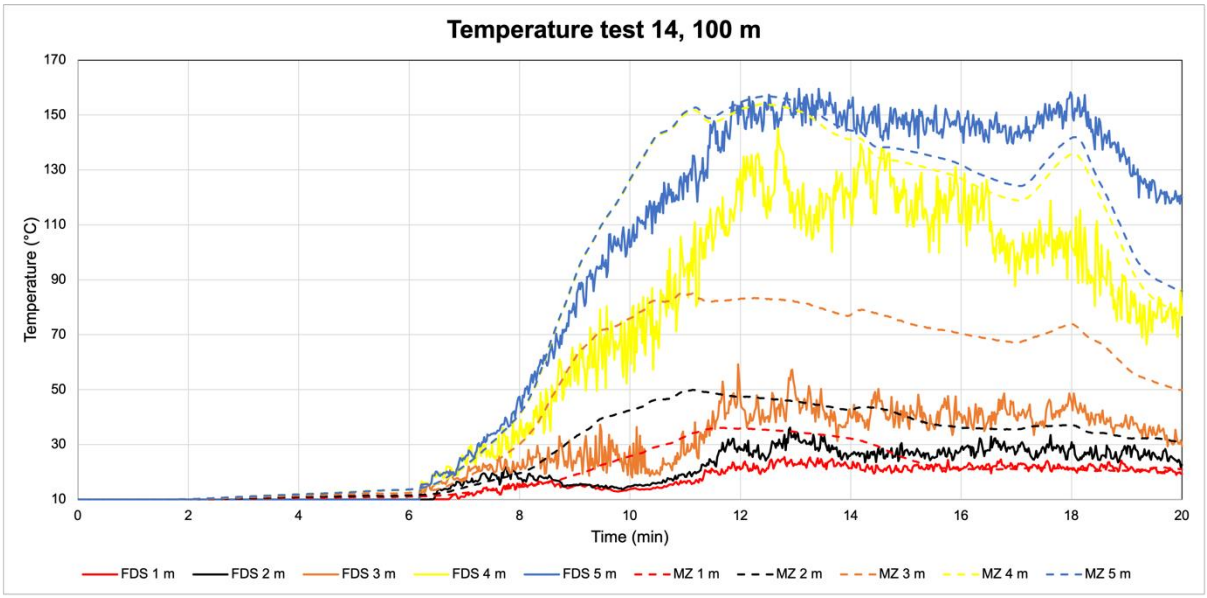

Figure A.40. Temperature calculated with FDS and MZ 100 m from fire source test 14.

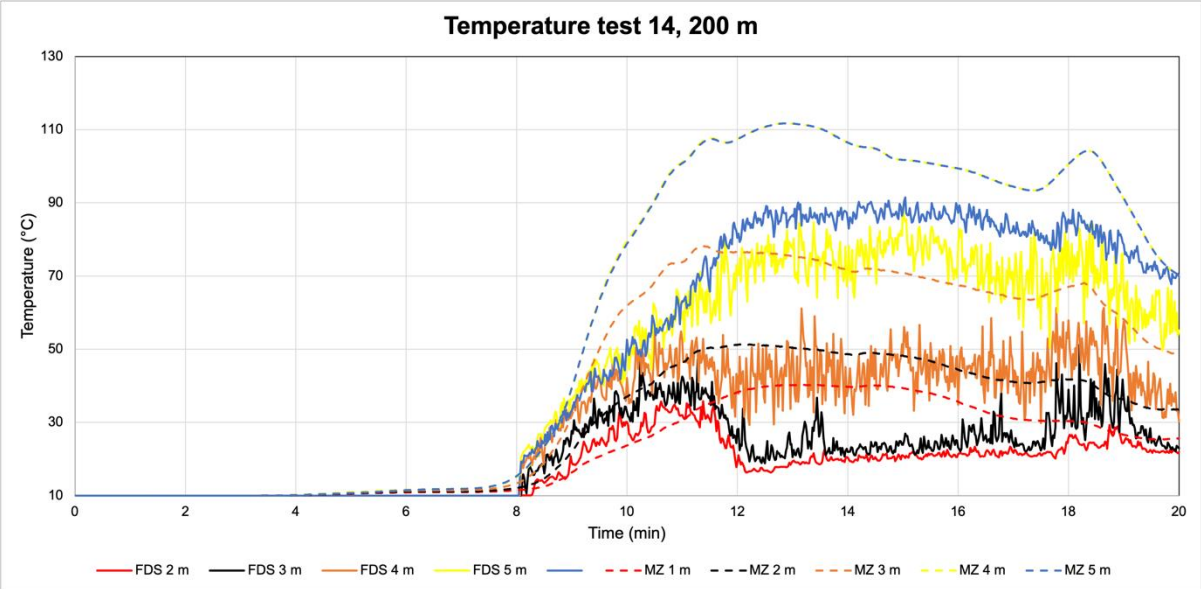

Figure A.41. Temperature calculated with FDS and MZ 200 m from fire source test 14.

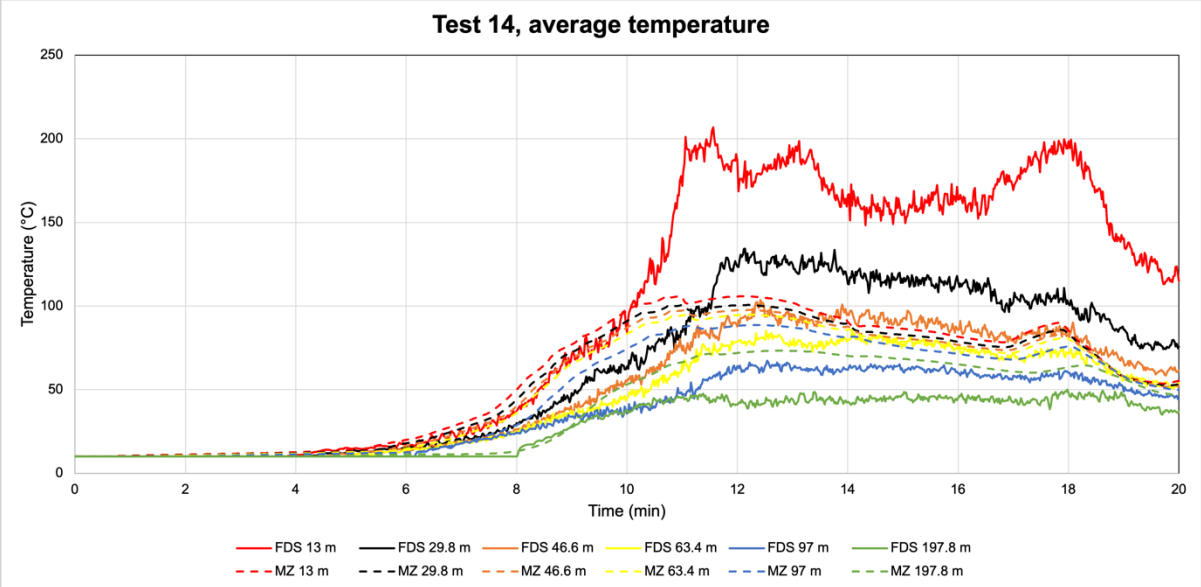

Figure A.42. Average cross section temperature calculated with FDS and MZ at different positions from fire source test 14.

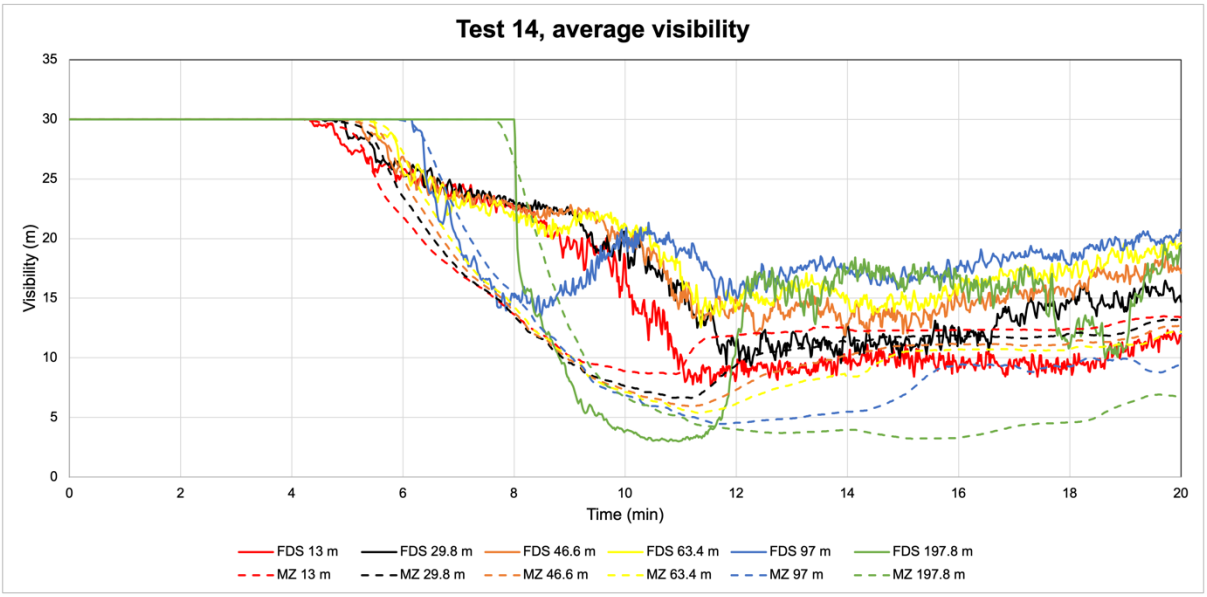

Figure A.43. Average cross section visibility calculated with FDS and MZ at different positions from fire source test 14.

Comment on the results test 14:

The overall correspondence between FDS and MZ is considered good for test 14. The average temperatures are higher for FDS closer to the fire source, this is mainly because the lower temperatures (1-2 m) are lower in MZ. Further away from the fire (> 50 m), the results from MZ are more conservative even at lower levels.

No comparison to experimental test data was done for Test 14.

Appendix B – Example inputs files used in Chapter 6

Longitudinal ventilation (2 m/s)

```
&MESH IJK= 10, 3, 8,  XB=0,40,0,12,0,4 / Recommended size of each zone is 4x4x0.5 m3
&TIME T_END=600 /
&MISC TMPA=10 ANGLE=0/

&FIRE XB=17,19,5,7,0,0, RAMP_ID=1  HRRPUA=1000, RADI=0.35, SOOT_YIELD = 0.015, HEAT_OF_COMBUSTION = 18700,  / FIRE VENT
&RAMP ID=1, T=0.0, F=0/
&RAMP ID=1, T=300, F=1/
&RAMP ID=1, T=600, F=1/

&MATL ID=1 CONDUCTIVITY=1.37, SPECIFIC_HEAT=880, DENSITY=2100, THICKNESS=0.3, EMISSIVITY=0.9 /

&VENT XB=0.0,0.0,0.0,12,0.0,4, VOLUME_FLOW=-96, RAMP_ID=2/

&RAMP ID=2, T=0, F=0/
&RAMP ID=2, T=150, F=0.5/
&RAMP ID=2, T=300, F=1/

&VENT XB=40,40,0,12,0,4/
&OBST XB=0.0,40,0.0,12,4,4, MATL_ID=1 / roof
&OBST XB=0.0,40,0.0,12,0.0,0.0, MATL_ID=1 / floor
&OBST XB=0.0,40,0.0,0.0,0.0,4, MATL_ID=1 / right wall
&OBST XB=0.0,40,12,12,0.0,4, MATL_ID=1 / left wall

&DEVC XYZ=10,6,0.25 QUANTITY='TEMPERATURE' /
&DEVC XYZ=10,6,0.75 QUANTITY='TEMPERATURE' /
&DEVC XYZ=10,6,1.25 QUANTITY='TEMPERATURE' /
&DEVC XYZ=10,6,1.75 QUANTITY='TEMPERATURE' /
&DEVC XYZ=10,6,2.25 QUANTITY='TEMPERATURE' /
&DEVC XYZ=10,6,2.75 QUANTITY='TEMPERATURE' /
&DEVC XYZ=10,6,3.25 QUANTITY='TEMPERATURE' /
&DEVC XYZ=10,6,3.75 QUANTITY='TEMPERATURE' /

&DEVC XYZ=14,6,0.25 QUANTITY='TEMPERATURE' /
&DEVC XYZ=14,6,0.75 QUANTITY='TEMPERATURE' /
&DEVC XYZ=14,6,1.25 QUANTITY='TEMPERATURE' /
&DEVC XYZ=14,6,1.75 QUANTITY='TEMPERATURE' /
&DEVC XYZ=14,6,2.25 QUANTITY='TEMPERATURE' /
&DEVC XYZ=14,6,2.75 QUANTITY='TEMPERATURE' /
&DEVC XYZ=14,6,3.25 QUANTITY='TEMPERATURE' /
&DEVC XYZ=14,6,3.75 QUANTITY='TEMPERATURE' /

&DEVC XYZ=30,6,0.25 QUANTITY='TEMPERATURE' /
&DEVC XYZ=30,6,0.75 QUANTITY='TEMPERATURE' /
&DEVC XYZ=30,6,1.25 QUANTITY='TEMPERATURE' /
&DEVC XYZ=30,6,1.75 QUANTITY='TEMPERATURE' /
```

```
&DEVC XYZ=30,6,2.25 QUANTITY='TEMPERATURE' /
&DEVC XYZ=30,6,2.75 QUANTITY='TEMPERATURE' /
&DEVC XYZ=30,6,3.25 QUANTITY='TEMPERATURE' /
&DEVC XYZ=30,6,3.75 QUANTITY='TEMPERATURE' /

&TAIL /
```

Tunnel gradient (2.5°)

```
&MESH IJK= 10, 3, 8,  XB=0,40,0,12,0,4 / Recommended size of each zone is 4x4x0.5 m3
&TIME T_END=600 /
&MISC TMPA=10 ANGLE=2.5/

&FIRE XB=17,19,5,7,0,0, RAMP_ID=1  HRRPUA=1000, RADI=0.35, SOOT_YIELD = 0.015, HEAT_OF_COMBUSTION = 18700,  / FIRE VENT
&RAMP ID=1, T=0.0, F=0/
&RAMP ID=1, T=300, F=1/
&RAMP ID=1, T=600, F=1/

&MATL ID=1 CONDUCTIVITY=1.37, SPECIFIC_HEAT=880, DENSITY=2100, THICKNESS=0.3, EMISSIVITY=0.9 /

&VENT XB=0.0,0.0,0.0,12,0.0,4/

&RAMP ID=2, T=0, F=0/
&RAMP ID=2, T=150, F=0.5/
&RAMP ID=2, T=300, F=1/

&VENT XB=40,40,0,12,0,4/
&OBST XB=0.0,40,0.0,12,4,4, MATL_ID=1 / roof
&OBST XB=0.0,40,0.0,12,0.0,0.0, MATL_ID=1 / floor
&OBST XB=0.0,40,0.0,0.0,0.0,4, MATL_ID=1 / right wall
&OBST XB=0.0,40,12,12,0.0,4, MATL_ID=1 / left wall

&DEVC XYZ=10,6,0.25 QUANTITY='TEMPERATURE' /
&DEVC XYZ=10,6,0.75 QUANTITY='TEMPERATURE' /
&DEVC XYZ=10,6,1.25 QUANTITY='TEMPERATURE' /
&DEVC XYZ=10,6,1.75 QUANTITY='TEMPERATURE' /
&DEVC XYZ=10,6,2.25 QUANTITY='TEMPERATURE' /
&DEVC XYZ=10,6,2.75 QUANTITY='TEMPERATURE' /
&DEVC XYZ=10,6,3.25 QUANTITY='TEMPERATURE' /
&DEVC XYZ=10,6,3.75 QUANTITY='TEMPERATURE' /

&DEVC XYZ=14,6,0.25 QUANTITY='TEMPERATURE' /
&DEVC XYZ=14,6,0.75 QUANTITY='TEMPERATURE' /
&DEVC XYZ=14,6,1.25 QUANTITY='TEMPERATURE' /
&DEVC XYZ=14,6,1.75 QUANTITY='TEMPERATURE' /
&DEVC XYZ=14,6,2.25 QUANTITY='TEMPERATURE' /
&DEVC XYZ=14,6,2.75 QUANTITY='TEMPERATURE' /
&DEVC XYZ=14,6,3.25 QUANTITY='TEMPERATURE' /
&DEVC XYZ=14,6,3.75 QUANTITY='TEMPERATURE' /

&DEVC XYZ=30,6,0.25 QUANTITY='TEMPERATURE' /
&DEVC XYZ=30,6,0.75 QUANTITY='TEMPERATURE' /
&DEVC XYZ=30,6,1.25 QUANTITY='TEMPERATURE' /
&DEVC XYZ=30,6,1.75 QUANTITY='TEMPERATURE' /
&DEVC XYZ=30,6,2.25 QUANTITY='TEMPERATURE' /
&DEVC XYZ=30,6,2.75 QUANTITY='TEMPERATURE' /
```

```
&DEVC XYZ=30,6,3.25 QUANTITY='TEMPERATURE' /
&DEVC XYZ=30,6,3.75 QUANTITY='TEMPERATURE' /

&TAIL /
```

Vertical cross-section (Scenario 1)

```
&MESH IJK= 10, 3, 8,  XB=0,40,0,12,0,4 / Recommended size of each zone is 4x4x0.5 m3
&TIME T_END=600 /
&MISC TMPA=10 ANGLE=0/

&FIRE XB=17,19,5,7,0,0, RAMP_ID=1  HRRPUA=1000, RADI=0.35, SOOT_YIELD = 0.015, HEAT_OF_COMBUSTION = 18700,  / FIRE VENT
&RAMP ID=1, T=0.0, F=0/
&RAMP ID=1, T=300, F=1/
&RAMP ID=1, T=600, F=1/

&MATL ID=1 CONDUCTIVITY=1.37, SPECIFIC_HEAT=880, DENSITY=2100, THICKNESS=0.3, EMISSIVITY=0.9 /

&RAMP ID=2, T=0, F=0/
&RAMP ID=2, T=150, F=0.5/
&RAMP ID=2, T=300, F=1/

&VENT XB=0,0,0,12,0,4/
&VENT XB=40,40,0,12,0,4/

&OB3D XB=0.0,40,0.0,2,3,3.6, /  OB3D should not overlap, the volume will be counted twice.
&OB3D XB=0.0,40,10,12,3,3.6, / OB3D should not overlap, the volume will be counted twice.
&OB3D XB=0.0,40,0,12,3.6,4, / OB3D should not overlap, the volume will be counted twice.

&OBST XB=0.0,40,0.0,12,4,4, MATL_ID=1 / roof
&OBST XB=0.0,40,0.0,12,0.0,0.0, MATL_ID=1 / floor
&OBST XB=0.0,40,0.0,0.0,0.0,4, MATL_ID=1 / right wall
&OBST XB=0.0,40,12,12,0.0,4, MATL_ID=1 / left wall

&DEVC XYZ=10,6,0.25 QUANTITY='TEMPERATURE' /
&DEVC XYZ=10,6,0.75 QUANTITY='TEMPERATURE' /
&DEVC XYZ=10,6,1.25 QUANTITY='TEMPERATURE' /
&DEVC XYZ=10,6,1.75 QUANTITY='TEMPERATURE' /
&DEVC XYZ=10,6,2.25 QUANTITY='TEMPERATURE' /
&DEVC XYZ=10,6,2.75 QUANTITY='TEMPERATURE' /
&DEVC XYZ=10,6,3.25 QUANTITY='TEMPERATURE' /
&DEVC XYZ=10,6,3.75 QUANTITY='TEMPERATURE' /

&DEVC XYZ=14,6,0.25 QUANTITY='TEMPERATURE' /
&DEVC XYZ=14,6,0.75 QUANTITY='TEMPERATURE' /
&DEVC XYZ=14,6,1.25 QUANTITY='TEMPERATURE' /
&DEVC XYZ=14,6,1.75 QUANTITY='TEMPERATURE' /
&DEVC XYZ=14,6,2.25 QUANTITY='TEMPERATURE' /
&DEVC XYZ=14,6,2.75 QUANTITY='TEMPERATURE' /
&DEVC XYZ=14,6,3.25 QUANTITY='TEMPERATURE' /
&DEVC XYZ=14,6,3.75 QUANTITY='TEMPERATURE' /

&DEVC XYZ=30,6,0.25 QUANTITY='TEMPERATURE' /
&DEVC XYZ=30,6,0.75 QUANTITY='TEMPERATURE' /
```

```
&DEVC XYZ=30,6,1.25 QUANTITY='TEMPERATURE' /
&DEVC XYZ=30,6,1.75 QUANTITY='TEMPERATURE' /
&DEVC XYZ=30,6,2.25 QUANTITY='TEMPERATURE' /
&DEVC XYZ=30,6,2.75 QUANTITY='TEMPERATURE' /
&DEVC XYZ=30,6,3.25 QUANTITY='TEMPERATURE' /
&DEVC XYZ=30,6,3.75 QUANTITY='TEMPERATURE' /

&TAIL /
```